

INDIVIDUAL-BASED MODELLING OF BIODIVERSITY IN MICROBIAL COMMUNITIES

Ward Quaghebeur

Studentennummer: 01201743

Aantal woorden: 19843

Promotors: prof. dr. Bernard De Baets
dr. ir. Jan Baetens

Tutors: Msc. Aisling Daly
dr. ir. Frederiek-Maarten Kerckhof

Masterproef voorgelegd voor het behalen van de graad:
master in de richting Bio-ingenieurswetenschappen.

Academiejaar: 2016 - 2017

Contents

Acknowledgements	i
Contents	iv
Summary	v
Samenvatting	vii
List of symbols	ix
1 Introduction and research objectives	1
1.1 Introduction	1
1.2 Outline and research objectives	2
2 Literature Review	3
2.1 Microbial biodiversity	3
2.1.1 Introduction	3
2.1.2 Competitive dynamics	5
2.1.3 Spatial partitioning	9
2.2 Modelling microbial systems	13
2.2.1 Population-level models	13
2.2.2 Individual-based models	14
2.2.3 Application portfolio of IBMs in microbial systems	17
3 Lattice-free modelling	19
3.1 Introduction	19
3.2 Lattice-based benchmark model	20
3.3 Lattice-free model	21
3.3.1 Identifying neighbours	22
3.3.2 Local interactions	25
3.3.3 Overlap avoidance	26

3.4	Experimental setup	27
3.5	Results and discussion	29
3.5.1	Model efficiency	29
3.5.2	Lattice-free versus lattice-based models	30
3.5.3	Interaction range	37
3.6	Conclusion	38
4	Continuous mobility	39
4.1	Introduction	39
4.2	Adapted movement mechanics	39
4.3	Chasing predators and escaping preys	40
4.4	Experimental setup	41
4.4.1	Adapted movement mechanism	41
4.4.2	Chasing predators and escaping preys	42
4.5	Results and discussion	42
4.5.1	Adapted movement mechanism	42
4.5.2	Chasing predators and escaping preys	44
4.6	Conclusion	52
5	Substrate dynamics	53
5.1	Introduction	53
5.2	Substrate-dependent reproduction	53
5.3	Experimental set-up	55
5.4	Results and discussion	55
5.5	Conclusion	59
6	Conclusion	61
6.1	Conclusion	61
6.2	Perspectives	63
	Bibliography	67
A	Evenness and patchiness for the systems under study in Chapter 3	79
B	Derivation of the expected value of total distance	81
C	Evenness and patchiness for the systems under study in Chapter 4	83

Summary

Biodiversity is a key factor underpinning the stability and productivity of microbial ecosystems. However, the mechanisms that give rise to and maintain biodiversity in microbial communities are not yet fully understood. This thesis builds on an individual-based model (IBM) developed by Reichenbach et al. (2007), which has been used extensively in literature to investigate biodiversity in microbial communities. It uses a three-species intransitive competition structure, found in real microbial communities, as a simplification of microbial competition. When interactions are localised on a lattice, bacteria arrange themselves in spatial structures, thereby maintaining coexistence. However, models are always an approximation of reality. To further close the gap, we modified and extended the original model in several significant ways, and investigated their influence on the maintenance of coexistence, thereby making the model more realistic.

First, we constructed a lattice-free variant of the model. We found that this approach maintains coexistence better than the lattice-based model. By having more spatial degrees of freedom, the spirals in the lattice-free model tend to be more robust, with small refuges able to survive, thereby maintaining coexistence. These findings agree with experimental results. Second, we adapted the movement mechanism of the model to mimic movement more realistically. We found similar qualitative dynamics, namely emerging spatial patterns and a jeopardising effect of mobility on coexistence. Subsequently, we extended the model with chasing and escaping behaviour. We found that, when no spatial structures are present, this behaviour is a disadvantage by increasing the probability of encountering a predator. However, when spatial structures are present, chasing is an advantage. Escaping is an advantage when being chased, but a disadvantage when not being chased, since it opens up space for a predator to expand into. Finally, we incorporated substrate-dependent growth. We found that a higher substrate availability allows the system to support more individuals, thereby retrieving the macroscopic concept of carrying capacity when using the bottom-up approach of an IBM. Furthermore, a higher substrate availability promotes the maintenance of coexistence by sustaining more individuals. Adding substrate-dynamics to the model promotes the maintenance of coexistence by lowering the rate of reproduction.

Samenvatting

Biodiversiteit is een belangrijke invloed op de stabiliteit en productiviteit van microbiële ecosystemen. De mechanismen die co-existentie in stand houden zijn echter nog niet compleet begrepen. Deze thesis bouwt verder op een individu-gebaseerd model ontwikkeld door Reichenbach et al. (2007), dat uitgebreid wordt gebruikt in de literatuur om biodiversiteit in microbiële gemeenschappen te onderzoeken. Het model gebruikt een intransitieve competitiestructuur met drie soorten, gebaseerd op *in vivo* microbiële culturen, als simplificatie voor microbiële competitie. Indien men de interacties lokaliseert op een raster ordenen de bacteriën zich in ruimtelijke structuren en behouden daardoor co-existentie. Modellen zijn echter altijd benaderingen van de werkelijkheid. Daarom pasten we het model op verschillende manieren aan, en onderzochten we de invloed op het behoud van co-existentie. Hierdoor maakten we het model realistischer.

Ten eerste construeerden we een rasterloze versie van het model. We vonden dat deze aanpak co-existentie beter in stand hield dan een raster-gebaseerd model. De spiralen in het rasterloos model waren robuuster door een grotere ruimtelijke vrijheid. Ruimtelijke schuilplaatsen konden overleven, en daardoor bleef co-existentie behouden. Deze bevindingen komen overeen met experimentele resultaten. Ten tweede pasten we het bewegingsmechanisme aan. We vonden soortgelijke kwalitatieve resultaten: ruimtelijke structuren en een negatief effect van mobiliteit op co-existentie. Vervolgens implementeerden we achtervolgings- en vluchtgedrag in het model. Indien geen ruimtelijke structuren aanwezig waren vonden we dat dit gedrag een nadeel was door de kans op een ontmoeting met een vijand te verhogen. Achtervolgingsgedrag was wel een voordeel indien ruimtelijke structuren aanwezig waren. Dan was vluchtgedrag ook een voordeel indien de bacterie achtervolgd werd. Het was echter een nadeel indien de bacterie niet achtervolgd werd door ruimte vrij te maken voor de vijand. Als laatste implementeerden we substraat afhankelijke groei. We vonden dat een hogere beschikbaarheid van substraat meer individuen kon onderhouden. Het macroscopisch concept van draagvermogen werd dus teruggevonden met de bottom-up benadering van een individu-gebaseerd model. Ook vonden we dat een hogere beschikbaarheid van substraat een positief effect had op het behoud van co-existentie door meer individuen te onderhouden.

List of symbols

d_{cell}	Side length of a grid cell
d_{ij}	Distance between the centres of bacteria i and j
d_{max}	Maximal distance travelled in the x - or y -direction during one time step
D_s	Diffusion coefficient
d_x	Distance travelled in the x -direction
d_y	Distance travelled in the y -direction
E	Expected value
\mathbf{F}	Force
F_{in}	Substrate inflow rate
G	Gini coefficient
K_s	Half-saturation constant
L	Length of the <i>in silico</i> environment
M	Mobility
N	Area of the <i>in silico</i> environment
P_{blue}	Probability of a monoculture dominated by the blue species
P_{ext}	Probability of extinction
p_i	Relative abundance of the species i
P_{red}	Probability of a monoculture dominated by the red species
P_{yellow}	Probability of a monoculture dominated by the yellow species
s	Number of species in the community
$S^t(i, j)$	Substrate concentration of cell (i, j) at time t
r_d	Radius of the daughter bacteria
r_i	Radius of bacterium i
\mathbf{r}_{ij}	Repulsion vector between bacteria i and j
r_{int}	Interaction range
r_{rep}	Minimal radius at replication
x	Number of growth steps needed between two subsequent reproduction events
Y_{max}	Apparent yield coefficient

α	Repulsion weight factor
β	Motility weight factor
ϵ	Mobility rate
η	Reproduction efficiency
θ	Angle of reproduction
μ	Reproduction rate
μ_{max}	Maximum growth rate
σ	Competition rate

CHAPTER 1

Introduction and research objectives

1.1 Introduction

Biodiversity is a key factor controlling the stability and productivity of natural and engineered microbial ecosystems (Bell et al., 2005). However, the mechanisms that give rise to and maintain microbial biodiversity are not yet fully understood. To properly comprehend and engineer microbial ecosystems, a deeper knowledge of this fundamental concept is required. Performing lab experiments is the major, yet not the only path towards gathering these insights.

In all scientific disciplines, complementing experiments with mathematical modelling has provided relevant knowledge that would be challenging to gather through experimentation alone (Ermentrout and Edelstein-Keshet, 1993; Hellweger et al., 2016). A model unifies our empirical insights of the system under study. It tests the assumptions made and their consequences, thereby possibly exposing gaps and inconsistencies in our understanding of the system. If correctly validated, a mathematical model can be used to make predictions under conditions not yet investigated empirically, or simulate experiments that might be troublesome to execute in the field (Ferrer et al., 2008; Kreft et al., 2013).

This thesis builds on an individual-based model (IBM) originally developed by Reichenbach et al. (2007), which has been extensively used in literature to investigate biodiversity in microbial communities. It uses a three-species intransitive competition structure, comparable to a rock-paper-scissor game where no strategy has an absolute advantage, as simplification for real microbial competition. This structure is also found in real-life microbial systems (Kerr et al., 2002; Hibbing et al., 2010). When interactions between bacteria are localised, the number of neighbours available to interact with is limited. The bacteria tend to arrange themselves in spatial structures, thereby maintaining coexistence. The effect on the maintenance of coexistence of various parameters, such as mobility or substrate dependence, has been investigated with variants of this model, thereby providing valuable knowledge into the dynamics of microbial communities (Hawick, 2011; Avelino et al., 2012; Szolnoki et al., 2014; Daly et al., 2016).

1.2 Outline and research objectives

Models are always an approximation of the reality. To further close the gap between model and reality, we will modify and extend the original model in several significant ways, and investigate their influence on coexistence, thereby making the model more realistic.

First, the bacteria in the original model use a lattice to position themselves, forcing themselves to align orthogonally. This is not in accordance with the behaviour of *in vivo* bacteria, which position themselves more freely. Furthermore, the model depicts bacteria as squares, an uncommon shape in the microbial world. In Chapter 3, we will develop a lattice-free approach with round bacteria, allowing for more realistic spatial dynamics. We will investigate the effect of this approach on the maintenance of coexistence.

As Adamson and Morozov (2012) remarked, the mobility of species implemented in the model by Reichenbach et al. (2007) does not resemble the real movement of species. In this model, an individual can only move by switching places with one of its neighbours, a very unconventional way of movement from a biological perspective. We will therefore implement a more realistic movement mechanism in Chapter 4. Furthermore, we will investigate the effect of motility on the maintenance of coexistence. Therefore, we will extend the model to allow for chasing predators and escaping prey, two forms of motile behaviour.

Furthermore, the model developed by Reichenbach et al. (2007) assumes that a bacterium can only reproduce when the carrying capacity in its neighbourhood has not been reached. This is implemented by requiring an empty cell to reproduce into. However, this is not in accordance with reality. *In vivo* reproduction happens when the bacteria attain a certain size through growth. Growth, on the other hand, is limited by the availability of substrate, which in turn is influenced by the presence of other bacteria. To model reproduction more realistically, we will extend the model to include substrate-dependent growth, and assess the effect on the maintenance of coexistence in Chapter 5.

The research objectives of this thesis are thus twofold:

1. To make existing models more representative with respect to real microbial systems, by adopting a lattice-free approach, more realistic movement, and substrate-dependent reproduction. To identify the influence of these adaptations on the maintenance of coexistence.
2. To identify the influence of individual adaptive behaviour, notably motility, on the maintenance of coexistence.

CHAPTER 2

Literature Review

The scope of this thesis is to model biodiversity in microbial systems. Therefore, we will introduce some relevant concepts at the basis of the maintenance of coexistence in Section 2.1. The focus is on two important factors: competitive dynamics and spatial partitioning. In Section 2.2, we will consider two relevant modelling approaches for microbial systems: population-level modelling and individual-based modelling.

2.1 Microbial biodiversity

2.1.1 Introduction

Biodiversity

Biodiversity is a complex concept that spans functional, phylogenetic, temporal, and spatial aspects of a community (Wittebolle et al., 2009). The most relevant components are species richness (the number of species) and evenness (the relative abundance of species)(Figure 2.1) (Sale, 2007). A rich population suggests a potential to perform a lot of functions (Tilman, 1996), whereas evenness controls the balance among these traits (Polley et al., 2003).

The first measure, species richness, is known to increase the productivity of an ecosystem (Cardinale et al., 2002; Bell et al., 2005). The coexistence of many unique species increases the probability that some will back up a given function when others fail (Lemieux and Cusson, 2014). Species richness therefore promotes temporal stability (Hooper et al., 2005; Isbell et al., 2009; Proulx et al., 2010), compositional stability (Sankaran and McNaughton, 1999), and resilience (the ability to cope with change) (Naeem and Li, 1997; Reusch et al., 2005). Moreover, species richness is a strong defence against invasion (Levine and D'Antonio, 1999; Kennedy et al., 2002).

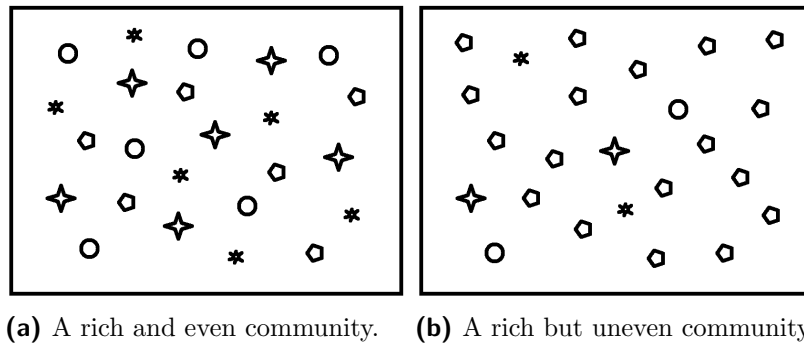


Figure 2.1: Richness versus evenness.

Evenness (or dominance, its antonym) has a similar importance in supporting the functioning of a population (Hillebrand et al., 2008). Evenness promotes adaptability to disturbance by ensuring that enough members of each species are present in every functional role. When one species is lost due to external factors, a sufficient number of the other species are present to substitute and guarantee its function, thereby promoting resilience (Wilsey and Potvin, 2000; Naeem, 2009). Moreover, uneven communities are more susceptible to invasion (Wilsey and Polley, 2002; Tracy and Sanderson, 2004; Fink and Wilson, 2011), although this effect does not hold when the community is under stress (De Roy et al., 2013). Additionally, a loss of evenness is often an early warning of biodiversity decline (Wilsey et al., 2009).

Although modelling studies on biodiversity generally assume maximal community evenness at the start of the simulation, research suggests this is often not the case (Wilsey, 2004). A study from Ashby et al. (2007) showed that 99% of unique rRNA tags identified in a soil sample belonged to fewer than one percent of the population. This finding demonstrates that taxa with a low abundance make a large contribution to the community richness and thus play a large role in the functioning and resilience of an ecosystem.

The paradox of the plankton

One of the core principles of conventional biodiversity thinking is the competitive exclusion principle, frequently referred to as Gause's law (Gause, 1934). It states that two species competing for the same niche cannot coexist. One of these two species will have a slight advantage over the other, leading to its dominance in the long run. The other one will either go extinct or shift towards another niche (Hardin, 1960). Contrary to what one would expect from Gause's law, a striking richness of species is present in many ecosystems, including microbial systems. Hutchinson (1961) encountered an astonishingly wide range of planktonic species supported by a narrow resource base, thereby defying the competitive exclusion principle. He famously formulated this observation as the paradox of the plankton.

To maintain this coexistence of species, an ecosystem needs stabilising actions that minimise average fitness differences among species (Chesson, 2000). Such actions can either be a rare species advantage, favouring the uncommon species (Wills et al., 2006), or a common species disadvantage, impairing the dominant species (Harpole and Suding, 2007). Various stabilising mechanics have been proposed to explain the paradox of the plankton (Scheffer et al., 2003; Roy and Chattopadhyay, 2007): spatial and temporal fluctuations in the environment (Richerson et al., 1970; Descamps-Julien and Gonzalez, 2005), oscillating (Huisman and Weissing, 1999) or size-selective (Wiggert et al., 2005) competitive dynamics, (non-)competitive interactions with other species (Huisman et al., 2001), and spatial partitioning among species (Miyazaki et al., 2006). Depending on the environmental context, all or some of these mechanisms work together towards maintaining biodiversity (Grman et al., 2010). The remainder of this section will investigate two of these mechanisms maintaining coexistence within the scope of this thesis: competitive dynamics and spatial partitioning, and will focus on microbial systems.

2.1.2 Competitive dynamics

Mechanisms of competitive advantages

Competition can be defined as a struggle among two or more species for the same niche that cannot be shared. Competition is a zero-sum game, meaning that one's gain is the other's loss, contrary to other interactions such as mutualism or commensalism (Keddy, 2001). By attaining a competitive advantage, bacteria can dominate their competitors and drive them to extinction in the long run. Using the available resources more economically than one's competitors is an obvious competitive advantage, but activities like toxin production, coordinated action, or motility can also tip the competitive balance (Hibbing et al., 2010).

A first mechanism affecting competitive dynamics is resource limitation. Tilman et al. (1997) were among the first to study the competition of species as a function of limiting resources. Their resource ratio model shows that different species can outcompete each other under certain limiting nutrient ratios. For example, Smith (2002) showed that the availability of nitrogen, phosphorus, and the ratio thereof affects the competition among different microbial species.

Secondly, the production of toxins often regulates competition patterns (Chao and Levin, 1981). By producing toxins harmful to other species, one lowers the functioning of its competitor or even kills it, and can thus gain a competitive advantage. However, this production of toxins comes at a metabolic cost, potentially paving the way to a resource utilisation advantage for a toxin-resistant species (Durrett and Levin, 1997). This chemical warfare by excretion of antimicrobial substances is widespread among bacteria (James et al., 2013).

Lastly, certain behaviour can influence competitive dynamics. Communication (e.g. quorum sensing) allows multiple bacteria to coordinate their actions (Miller and Bassler, 2001; Waters and Bassler, 2005), giving them a competitive advantage (Shapiro, 1998; Henke and Bassler, 2004; Diggle et al., 2007). Motile behaviour, such as chemotaxis (Hibbing et al., 2010) or chasing behaviour (Flannagan et al., 2004), have also an influence on the competitive dynamics.

Competition structures

A competition structure is defined by the number of partaking species and their mutual interactions. A tournament graph visualises a complex interaction network among species (Figure 2.2). It shows the pairwise interactions between all species, by drawing an arrow from the inferior to the superior species (Allesina and Levine, 2011; Laird and Schamp, 2015).

In ecosystems with two species, only one competition structure is possible: one species has an advantage over the other. Nevertheless, these advantages are not always absolute. For example, there is a metabolic trade-off between the costs and benefits of production of the toxin colicin (Riley and Gordon, 1999). Models with *Escherichia coli* bacteria show that, depending on the conditions, both the colicin-producing and colicin-sensitive strategies can be advantageous (Levin et al., 1988; Durrett and Levin, 1997).

In populations of three species, the picture is more complex. Competition can be transitive (Figure 2.2a), where one apex predator dominates all others, or intransitive (Figure 2.2b), where no apex predator is present and all species are preyed upon. Literature also refers to these as hierarchical (transitive) and cyclic (intransitive) competition. One can intuitively determine that transitive competition results in extremely uneven communities, and possibly monocultures (May and Leonard, 1975).

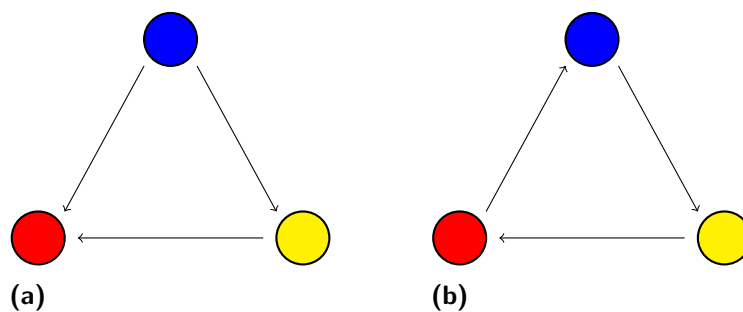


Figure 2.2: Transitive (hierarchical) (a) and intransitive (cyclic) (b) three-species tournament graph.

The rock-paper-scissors game is often used to explain the coexistence of species under intransitive competition. When rock smashes scissors, scissors cuts paper, and paper covers rock, no object is strictly dominant, and the competition is thus intransitive. This intransitive competition is present in a community of three *E. coli* strains (Kerr et al., 2002). A producing strain (P) synthesises the toxin colicin, harmful to a sensitive strain (S). However, a resistant strain (R) is not influenced by the colicin. The latter does not have the metabolic cost imposed on P for producing colicin, thereby gaining a resource utilisation advantage and outgrowing P. Furthermore, S does not have the metabolic cost of the resistance genes, thereby outcompeting R. So, S outcompetes R, R outcompetes P, and of course, P kills S (Figure 2.3). This dynamic is thus an intransitive competition structure (Kirkup and Riley, 2004). Narisawa et al. (2008) reported a similar toxin-mediated intransitive competitive dynamic across species, with a pyocyanin producing *Pseudomonas*, a resistant *Raoultella*, and a sensitive *Brevibacillus*.

These colicin-driven intransitive dynamics are not a marginal phenomenon (Achtman et al., 1983). 35% of tested *E. coli* strains are reported to be colicinogenic, whereas most of the strains were sensitive to at least one of the 20 types of colicin tested. Multiple resistance is common, and some 22% of the strains were found to be resistant to all colicines (Riley and Gordon, 1992). Furthermore, similar intransitive dynamics have been found in other taxonomic groups, including plants (Taylor and Aarssen, 1990; Lankau and Strauss, 2007), sessile marine organisms (Buss, 1979; Jackson, 1983; Buss, 1990; Taylor and Aarssen, 1990), and mating strategies of lizards (Sinervo et al., 2007).

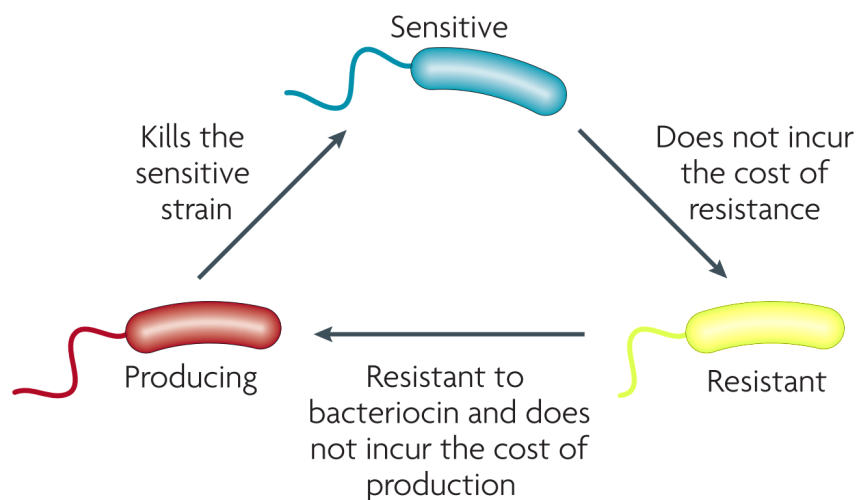


Figure 2.3: Visualisation of an *E. coli* intransitive competition network (adapted from Hibbing et al. (2010)).

Intransitivity can stabilise an ecosystem through enemy's enemy indirect facilitation (Laird and Schamp, 2006). If one species improves its situation at the expense of its prey, it gives an advantage to its enemy by reducing competition by the predator of its predator. By indirectly giving an advantage to its predators, it loses its temporarily dominant position, thereby balancing the competitive dynamics. Within certain parameter ranges, coexistence is thus promoted by an intransitive competition structure (Czárán et al., 2002).

When coexistence is lost in a three-species intransitive community, it follows the survival of the weakest law. A species that is temporarily dominating the community (e.g. the blue species in Figure 2.2b) will induce a sharp drop in the number of its prey (the yellow species), consequently lowering the pressure on the prey of its prey (the red species). This advantage for the red species, in combination with the abundance of its blue prey, leads to a rapid growth of the red species, thereby driving the blue species to extinction. The yellow species, initially the weakest, finds itself without a predator and drives the preyless red species to extinction, leaving only the yellow species to survive (Frean and Abraham, 2001; Adamson and Morozov, 2012). Berr et al. (2009) remarked that this law only holds with a sufficient number of individuals in the population.

When looking at competition structures involving a higher number of species, communities often contain one or more intransitive substructures. Four-species communities are widely studied (Laird and Schamp, 2006, 2008; Rojas-Echenique and Allesina, 2011). A fully connected variant is unstable and will collapse to the classic rock-paper-scissors game by elimination of one species (Cheng et al., 2014; Daly et al., 2015). Five-species variants (Laird and Schamp, 2009; Hawick, 2011; Kang et al., 2013; Vukov et al., 2013) and six-species or higher (Roman et al., 2016) have also been studied. Allesina and Levine (2011) reported that every fully-connected network of an even number of species will contain a subnetwork of an odd number of species that collectively wins against each of the remaining species more often than it loses. Thus, only a competition structure containing an uneven number of species can maintain coexistence in the long run. If each species is dominated by exactly half of the other species and dominates the other half, the network is considered balanced.

A competition structure can be written down in a tournament matrix, from which a relative intransitivity index can be calculated to quantify the level of intransitivity (Petraitis, 1979). Theoretical models have shown that these indices are a powerful predictor of the maintenance of coexistence (Laird and Schamp, 2006, 2008). However, care should be taken, since a lot of information is compressed into a single metric. Moreover, since indices do not take into account other influencing factors (e.g. spatial dynamics), two communities with the same level of intransitivity can produce different coexistence outcomes (Laird and Schamp, 2009).

Real ecosystems are defined by complex competitive interactions involving a lot of different species, often including intransitive substructures (Laird and Schamp, 2008). Increasing the number of competing species opens a whole range of possible levels of intransitivity, with networks that contain multiple intransitive subloops (Petraitis, 1979; Allesina and Levine, 2011). The rock-paper-scissors game used by Kerr et al. (2002) is therefore an interesting simplification to study the basic interaction in communities. Investigating this simple system can potentially lead to insights into the dynamics of communities with more species, where plenty of species have relative resource advantages or excrete toxins to inhibit some of their competitors (Vetsigian et al., 2011; Kinkel et al., 2014).

2.1.3 Spatial partitioning

From local interactions to spatial patterns

Kerr et al. (2002) placed the intransitive community of *E. coli* described in Section 2.1.2 in a well-mixed flask, where each bacterium can interact with every other bacterium. He found that two out of three strains go extinct, with one strain dominating the system (Figure 2.4a). However, when the same community is placed on a static plate, where interactions are limited to neighbouring individuals only, coexistence can be maintained over an ecologically significant time frame (Figure 2.4b).

The degree of localisation of interactions among individuals thus appears to facilitate coexistence. These findings have been confirmed by modelled intransitive communities under global and local interaction (Durrett and Levin, 1998). When each individual has an equal chance to interact with any other, irrespective of the distance between them, long term coexistence is threatened. When the interactions are limited by the distance to the neighbour (i.e., local interactions), coexistence can be maintained (Frean and Abraham, 2001; Kerr et al., 2002).

When the same intransitive community of *E. coli* is placed on a plate, but is rubbed on from time to time with a velvet, interactions are an intermediate between local and global. In this system, coexistence is lost as well, but preserved longer than in a well-mixed flask (Kerr et al., 2002). Similarly, a study by Abrudan et al. (2016) showed that a model where every modelled bacterium has six neighbours to interact with, maintains coexistence longer than a model where every bacterium has eight neighbours. Thus, in the whole range of intermediates between local and global interactions, systems with more localised interactions maintain biodiversity longer.

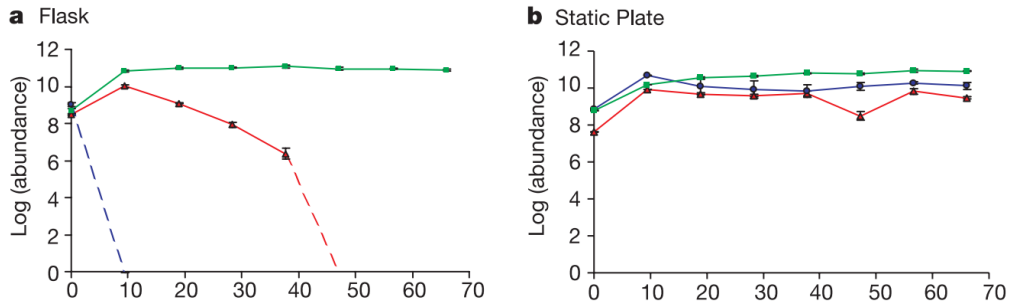
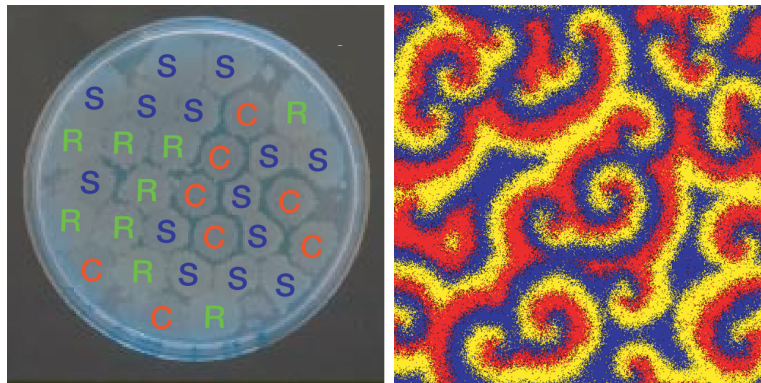


Figure 2.4: Dynamics of an intransitive three-species community in a well-mixed flask (a) and on a static plate (b). Dashed lines indicate that the abundance of the relevant strain has decreased below its detection limit (adapted from Kerr et al. (2002)).

It has been shown that when interactions between individuals are localised, spatial patterns emerge in both *in vivo* and *in silico* communities (Figure 2.5) (Hassell et al., 1994; Kerr et al., 2002; Kéfi et al., 2007; Perc et al., 2007; Scanlon et al., 2007; Szabó and Fátth, 2007). A balanced chase arises, where each patch outcompetes its prey at the expanding edge of its territory, while simultaneously being outcompeted by its predator at the shrinking edge (Laird and Schamp, 2008). Reichenbach et al. (2007) describe it as an endlessly spinning wheel of species chasing each other.

Laird (2014) examined the origin of preserved coexistence under local interactions. Is it merely attributed to the limited number of neighbours available to interact with, or are the spatial structures responsible? He compared rock-paper-scissors games on lattices (where spatial structures are present) with random regular graphs (without spatial structures). Although both systems limit the number of neighbours, coexistence could only be maintained in the former. Furthermore, when using a small-world network (an intermediate form, where a certain degree of spatial structures is present), coexistence is rapidly lost when the degree of localisation is lowered. This suggests that coexistence is not maintained due to the limited number of neighbours, but due to the spatial structures that arise.

Adamson and Morozov (2012) subdivided these spatial patterns into symmetric spiral waves, intermingled spirals and chaotic patches. Perfect symmetric spiral waves can only arise and survive under exact cyclic symmetry in mobility and competition with no stochasticity. This might clarify why symmetric spiral waves are often encountered in theoretical studies, but are absent in experimental results (Rohani et al., 1997), where the characteristics of these species are generally not equal.



(a) Experimental *E. coli* system (b) *In silico* system (adapted from Kerr et al. (2002)). from Reichenbach et al. (2007)).

Figure 2.5: Emergence of spatial patterns in a three-species intransitive community under local interactions.

Nevertheless, Laird and Schamp (2008) remarked that in some cases global interactions favour coexistence. If a species become surrounded by superior competitors, its extinction is inevitable under local interactions. Under global interactions, the inferior species has the opportunity to escape. The same dynamics can also assist coexistence, for example when a few individuals of a species remain, completely surrounded (and thus protected) by harmless neighbours. Abrudan et al. (2016) dubbed this effect as "coexistence by small numbers". However, it is worth noting that these findings can also be an artefact of the used model architecture.

Influence of mobility

Mobility influences the degree of localisation of the interactions. When the mobility of bacteria is minimal, the dynamics of the system are governed by the local interactions. The individuals arrange themselves in spatial structures, ensuring the long-term coexistence of the system. However, if mobility increases, bacteria move further, making the interactions less local. The spirals increase in size, increasing the chance that one of the species becomes dominant and drives the others out of existence. When mobility reaches a certain critical mobility, the local characteristics of the interactions disappear. The spirals outgrow the system, leaving one species to dominate the ecosystem (Figure 2.6a) (Reichenbach et al., 2007).

Which species survives is dependent on random processes, therefore each species has an equal chance of being the sole survivor. Since mobility is expressed relative to the dimensions of the lattice, coexistence in a larger system is more easily maintained than in a smaller one (Figure 2.6b). This is comparable to the ecological concept of carrying capacity (Reichenbach et al., 2007).

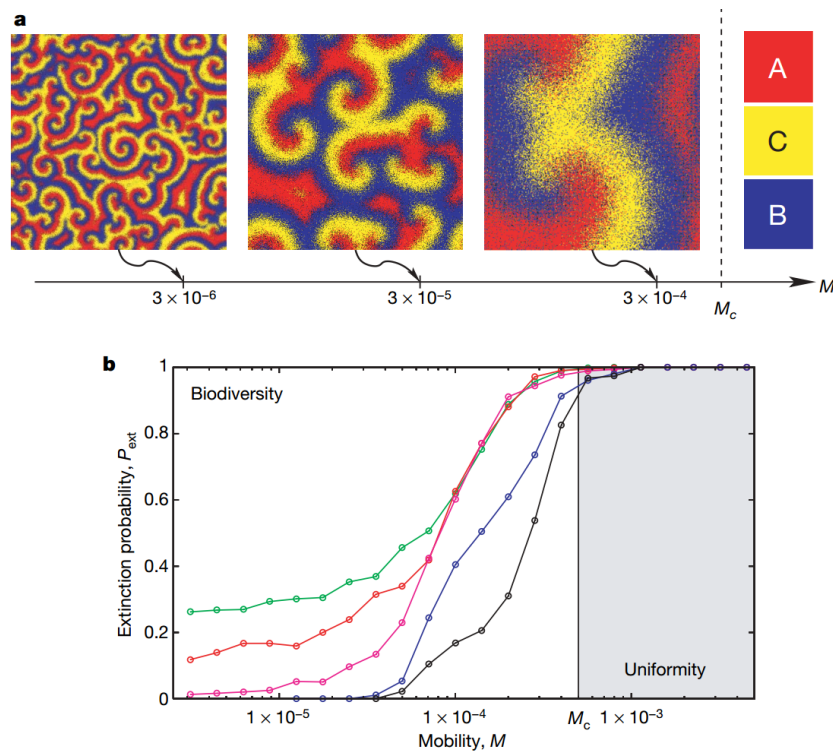


Figure 2.6: Snapshots obtained from lattice simulations for different values of the mobility M (a). Extinction probability P_{ext} as a function of M for different system sizes: 20×20 (green), 30×30 (red), 40×40 (purple), 100×100 (blue), and 200×200 (black) (b) (adapted from Reichenbach et al. (2007)).

Similar dynamics are found in other types of ecosystems. Karolyi et al. (2005) observed that chaotic mixing induces oscillations in phytoplankton systems by altering the spatial structure. They identified a critical mixing rate, beyond which coexistence is lost. Levin (1974) experimentally found a critical mobility when studying movement of animals between different patches. Nevertheless, Adamson and Morozov (2012) remarked that the mobility of species implemented in certain models (e.g. Reichenbach et al. (2007)) does not resemble real movement of species. In these models, an individual can only move by switching its place with its closest neighbour. This movement mechanism is unrealistic from a biological perspective.

Differences in mobility among species have an impact on the maintenance of biodiversity as well. Durrett and Levin (1998) showed that a faster moving species can potentially overcome a dominant predator. In certain habitats where coexistence would be lost, it can be preserved under unequal mobility. However, this effect is not always positive. Changing the dispersal rate of one of the species alters the arising spatial patterns. In some systems, even a small disparity in the mobilities results in loss of biodiversity (Adamson and Morozov, 2012).

To recap, a three-species intransitive competition structure offers an interesting simplification to study competition in microbial communities. When interactions between bacteria are localised, the number of neighbours available to interact with is limited. The bacteria tend to arrange themselves in spatial structures, thereby possibly maintaining coexistence.

2.2 Modelling microbial systems

Aside from experiments, mathematical models can provide us with valuable insights in biodiversity that would be difficult to obtain through experimentation alone. Integrating the experimental and modelling approach is therefore an intelligent way to both increase understanding and accurately predict microbial ecosystems (Hellweger et al., 2016). In this section, we will discuss and compare two relevant modelling paradigms for microbial ecosystems: population-level models (PLMs) and individual-based models (IBMs).

2.2.1 Population-level models

The conventional approach to modelling a bacterial ecosystem is based on PLMs. These models are derived from a set of governing laws at population level, consistent with a collection of assumptions about the behaviour at individual level (Standaert et al., 2004). They consider a macroscopic variable (e.g. total cell number) and model this as a function of other macroscopic parameters. This relation is typically written down in the form of differential equations (DEs). These models are ideal for discovering general principles that apply across a broad range of systems, such as the tendency of predator-prey systems to evolve towards oscillations (Rosenzweig and MacArthur, 1963). PLMs can be extended to incorporate spatial dynamics by using partial differential equations (PDEs). For example, the spatial structures discussed in Section 2.1.3 can be modelled using either stochastic PDEs (Mimura and Tohma, 2015) or the complex Ginzburg-Landau equation (Reichenbach et al., 2008).

Because of the mathematical nature of PLMs, they are typically simple and understood by a broad audience. Their macroscopic variables and parameters are straightforward to measure, and the underlying equations are generally computationally efficient to solve (Hellweger and Bucci, 2009). Due to these advantages, PLMs have been extensively used and tested for applications in microbial systems, such as biofilm formation (Klapper and Dockery, 2010) or competition dynamics (Frey and Reichenbach, 2011).

However, this macroscopic top-down approach poses some drawbacks. First, solving the DEs numerically introduces approximation errors into the solution. Furthermore, the modelled population level processes are not always related to the actions undertaken by the individuals, and can easily fail to validate the assumptions made at the individual level (Ferrer et al., 2008). Whereas PLMs can simulate certain macroscopic dynamics of a system, it is impossible to trace these back to the individual behaviour of the organisms (Hellweger et al., 2016). Moreover, these models imply a mean-field-approximation (Ferrer et al., 2008). Neither the inherent individual variability and life cycles of bacteria can be taken into account, nor can the broad range of different biotic and abiotic interactions between bacteria and their environment be incorporated (Grimm, 1999; Hellweger et al., 2016). Likewise, it is impossible to include individual adaptive behaviour (Grimm et al., 2006). Lastly, spatial PLMs require partial differential equations, whose implementation can be complex and might lead to numerically unstable solutions (Standaert et al., 2004).

2.2.2 Individual-based models

In contrast to PLMs, an IBM tracks all organisms individually, or sometimes grouped into cohorts, with their corresponding state and behaviour (Kreft et al., 1998; Standaert et al., 2004; Hellweger and Bucci, 2009). Their state can include properties like biomass, size, species, or age of the individual; whereas their behaviour can include processes such as substrate uptake, competition, or biomass synthesis. This behaviour can be described by equations (e.g. growth) or rules (e.g. division) (Hellweger et al., 2016). All individuals execute their procedural activities once every time step (Ferrer et al., 2008). Their collective action reveals population level dynamics (Hellweger et al., 2016). In other words, IBMs incorporate biological, chemical, and physical insights at the individual bacterium level to generate the output at the population level (Standaert et al., 2004).

IBMs are based on more realistic assumptions at the individual level than PLMs (Grimm, 1999). By taking an individual as the basic modelling entity, this bottom-up approach circumvents the use of mean-field approximations. IBMs eliminate the need to specify global laws, which are inherently empirical (Standaert et al., 2004). If such a global phenomenon occurs, it is due to the established procedural rules of the modelled bacteria (Kreft et al., 1998). For example, PLMs often model resource dependency implicitly by assuming a carrying capacity. Since underlying individual processes like growth, dispersal, and reproduction are resource dependent, it is possible to model the system more realistically with an IBM (Grimm, 1999). The structural correctness of IBMs can thus be assessed by verifying whether they reproduce both the individual and population level dynamics observed experimentally (Kreft et al., 2013).

In contrast to the mean-field approach PLMs stand for, IBMs can account for individual variability and life cycles of bacteria, the broad range of different biotic and abiotic interactions between bacteria and their environment, as well as individual adaptive behaviour. IBMs can thus closely mimic the natural variability in the real system (Standaert et al., 2004; Ferrer et al., 2008). Moreover, in contrast to PLMs, adapting a model to simulate diverse communities consisting of many different species is easily done.

As discussed before, spatial phenomena are a key to the behaviour of microbial communities (Wimpenny, 1992). The individual basis of the modelled processes means that IBMs can naturally take into account the local interactions and spatial dynamics. (Standaert et al., 2004).

However, IBMs have their drawbacks. Since IBMs are often described verbally without clear equations, rules, or schedules, they lack the mathematical formulation and simplicity of PLMs. Despite efforts to construct a generic modelling framework (most notably the ODD protocol (Grimm et al., 2006, 2010)), it remains difficult to communicate about them and reproduce other's findings (Hales et al., 2003). IBMs can also become very complex, since slight modifications in the local governing laws can lead to substantial differences at the macroscopic level. This makes it difficult to quantitatively analyse them (Standaert et al., 2004; Ferrer et al., 2008).

In contrast to the macroscopic data needed to construct PLMs, an IBM requires a large amount of microscopic individual-based data (Kreft et al., 1998). Recent advances in the field pose new exciting ways to experimentally confine (microfluidics, hydrogels, ...) and analyse (microscopy, spectrometry, flow cytometry, ...) single cells or communities (Wessel et al., 2013). This opens possibilities for microbiologists to study what plant and animal ecologists have done for a long time: assessing where, when, and with whom an individual does something. This approach is known as microbial individual-based ecology (μ IBE), which complements IBMs (Kreft et al., 2013). Data acquisition will become more comprehensive in the future and can thereby improve the current models (Ferrer et al., 2008).

Lastly, IBMs typically pose a higher computational demand than PLMs (Kreft et al., 1998; Standaert et al., 2004). Luckily, the continuing hardware and software enhancements make this less of an issue nowadays. Still, one can always consider lowering the number of simulated individuals. Nonetheless, this gives rise to irregular dynamics, loss of variability and sensitivity to random processes, especially when simulating a microbial community containing large numbers of individuals (Scheffer et al., 1995). One can also opt to model a smaller ecosystem as a representative space for a bigger ecosystem, but one should not overlook larger levels of heterogeneity (Hellweger and Bucci, 2009). An alternative approach is to aggregate the individual species into functional groups or super-individuals (Scheffer et al., 1995).

The ability of IBMs to make predictions is equally promising. Since certain experiments are too complicated or unpractical to perform, IBMs can offer a way to run them *in silico*. IBMs can test experimental setups and support experimental design, or explore parameter ranges impossible to achieve in a laboratory (Ferrer et al., 2008; Kreft et al., 2013). Because of the mechanistic nature, they can potentially make predictions for a wide range of conditions and environments (Kreft et al., 2013).

The bottom-up approach of IBMs and top-down approach of PLMs are not mutually exclusive, but can complement each other (Nisbet et al., 2016). Acknowledging that each modelling paradigm has its advantages, a good choice should be motivated by the research objective (Evans et al., 2013). Comparing the same system modelled by different paradigms also has its merits. For example, by comparing a PLM and IBM of the same ecosystem, one can isolate the effects of individual variability and adaptability (Hellweger et al., 2016).

For the sake of completeness, it is worth mentioning a third modelling paradigm, namely cellular automata (CA). These models are discrete in space and time. CA concentrate on the cells of the grid themselves and study the geometric patterns arising from local interactions. They differ from IBMs by focusing on the grid cells instead of the individuals that might be in a certain cell, and do not explain individual diversity and the effect thereof on the behaviour of the population (Ben-Jacob et al., 1994; Ferrer et al., 2008). Since CA focus on geometric patterns, they are often used to explain the growth and structure of biofilms (Wimpenny and Colasanti, 1997; Picioreanu et al., 1998a,b).

A comparison of the advantages and disadvantages of PLMs and IBMs is given in Table 2.1. An example of the same system modelled using both paradigms is shown in Figure 2.7.

Table 2.1: Comparison of population-level and individual-based models.

Population-level models (PLMs)	Individual-based models (IBMs)
Model population dynamics	Dynamics emerge from individual behaviour
Individual dynamics not validated	Defined by individual dynamics
Macroscopic parameters/variables	Individual-based parameters/variables
Mean-field parameters/variables	Individual variability, adaptability, ...
DE	Textually described
Spatial PDE	Spatially explicit
Well-established	Relatively new

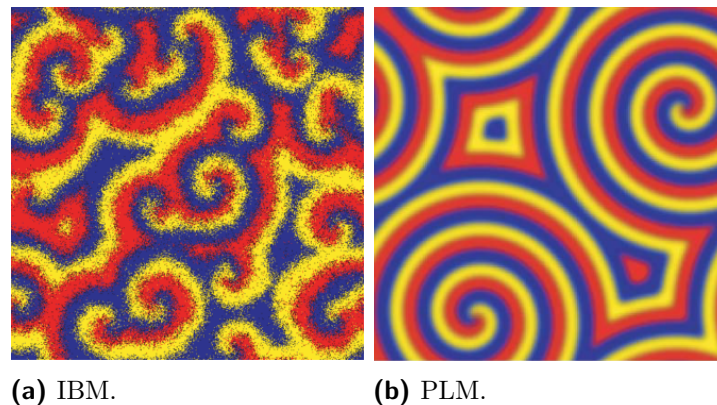


Figure 2.7: Visualisation of an *in silico* microbial system using both modelling paradigms (adapted from Reichenbach et al. (2007)).

2.2.3 Application portfolio of IBMs in microbial systems

IBMs simulating the growth of pure cultures have been developed for *E. coli* (Domach et al., 1984) and *Bacillus subtilis* (Jeong et al., 1990). These studies integrate subcellular biochemical processes and use experimental data from one specific species. Therefore, these models only allow accurate predictions for that certain species and should neither be used for other species, nor for mixed cultures.

Kreft et al. (1998) proposed a more generic approach with the BacSim model (Figure 2.8). By treating the biochemistry of the bacteria as a black box, the model is simplified and uses only eight parameters. Whereas the bacteria occupy a continuous space, the substrate dependency of the bacteria is modelled by defining a substrate concentration in each discrete lattice cell. Diffusion allows the substrate to move, replenished by a reservoir. The substrate uptake by the bacteria is modelled with the Michaelis-Menten equation (Michaelis et al., 1913). The metabolism allows for growth by converting substrate into dry biomass and waste, which is then excreted. Likewise, maintenance reactions convert substrate into waste. When substrate uptake is lower than the maintenance requirements, the cell biomass is consumed, implying a shrinkage of the bacterium. If the biomass drops below a certain minimum value, the individual dies, releasing its biomass into the environment as substrate. If the bacterium reaches a certain size, it divides into two identical daughter cells. It succeeds in correctly reproducing certain population-level characteristics such as exponential growth. Standaert et al. (2004) extended this model.

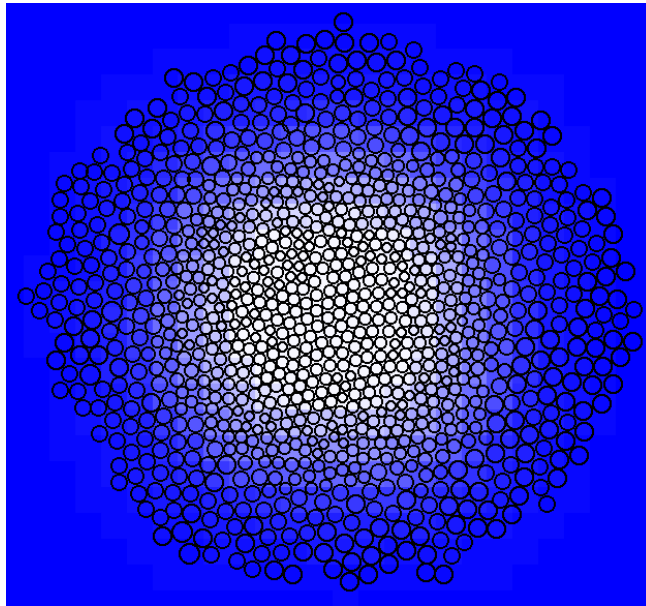


Figure 2.8: Example of output generated by BacSim (Kreft et al., 1998).

INDividual DIcrete SIMulations (INDISIM) was developed by Ginovart (2002). In contrast to BacSim, it uses a discrete lattice to simulate the habitat of the bacteria. Only four input parameters are needed, making it a simple, yet effective model. The model incorporates the uptake and metabolism of nutrients, reproduction, cell lysis, and movement. The simulation results correspond with experimental data. Ferrer et al. (2008) extended this model.

Reichenbach et al. (2007) proposed an interesting framework, which other researchers have built further on (Hawick, 2011; Avelino et al., 2012; Szolnoki et al., 2014; Daly et al., 2016). Since this dissertation uses this model as a basis, we refer the reader to Section 3.2 for more details.

Lastly, a number of modelling platforms are available. General tools like NetLogo (Wilensky, 1999) and FLAME (Flexible Large-scale Agent Modelling Environment) (Holcombe et al., 2012) focus on building generic IBMs, and are widely used by ecologists. Specific tools, like CellModeller (Rudge et al., 2012), CHASTE (Cancer, Heart And Soft Tissue Environment) (Mirams et al., 2013), and CompuCell3D (Popławski et al., 2008) were developed for modelling plant or animal tissues. Since biofilms behave similarly, the latter tools have been used to model them.

CHAPTER 3

Lattice-free modelling of microbial communities

3.1 Introduction

The model originally developed by Reichenbach et al. (2007) has been used extensively in literature to investigate spatial interactions, with many other researchers amending it (see Section 2.1.3). However, this model uses a lattice, forcing the bacteria to align orthogonally and thereby limiting the degrees of freedom to arrange themselves. This dissimilarity between the real and modelled world becomes clear by visually comparing a simulated spatial microbial distribution with a microscopic image of a microbial culture (Figure 3.1).

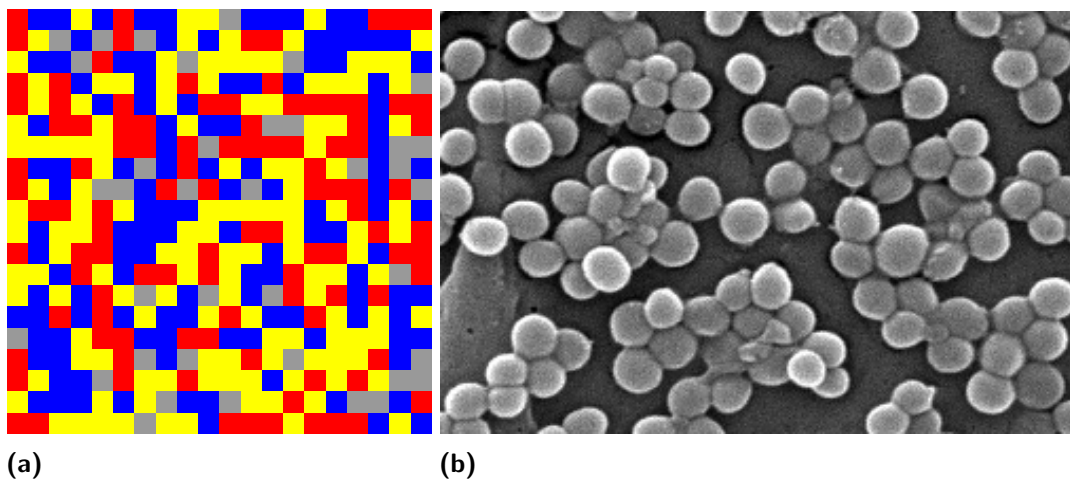


Figure 3.1: Comparison of a microbial community modelled on a lattice according to Reichenbach et al. (2007) (a) and an *in vivo* community viewed through an electron microscope (b).

To mimic the microbial world in a more realistic manner, we will construct a model allowing the bacteria to position themselves in continuous space. We will compare the dynamics of the lattice-based benchmark model used by Reichenbach et al. (2007) (Section 3.2) to this lattice-free model (Section 3.3).

3.2 Lattice-based benchmark model

May and Leonard (1975) proposed an intransitive interaction scheme, with three species, A, B, and C, performing actions according to a set of game theoretical rules. A bacterium can reproduce with rate μ if an empty space is available in its neighbourhood, and can compete with rate σ , following intransitive relations. Reichenbach et al. (2007) extended this model by allowing mobility. A bacterium can switch position with its neighbour with rate ϵ . The model interactions can be summarised by

$$\left\{ \begin{array}{l} A\emptyset \xrightarrow{\mu} AA \\ B\emptyset \xrightarrow{\mu} BB \\ C\emptyset \xrightarrow{\mu} CC \end{array} \right. , \quad \left\{ \begin{array}{l} AB \xrightarrow{\sigma} A\emptyset \\ BC \xrightarrow{\sigma} B\emptyset \\ CA \xrightarrow{\sigma} C\emptyset \end{array} \right. , \quad \left\{ \begin{array}{l} A\emptyset \xrightarrow{\epsilon} \emptyset A \\ B\emptyset \xrightarrow{\epsilon} \emptyset B \\ C\emptyset \xrightarrow{\epsilon} \emptyset C \end{array} \right. , \quad (3.1)$$

where \emptyset is an empty space. This game theoretical framework can be implemented in a spatially explicit IBM, where interactions take place on a two-dimensional lattice. Each lattice cell is either occupied by one of the three species, or is empty. The model defines the neighbourhood of a cell as the so-called von Neumann neighbourhood, i.e., the four cells orthogonally surrounding the focal cell.

An algorithm designed by Gillespie (1976), originally intended to simulate chemical reactions, simulates the interactions between *in silico* bacteria. At each simulation step, the bacterium in one randomly chosen cell can perform one of the three basic interactions with a randomly chosen bacterium in its neighbourhood: reproduction, with probability $\mu/(\mu + \sigma + \epsilon)$; competition, with probability $\sigma/(\mu + \sigma + \epsilon)$; or movement, with probability $\epsilon/(\mu + \sigma + \epsilon)$. After performing one of these actions, the lattice is updated accordingly. One generation is defined as the number of steps needed so that each cell had the chance to interact on average once (Figure 3.2).

A reproduction event can occur when an individual finds itself next to an empty cell. A new individual of the same species fills this site. A competition event can happen between two individuals of different species, the outcome being determined by the intransitive competition scheme (Figure 2.2b). The defeated individual is discarded from the lattice, leaving an empty site. Mobility takes place between two individuals or an individual and an empty site, switching their positions. Figure 3.3 gives a visualisation of these interactions.

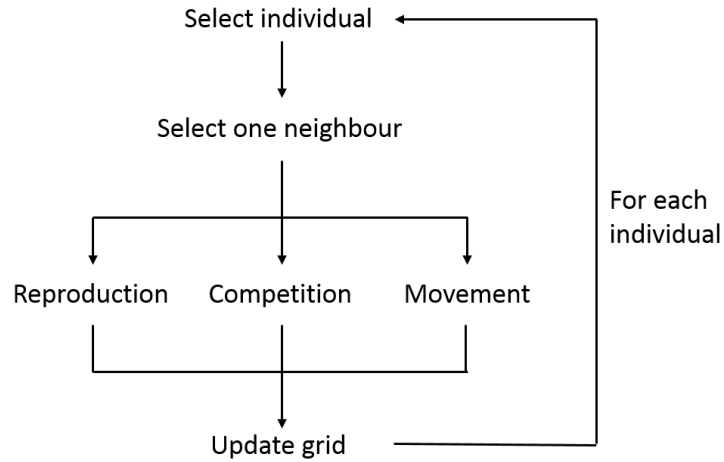


Figure 3.2: Flowchart outlining the processes making up one generation according to the algorithm by Gillespie (1976).

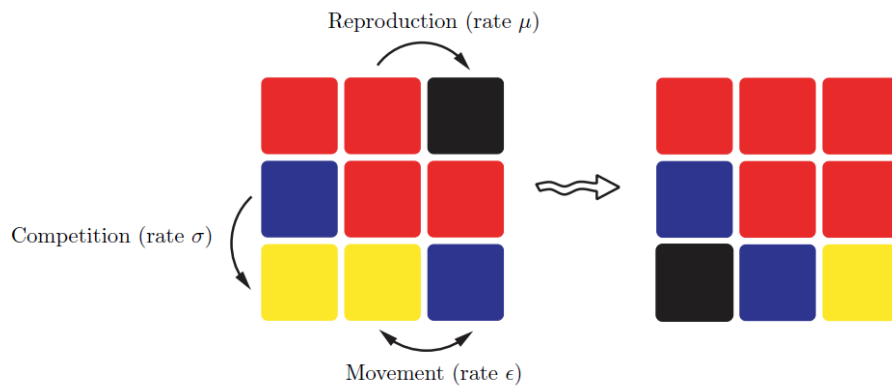


Figure 3.3: Visualisation of the three basic processes for three species (red, blue, and yellow) and empty sites (black) (adapted from Reichenbach et al. (2007)).

3.3 Lattice-free model

To assess the effect of continuous space on the maintenance of coexistence, we construct a model that resembles the benchmark model as closely as possible, except for the spatial component. The same game theoretical framework is implemented according to the Gillespie algorithm described in Section 3.2. However, the bacteria do not position themselves in lattice cells, but in continuous space. A circle of a certain radius centred at a certain point represents each bacterium. To resemble the size of the bacteria in the benchmark model as closely as possible, all bacteria are equally sized with radius 0.5 (i.e., half of a cell side in the lattice-based model).

3.3.1 Identifying neighbours

Since we cannot use the von Neumann neighbourhood, the lattice-free approach requires another definition. Consider a concentric circle around a focal individual with radius r_{int} . Each *in silico* bacterium with its centre in this circle is considered a neighbour of that focal individual (Figure 3.4a). In the special case of $r_{int} = 1$, only touching and overlapping bacteria are considered to be neighbours (Figure 3.4b).

The naive method of determining the neighbours of a given bacterium would be to calculate the Euclidean distance between that bacterium and every other, after which the ones within a distance smaller than r_{int} are selected. However, increasing the number of *in silico* bacteria n would not only increase the number of interactions in one generation, it would also increase the complexity of these interactions, because one interaction requires calculating the distance between a bacterium and n other bacteria. This naive approach is thus an $\mathcal{O}(n^2)$ algorithm, meaning that the computational load of the model scales quadratically with the number of individuals. To make the simulation of a large number of individuals practically feasible, we have optimised the model implementation by using two specialised data structures: cell lists and Verlet lists (Mattson and Rice, 1999; Heinz and Hunenberger, 2004).

To construct a cell list, the continuous space inhabited by the bacteria is divided into squares with side d_{cell} . Subsequently, an array is constructed representing this grid. For each bacterium, we check in which square it resides, and add its index to the corresponding place in the array. The resulting array is called a cell list (Figure 3.5). Note the differences in notation convention between a grid, with $(1,1)$ positioned on the bottom left, and an array, with $(1,1)$ positioned on the top left.

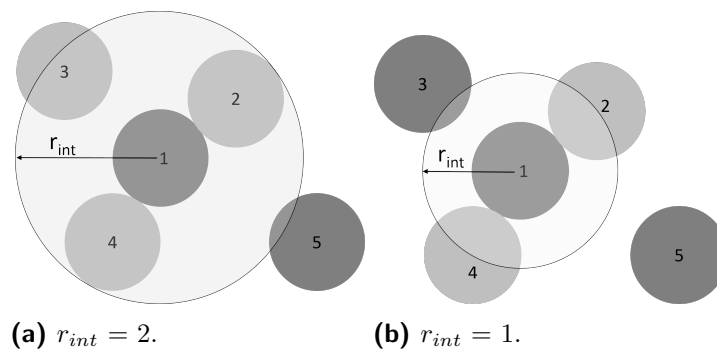


Figure 3.4: Definition of a neighbourhood with radius r_{int} where neighbouring cells of bacterium 1 are coloured light gray.

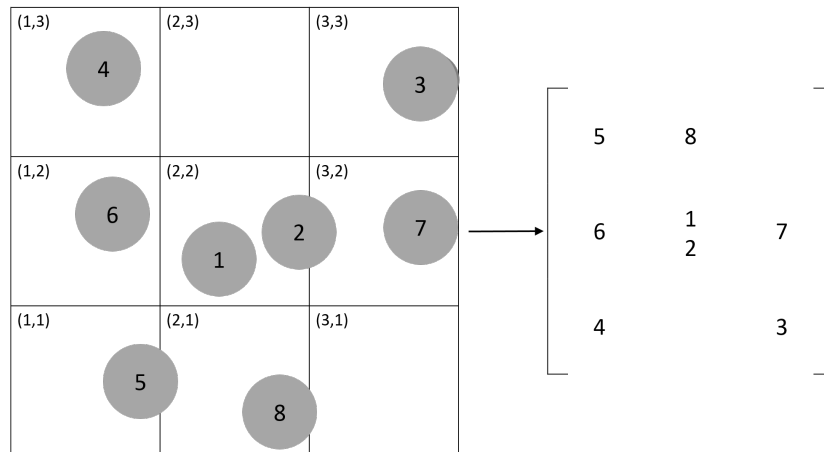


Figure 3.5: The construction of a cell list (from grid to array).

When we choose $r_{int} \leq d_{cell}$, the neighbours of a given focal bacterium can only reside in the eight neighbouring cells of the grid cell where the bacterium resides in (Figure 3.6a). This holds even in the limit case, where $r_{int} = d_{cell}$ and the bacterium resides in the corner of its grid cell (Figure 3.6b). One can now use the cell list to look up the indices of the bacteria that are in the eight surrounding cells, and are thus possibly within r_{int} of the focal bacterium. By calculating the distances between these bacteria and the focal bacterium, it is possible to efficiently determine its neighbours. The use of a cell list thus significantly reduces the number of distances that need to be calculated to determine the neighbours of a given bacterium. A smaller d_{cell} decreases the number of possible neighbours, but increases the size of the cell list.

It is possible to further improve the efficiency of the model implementation using Verlet lists (Verlet, 1967). Instead of determining the neighbours of a bacterium at each interaction, it is more efficient to determine them only once, save this information and update it when needed. By doing this, we obtain a Verlet list, containing the indices of the neighbours of each bacterium (Figure 3.7 and Table 3.1). Since, by definition, neighbourhoods are symmetric, each bacterium should occur in the entries of each of their neighbours. E.g. bacterium 8 is a neighbour of bacterium 5, and the Verlet (Table 3.1) list correctly shows that bacterium 5 is a neighbour of bacterium 8. This property can be used to check the validity of a Verlet list.

When the neighbours of a given bacterium need to be identified, one can now simply look up this information in the Verlet list. Therefore, increasing the number of simulated individuals does not increase the complexity of finding its neighbours. This algorithm is theoretically $\mathcal{O}(n)$, meaning that the computational load is linearly related to the number of bacteria.

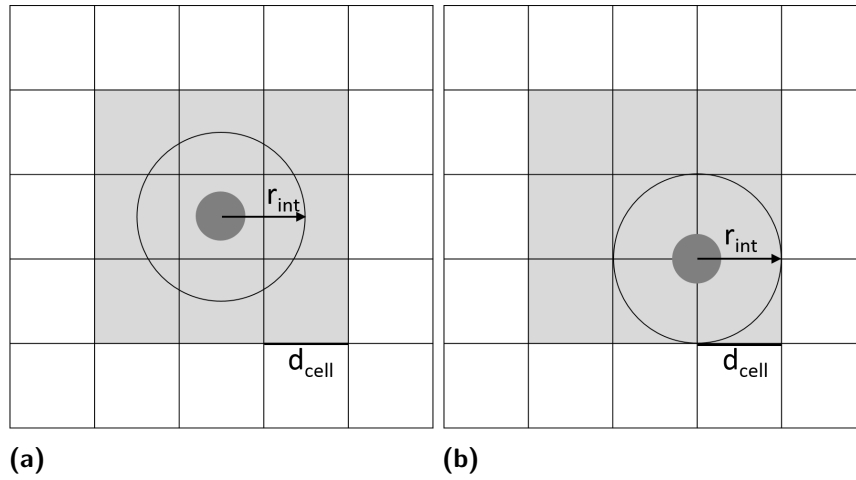


Figure 3.6: When $r_{int} \leq d_{cell}$, only bacteria in the grey cells can possibly be a neighbour.

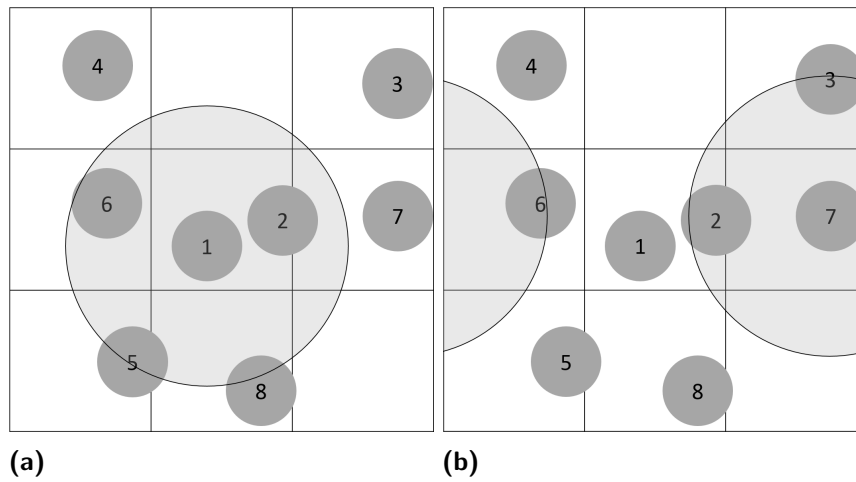


Figure 3.7: Visualisation of bacteria within r_{int} for focal bacterium: bacterium 1 (a) and bacterium 7 (b).

Table 3.1: The Verlet list constructed from the example in Figure 3.7.

Focal bacterium	Neighbours
1	2, 5, 6
2	1, 7
3	4, 7
4	3, 6
5	1, 8
6	1, 4, 7
7	2, 3, 6
8	5

At the start of each generation, a cell list is constructed, from which a Verlet list is derived. When bacteria perform interactions, their neighbours might change, implying that the Verlet list needs to be updated accordingly, as not only its own entry should be changed, but also the entries of its former neighbours.

3.3.2 Local interactions

Similar to the benchmark model, three basic interactions occur in the lattice-free model. The Gillespie algorithm, as described in Section 3.2, simulates these interactions. In the benchmark model, reproduction can occur when an empty site is available. The notion of empty spots is not defined in the lattice-free model, reproduction can therefore occur when the neighbourhood of a bacterium is not fully populated. The neighbourhood of a bacterium is considered fully populated when the bacterium has six or more neighbours (Figure 3.8). A bacterium at (x, y) splits into two equally-sized slightly-overlapping daughter bacteria positioned at

$$\begin{aligned} &\left(x + r \frac{\cos(\theta)}{2}, y + r \frac{\sin(\theta)}{2}\right), \\ &\left(x - r \frac{\cos(\theta)}{2}, y - r \frac{\sin(\theta)}{2}\right), \end{aligned} \quad (3.2)$$

where θ is a randomly chosen angle between $[0, \pi]$, and r the radius of the bacterium. The Verlet list is updated accordingly.

A competition event can happen between two individuals of different species, the outcome being determined by the intransitive competition scheme. The defeated individual is removed from the community and the Verlet list is updated accordingly. Movement takes place between two individuals, switching their positions. Again, the Verlet list is updated correspondingly. Figure 3.9 gives a summary of these interactions.

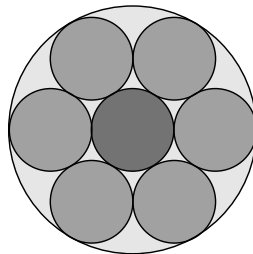


Figure 3.8: A fully populated neighbourhood of a bacterium contains six bacteria.

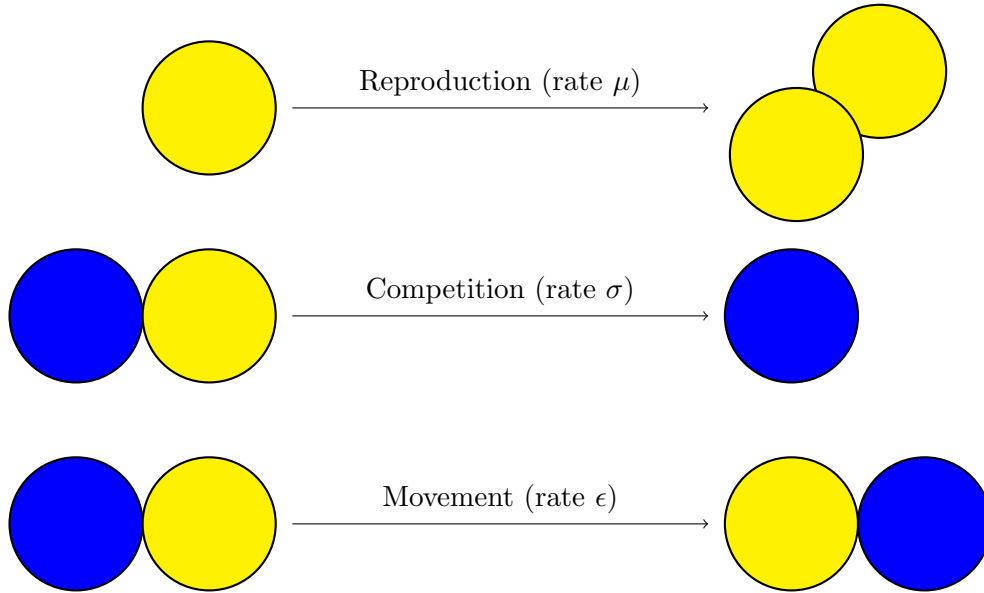


Figure 3.9: Visualisation of the three simulated demographic processes.

3.3.3 Overlap avoidance

As described above, reproduction gives rise to two overlapping bacteria. Furthermore, it is possible that the resulting bacteria are overlapping with their surrounding bacteria. Since space can only be occupied by one *in vivo* bacterium (Figure 3.1b), and spatial dynamics are key to these models (see Section 2.1.3), it is mandatory that *in silico* bacteria do not overlap. To achieve this, the model incorporates a repulsive force between overlapping bacteria.

In vivo bacteria are deformable (Arnoldi et al., 1998), we can thus model them as soft bodies. The repulsion between two soft bodies is given by (Landau and Lifshitz, 1986)

$$\mathbf{F}_{ij} = \begin{cases} \alpha \left(1 - \frac{d_{ij}}{r_i + r_j}\right)^{\frac{5}{2}} \mathbf{r}_{ij}, & \text{if } d_{ij} < r_i + r_j, \\ \mathbf{0} & \text{, otherwise,} \end{cases} \quad (3.3)$$

where \mathbf{F}_{ij} is the resulting repulsive force on bacterium i induced by bacterium j , α a weight, d_{ij} the distance between the centres of the bacteria, r_i and r_j the radii of bacteria i and j , \mathbf{r}_{ij} the vector defined by the centres of the two bacteria, pointing outwards from the centre of bacterium i (Figure 3.10a), and $\mathbf{0}$ the zero vector.

Figure 3.10b shows a plot of \mathbf{F}_{ij} for $r_i = r_j = 0.5$ and $\alpha = 5$. One can see that a large overlap, i.e., small d_{ij} , induces a greater repulsion than a smaller overlap, i.e., larger d_{ij} . No overlap, i.e., $d_{ij} \geq 1$, induces no repulsion.

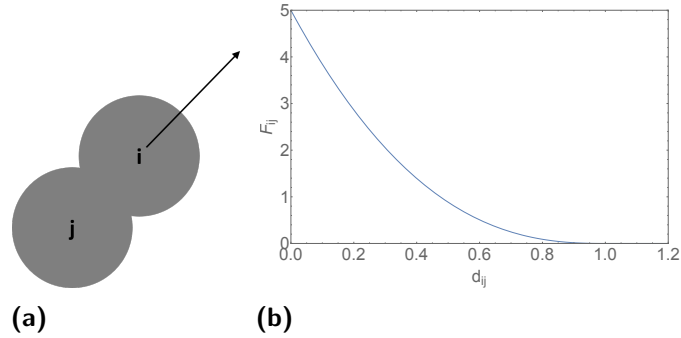


Figure 3.10: Direction (a) and magnitude (b) of the repulsive force \mathbf{F}_{ij} for $r_i = r_j = 0.5$ and $\alpha = 5$.

When multiple bacteria overlap with a given bacterium, vector addition of the individual forces applies. Each generation, the model calculates the repulsive force for all bacteria, changing their positions. *In vivo* elastic bacteria can cave into each other, small overlaps are therefore allowed (Touhami et al., 2003). Iterations are executed until a predefined minimal d_{ij} is obtained. Provided that fewer bacteria are present than can pack into space, this procedure will avoid overlapping bacteria.

Combining all these procedures, Figure 3.11 shows a flowchart summarizing the steps taken during one generation. Since this model is purely theoretical and not calibrated to a real microbial system, we choose to omit any units, as is conventional in literature. However, the dimensions of the variables and parameters are consistent throughout the model. One can therefore easily introduce units during a calibration effort.

3.4 Experimental setup

General setup

All simulations were initialized and executed in the same way, except when noted otherwise. The 100×100 space was randomly and evenly seeded with individuals of the three species with radius 0.5. Periodic boundary conditions were imposed to avoid boundary effects. The reproduction rate μ and competition rate σ were set at one. The interaction distance r_{int} was set at one, meaning that only touching and overlapping bacteria were considered neighbours. The side length of a grid cell d_{cell} was set at one, thus satisfying $r_{int} \leq d_{cell}$. The repulsion subroutine was iterated with α set at five until the minimal d_{ij} between any two bacteria was 0.95, which we consider a realistically small overlap.

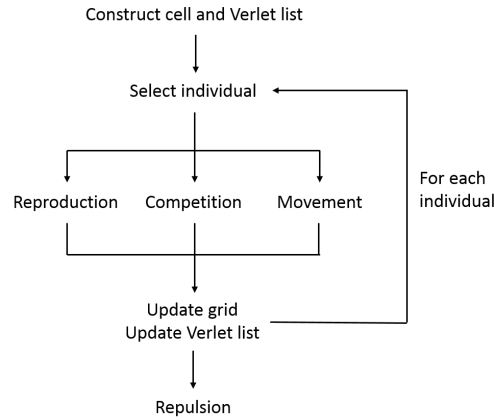


Figure 3.11: Flowchart outlining the processes making up one generation according to the algorithm by Gillespie (1976).

Each 100 generations, the spatial structure was exported. The number of individuals of each species was recorded at the end of each generation, allowing us to calculate the evolution of the species density through time. The probability of extinction P_{ext} can be calculated as the fraction of simulations with at least one extinction event.

Moreover, the evenness of the system was calculated by the Gini coefficient (Rousseau and Van Hecke, 1999). The Gini coefficient is based on Lorenz curves, plotting the cumulative proportion of species against the cumulative proportion of individuals. The index ranges from zero (perfect inequality) to 1 (perfect equality) according to

$$G(\mathbf{p}) = \frac{2}{s-1} \left(s - \frac{\sum_{i=1}^s i p_i}{\sum_{i=1}^s p_i} \right), \quad (3.4)$$

where s is the number of species in the community and p_i is the relative abundance of the species i , sorted such that $p_i < p_{i+1}$. Lastly, the patchiness is calculated as the average fraction of neighbours of the same species. A high patchiness suggest spatial structures, whereas a low patchiness suggests dispersed individuals. A patchiness of 1 suggests a monoculture.

The model was implemented in Mathematica (Version 11.0.1, Wolfram Research Inc., Champaign, USA). Simulations were carried out on the UGent High-Performance Computer (HPC). The VSC (Flemish Supercomputer Center), funded by Ghent University, the Hercules Foundation, and the Flemish Government (department EWI), provided these computational resources (Stevin Supercomputer Infrastructure).

Model efficiency

To investigate the efficiency of the Verlet list encoding, a 20×20 , 40×40 , 60×60 , 80×80 , and 100×100 space were considered. For each size, we carried out ten simulations and recorded their execution times.

Lattice-free versus lattice-based models

To investigate the influence of the mobility rate ϵ in the lattice-free model, ϵ was varied between 1 and 80, while all other parameters were kept constant. We computed 10 000 generations, with 50 simulations for each value of mobility rate ϵ .

For the benchmark lattice-based model, a 100×100 lattice was initialised with 10% empty cells and the remaining cells evenly distributed among the three species. The mobility rate ϵ was varied between 1 and 80. We ran the Gillespie algorithm (Figure 3.2) for 10 000 generations, with 50 simulations for each value of the mobility rate ϵ .

Interaction range

To investigate the influence of the interaction range r_{int} , this parameter was varied between 1 and 1.5. For that purpose, the mobility rate ϵ was set at 30. We simulated 10 000 generations, with 50 simulations for each value for r_{int} .

3.5 Results and discussion

3.5.1 Model efficiency

Figure 3.12 displays the number of simulated individuals versus execution time. The bacteria tend to fully pack the space, therefore approximately L^2 bacteria are present. The curve shows a quasi-linear relationship. The slight deviation from linearity is due to the computational overhead associated with larger sizes. As a result of this linear relationship between the number of simulated individuals and the execution time, increasing the simulation size is feasible without inflating the computational demand. However, the lattice-free models poses a significantly higher computational load, with an execution time of approximately 9 hours for 1000 generations, compared to 30 minutes for the lattice-based model.

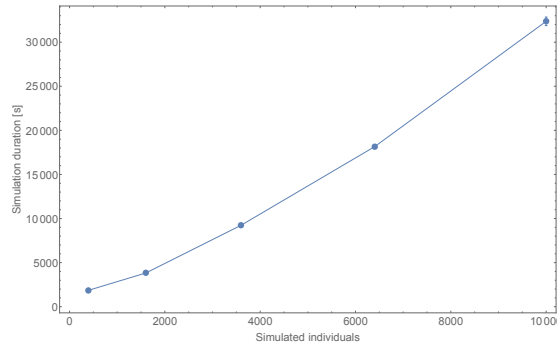


Figure 3.12: Execution time for 1000 generations in function of the number of simulated individuals, averaged over 10 simulations.

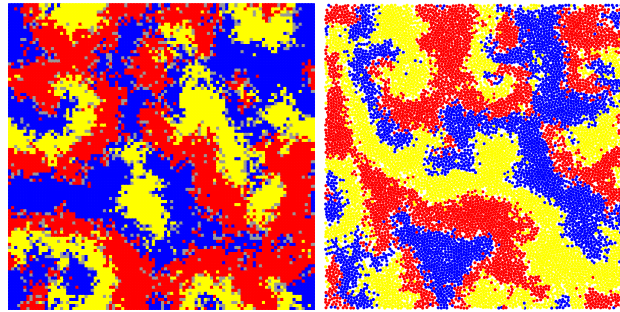
3.5.2 Lattice-free versus lattice-based models

General observations

Figure 3.13 shows an example of spatial dynamics arising using both approaches. Both models show the same qualitative behaviour, with the bacteria arranging themselves in spatial structures of approximately the same size, thereby facilitating coexistence.

Figure 3.14 shows the extinction probability P_{ext} as a function of mobility rate ϵ for both approaches. For both models, we can see a qualitative behaviour similar to the findings of (Reichenbach et al., 2007), with a higher probability of extinction P_{ext} for higher values of mobility rate ϵ . The extinction probability P_{ext} for the lattice-based model is consistently higher than for the lattice-free model. For the lattice-based benchmark model, the transition from stable coexistence ($P_{ext} = 0$) to extinction ($P_{ext} = 1$) sharpens at the critical mobility rate $\epsilon = 25 \pm 5$. For the lattice-free model, this happens at critical mobility rate $\epsilon = 65 \pm 5$. This means that the lattice-free model can maintain coexistence at a higher mobility than the lattice-based model, and can thus be considered more robust.

Figure 3.15 plots the average final evenness in function of mobility ϵ for both approaches. The final average evenness decreases with increased mobility rate ϵ , but it is consistently higher for the lattice-free model. Increasing the mobility increases the size of the spirals, leading to more uneven communities. Furthermore, by increasing the extinction probability P_{ext} , ecosystems with one remaining species (i.e., Gini coefficient of 0) occur more often, further lowering the average Gini coefficient. Once the critical mobility rate is exceeded, the average Gini coefficient drops to zero.



(a) Lattice-based model. (b) Lattice-free model.

Figure 3.13: Example of the spatial dynamics arising for both models with $\epsilon = 1$.

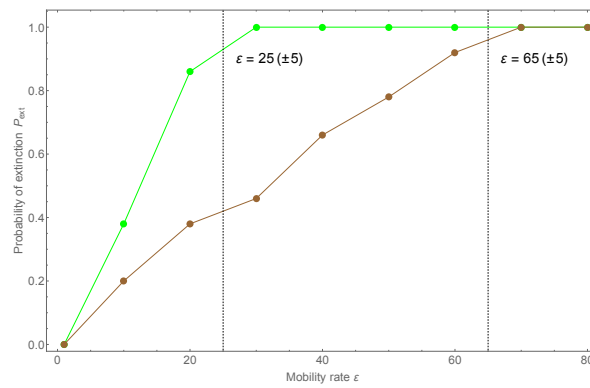


Figure 3.14: Extinction probability P_{ext} (50 simulations, 10 000 generations) versus mobility rate ϵ for the lattice-based (green) and lattice-free model (brown).

Spatial dynamics

In order to have a better insight into the spatial dynamics and their effect on coexistence, representative temporal evolutions are visualised for both models for four different mobility rates: $\epsilon = 1$, far below the critical mobility rate for both models (Figure 3.16); $\epsilon = 10$, below the critical mobility rate for both models (Figure 3.17); $\epsilon = 30$, above the critical mobility rate for the lattice-based model but below that for the lattice-free model (Figure 3.18); and $\epsilon = 70$, above the critical mobility rate for both models (Figure 3.19).

For each simulation, three plots are displayed. The plots at the left side show the temporal evolution of the species densities. The plots in the middle show a projection of the evolution on a simplex plot. When the density of a species is higher, the resulting point on the simplex is closer to the corresponding vertex. When one species goes extinct, the trajectory has reached the edge opposite of the vertex of the extinct species, from where it will follow the edge towards one of the vertices, indicating a second extinction event. The plots on the right visualise the spatial dynamics. Additionally, Appendix A gives the evenness and patchiness through time.

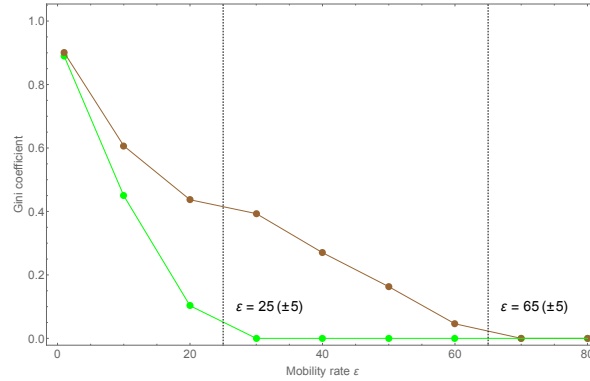


Figure 3.15: Final average Gini coefficient (50 simulations, 10 000 generations) in function of mobility rate ϵ for the lattice-based model (green) and lattice-free model (brown).

Figure 3.16 shows a representative evolution of a community with mobility rate $\epsilon = 1$, far below the critical mobility rate of both models (Figure 3.14). For both models, the densities of the three species oscillate with a small amplitude and high frequency around the equilibrium density of 0.33. The trajectories on the simplex are situated in the centre of the triangle, far away from the edges, indicating coexistence. Besides, we see spatial patterns of approximately the same size, thereby facilitating coexistence, regardless of the model. Figures A.1a and A.1b show the same patchiness and evenness for both systems.

Figure 3.17 shows a representative evolution of a community with mobility rate $\epsilon = 10$, still below the critical mobility rate of both models (Figure 3.14). The densities of the species in both models oscillate with a higher amplitude and lower frequency than at $\epsilon = 1$ (Figure 3.16). This is also visible from the simplex trajectory, which is less concentrated around the centre than at $\epsilon = 1$. Therefore, the probability that the trajectory reaches an edge and an extinction event occurs is higher than at lower mobility, as is visible in Figure 3.14. Again, we see the emergence of spiral patterns of approximately the same size for both models, but larger than at $\epsilon = 1$, explaining the higher P_{ext} .

However, the population densities obtained with the lattice-based model oscillate more regularly compared to those in the lattice-free model. This is visible from the simplex trajectory, which repeatedly follows the same path and rarely returns to the equilibrium. In contrast, the densities attained with the lattice-free model oscillates less regularly, the amplitude varies much more. The populations stay closer to the equilibrium. This is visible from the simplex trajectory, which is less regular and reverts back to the centre from time to time. Figures A.1c and A.1d show the same patchiness, although the evenness of the lattice-based system is lower.

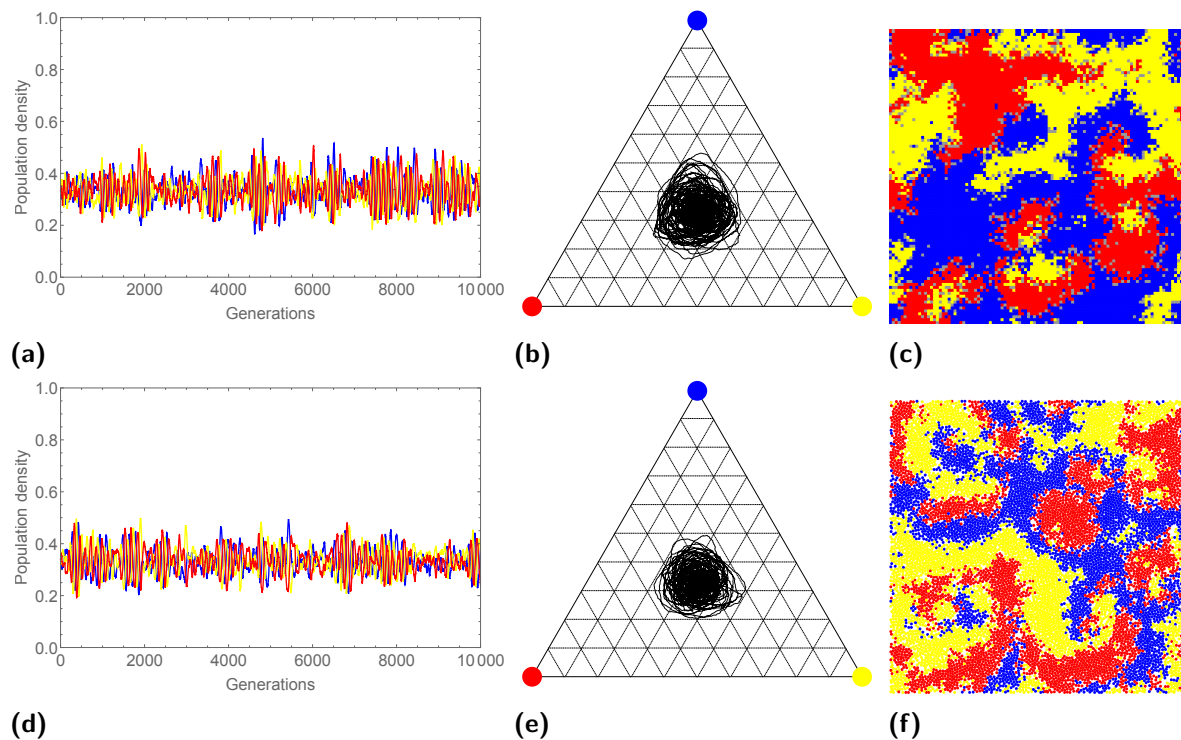


Figure 3.16: The population density plotted through time (a and d) and as a trajectory on a simplex (b and e), and the spatial configuration after 10 000 generations (c and f) for $\epsilon = 1$, for a representative evolution of the lattice-based (a-c) and lattice-free model (d-f).

Figure 3.18 shows a representative evolution of a community with mobility rate $\epsilon = 30$, still below the critical mobility rate for the lattice-free model, but above that for the lattice-based model (Figure 3.14). Therefore, it is inevitable that the community goes extinct in the lattice-based model, as can be seen in Figure 3.18a. On the simplex plot, we see a rapid approach towards one of the edges, with the trajectory ending at the vertex of the yellow species. Figure A.1f shows an evenness converging towards zero, and a patchiness going towards one, representing a monoculture.

When we take a look at a representative simulation result obtained with the lattice-free model, specifically selected for maintenance of coexistence, we see that the densities oscillate with a higher amplitude and lower frequency than at lower mobility, albeit still irregularly. Some highly uneven communities emerge over time, but the ecosystem is able to recover and maintain coexistence. In space, large diffuse spirals can be seen.

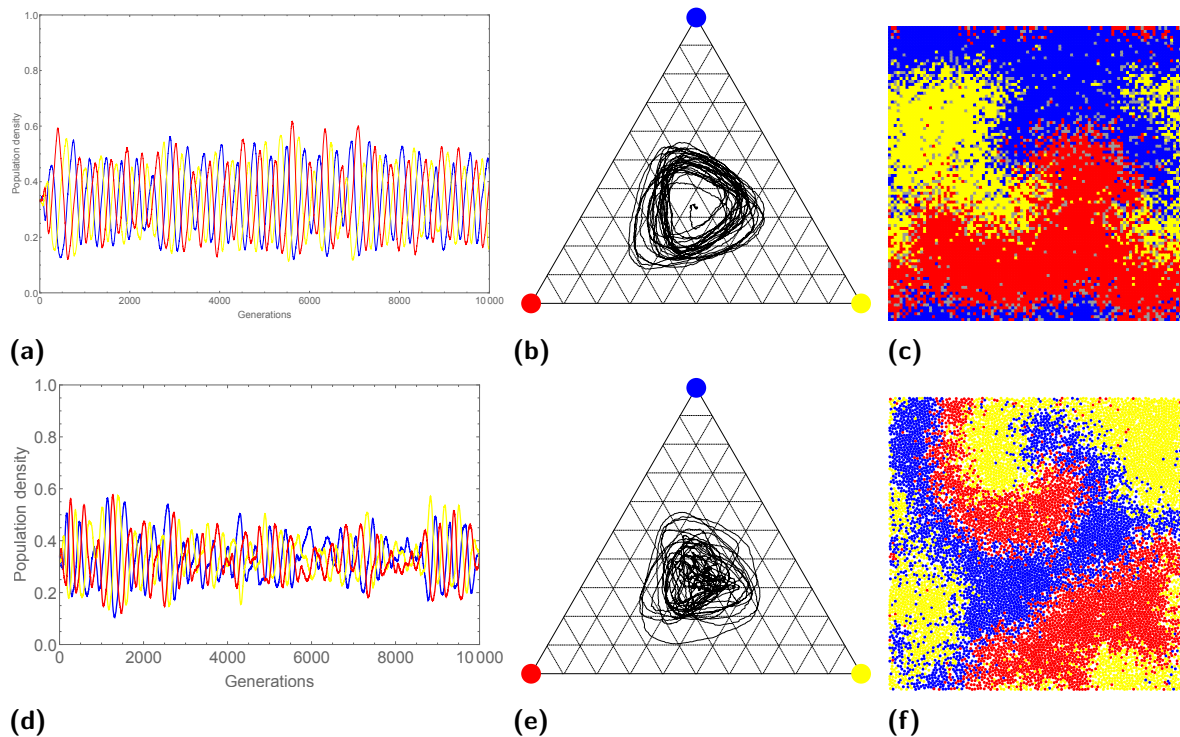


Figure 3.17: The population density plotted through time (a and d) and as a trajectory on a simplex (b and e), and the spatial configuration after 10 000 generations (c and f) for $\epsilon = 10$, for a representative evolution of the lattice-based (a-c) and lattice-free model (d-f).

Figure 3.19 shows a representative evolution of a community with mobility rate $\epsilon = 70$, well above the critical mobility rate of both models (Figure 3.14). Both evolve quickly towards a first extinction event, with a second one following soon. The lattice-free model maintains coexistence slightly longer, but the ultimate fate of both is the same.

Remarks on the critical mobility rate

To acquire a deeper understanding of the dissimilarity in critical mobility rate between the two approaches, it is important to understand the differences between the lattice-based and lattice-free models, and their effect on the maintenance of coexistence.

First, an empty cell in the lattice-based model can be chosen to take part in an interaction event. In contrast, empty areas in the lattice-free model cannot be chosen to take part in an interaction event. A bacterium can thus only compete or switch places with another bacterium. This implies that bacteria in the lattice-free approach cannot move into empty space. However, empty space still influences the reproduction mechanism, since reproduction only occurs when the neighbourhood of the bacteria is not overpopulated, and there is thus enough empty space.

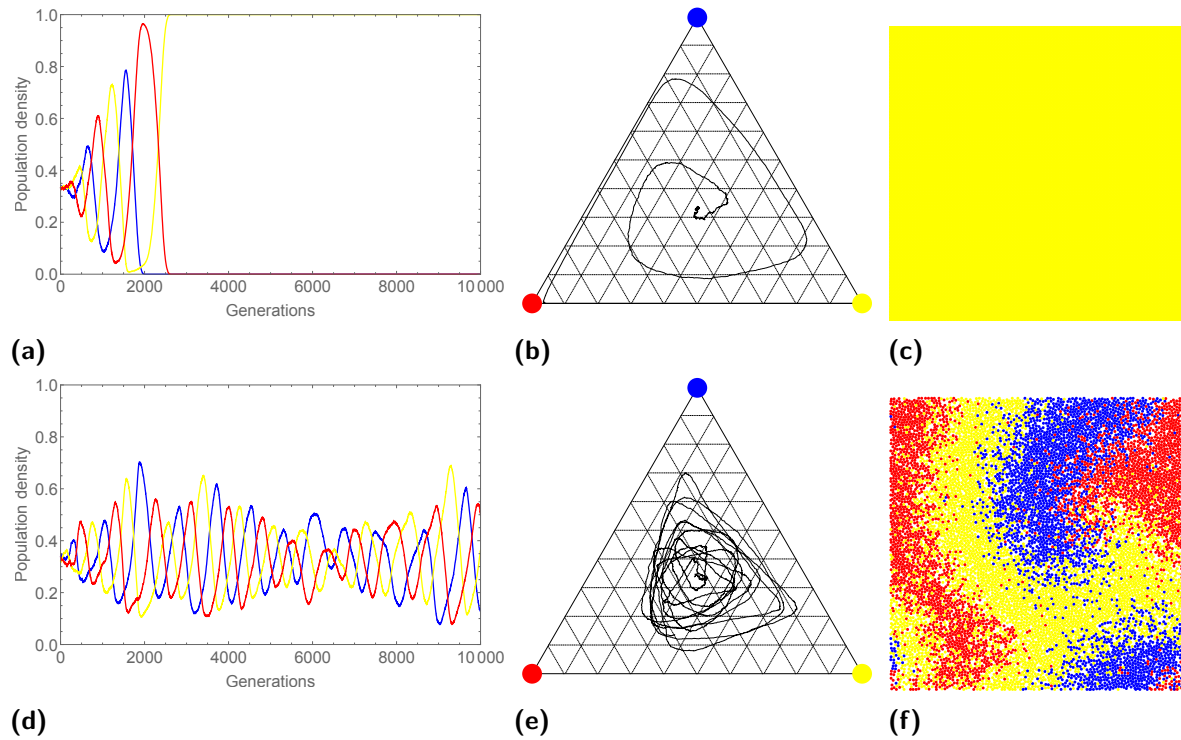


Figure 3.18: The population density plotted through time (a and d) and as a trajectory on a simplex (b and e), and the spatial configuration after 10 000 generations (c and f) for $\epsilon = 30$, for a representative evolution of the lattice-based (a-c) and lattice-free model (d-f).

Secondly, a generation in the lattice-based model consists of a fixed number of interaction attempts (i.e., the number of lattice cells L^2). However, a generation in the lattice-free model consists of a variable number of interactions (i.e., equal to the number of species at the start of the generation), and can thus be longer or shorter. However, the simulations show that the bacteria tend to tightly pack the whole space, with around L^2 bacteria present, making this difference negligible.

Furthermore, each bacterium has exactly four neighbours in the lattice-based model. On the other hand, the bacteria in the lattice-free model have a variable number of neighbours. Abrudan et al. (2016) found that a model where bacteria can interact with six neighbours maintains coexistence better than with eight neighbours, since the interactions are less local in the latter case. In a fully packed continuous space, bacteria have six neighbours. The higher number of neighbours suggests a reduced ability to maintain coexistence compared to the lattice-based model with four neighbours, due to the interactions being slightly less localised.

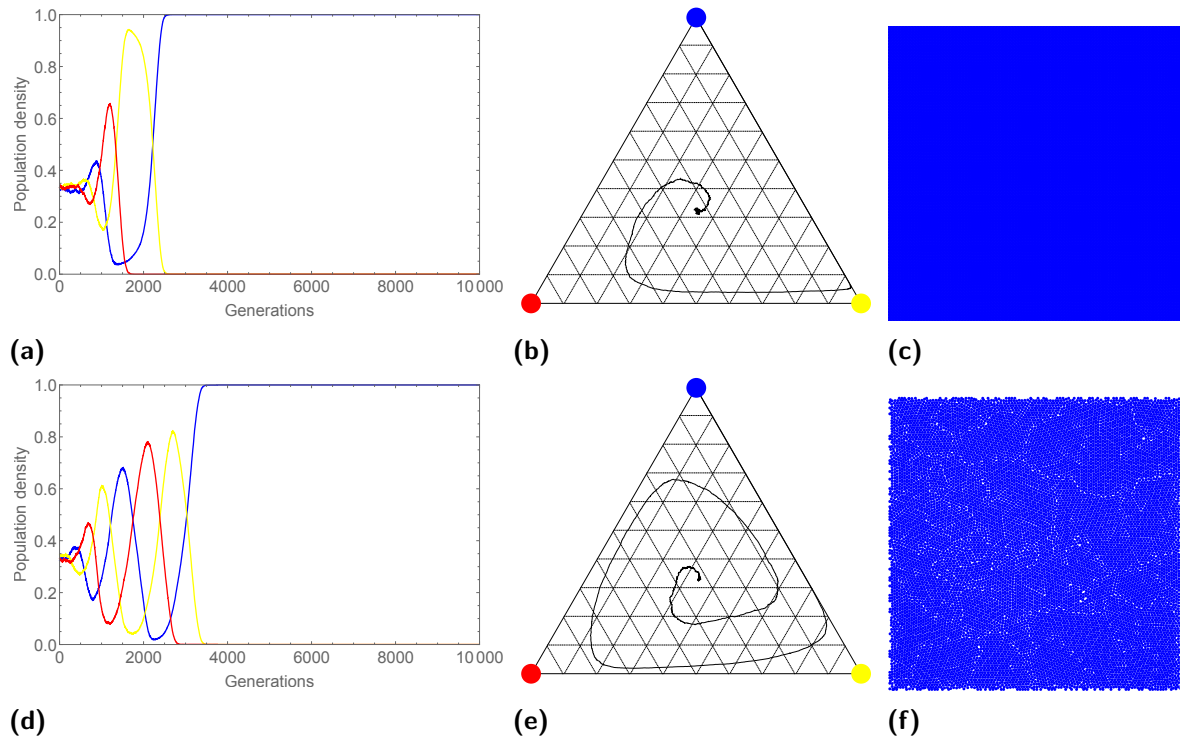


Figure 3.19: The population density plotted through time (a and d) and as a trajectory on a simplex (b and e), and the spatial configuration after 10 000 generations (c and f) for $\epsilon = 70$, for a representative evolution of the lattice-based (a-c) and lattice-free model (d-f).

Additionally, the overlap avoidance mechanism used in the lattice-free approach adds extra movement to the system. More specifically, reproduction increases the mobility by producing overlapping bacteria, which then repulse each other. This suggests a lower ability to maintain coexistence, due to the increased mobility further reducing the localisation of interactions.

Lastly, the lattice-free approach permits more freedom for the bacteria to position themselves, influencing the formation of the spatial structures. At the same mobility rate, the structures tend to be of the same size in both models (Figure 3.13). The structures in the lattice-based model outgrow the system size when the mobility rate ϵ increases, raising the chance of extinction events. In the lattice-free model, the structures also grow with higher mobility rates, but the communities tend to be less prone to extinction compared to the lattice-based model.

Nearly extinct species often retreat in refuges, a small spatial structure encompassing the last remaining individuals (Laird and Schamp, 2008). Closer inspection of the results reveals that these refuges tend to be more resilient in the lattice-free model, due to the more degrees of freedom available to arrange themselves, thereby decreasing the extinction probability.

It seems that this last difference has a decisive influence on the ability to maintain coexistence in the lattice-free model. The increased spatial degrees of freedom makes spatial refuges more robust by allowing them to optimise their spatial structure, as such increasing their chances of survival. Uneven communities that would go extinct in lattice-based models, can maintain coexistence in the lattice-free model. This reflects the composition of real microbial ecosystems, which are uneven and dynamic in time, and are typically dominated by a few species and many other species are present in small numbers (Wilsey, 2004; Ashby et al., 2007). We can thus conclude that, by constraining the bacteria in a lattice, the lattice-based model tends to underestimate the ability to maintain coexistence, compared to the more realistic lattice-free approach.

However, this more realistic approach comes at a computational cost, and this cost needs to be balanced against its benefits. The qualitative behaviour of both models is the same (i.e., emergence of spatial structures, which is key to the maintenance of coexistence), but the quantitative behaviour is different (i.e., different P_{ext}). It can therefore be justified to keep using the lattice-based models, as long as one is merely interested in the qualitative behaviour. The use of a lattice-free model is recommended once quantitative behaviour becomes important, e.g. calibration of the model to a real world microbial community (see Section 6.2). Moreover, when incorporating specific behaviour, e.g. specific movement (see Chapter 4) or volume-dependent growth (see Chapter 5), which is impossible in lattice-based models, the use of lattice-free models is a prerequisite.

3.5.3 Interaction range

Figure 3.20 gives the probability of extinction P_{ext} versus the interaction range r_{int} at a fixed mobility $\epsilon = 30$. One can see that a higher r_{int} increases the extinction probability P_{ext} .

A larger interaction range r_{int} means that bacteria have more neighbours to interact with, making the interactions less localised. This agrees with Abrudan et al. (2016), who found that a higher number of neighbours increases the probability of extinction. Laird (2014) found similar dynamics in small-world networks, where individuals can interact with others who are not positioned directly next to them. Furthermore, a larger interaction range allows bacteria to switch places with bacteria positioned further away, thereby increasing their mobility, and thus increasing the probability of extinction P_{ext} .

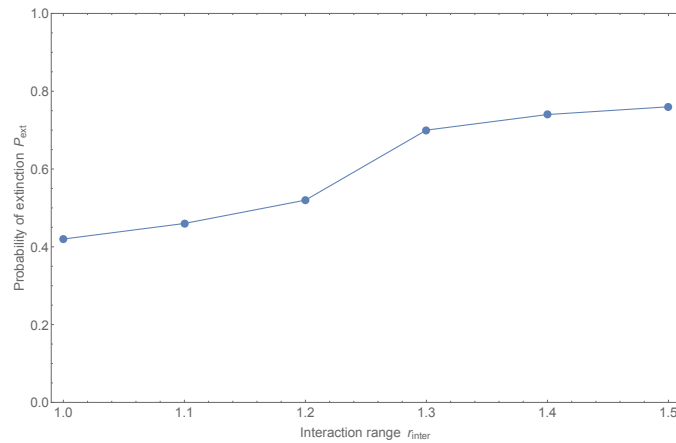


Figure 3.20: Extinction probability P_{ext} (50 simulations, 10 000 generations) as a function of the interaction rate r_{int} at $\epsilon = 30$.

3.6 Conclusion

A lattice-free model has been constructed and compared to a lattice-based model. We found that the former maintains coexistence better, as shown by a higher critical mobility rate. Both models show the same qualitative behaviour, with spatial structures allowing coexistence. However, having more spatial freedom, the structures in the lattice-free model tend to be more robust. Small spatial refuges that would go extinct in the lattice-based model, can survive, thereby maintaining coexistence. However, the increased realism comes at a computational cost, one thus needs to consider whether the advantages are worth the cost. Furthermore, the effect of the interaction range has been investigated. A larger interaction range diminishes the localisation of interactions, thereby increasing the probability of extinction. We can conclude that the lattice-free approach is more realistic and allows us to retrieve behaviour not seen with lattice-based models.

CHAPTER 4

Continuous mobility

4.1 Introduction

As Adamson and Morozov (2012) remarked, the mobility of species implemented in the model by Reichenbach et al. (2007) does not resemble the real movement of species. In this model, an individual can only move by switching places with one of its neighbours. Although this is the only possibility to include mobility in a lattice-based model, it is a very unconventional way of movement from a biological perspective. Since the model described in Section 3.3 is lattice-free, a more realistic movement mechanism will be implemented in Section 4.2.

Certain species exhibit motile behaviour, the ability to move deliberately and actively. This should not be confused with mobility, which simply describes the ability to be moved. In Section 4.3, we will extend the model to allow for chasing predators and escaping prey, two forms of motile behaviour. Whereas this is difficult to implement properly in a lattice-based model, the lattice-free model with an improved movement can easily be extended with motility.

4.2 Adapted movement mechanics

We use the model described in Section 3.3, but adapt the underlying movement mechanism. Instead of switching places with one's neighbour, a bacterium positioned at (x, y) moves a random distance in space, according to

$$(x, y) \xrightarrow{\epsilon} (x + d_x, y + d_y) , \quad (4.1)$$

with d_x and d_y independently and randomly chosen from $[-d_{max}, d_{max}]$, where d_{max} is the maximal distance a bacterium can move in the x - or y -direction during one time step.

Note that two parameters, the mobility rate ϵ and the maximal distance d_{max} , influence the mobility of the individuals. However, from a macroscopic perspective, moving a small distance at a high rate results in the same mobility as moving a large distance at a small rate. Both parameters are thus linked by mobility M . Reichenbach et al. (2007) defines mobility M as the typical proportional area explored by one mobile individual per time unit. In his lattice-based model, with two bacteria taking part in a movement interaction, this is proportional to $M \propto 2\epsilon N^{-1}$, with $N = L^2$ the area of the system. In the lattice-free model with adapted movement, the expected Euclidean distance travelled during one movement action equals $0.76 d_{max}$, as derived in Appendix B. Taking a circle as the typical region explored per time unit, mobility can be redefined as being proportional to $M \propto \epsilon (0.76 d_{max})^2 \pi N^{-1}$ or, after neglecting the constants, $M \propto \epsilon d_{max}^2 N^{-1}$.

4.3 Chasing predators and escaping preys

It is known that certain bacteria use motility to tip the competitive balance in their favour (Hibbing et al., 2010). Both *Bdellovibrio bacteriovorus* and *Myxococcus xanthus* have been shown to chase their preys (Flannagan et al., 2004), whereas *Agrobacterium tumefaciens* actively escapes its dominant competitor *Pseudomonas aeruginosa* (An et al., 2006).

To simulate motility, we introduce the following mechanism. A bacterium chasing its prey experiences an attraction force according to

$$\mathbf{F}_i = \beta \sum_{j=1}^n \begin{cases} \frac{\mathbf{r}_{ij}}{d_{ij}^2}, & \text{if } i \text{ is a predator of } j, \\ \mathbf{0} & , \text{ if } i \text{ is not a predator of } j, \end{cases} \quad (4.2)$$

where \mathbf{F}_i is the attraction force experienced by bacterium i towards n bacterium j in its neighbourhood, β a weight factor, \mathbf{r}_{ij} the vector pointing from the centre of bacterium i towards the centre of bacterium j , and d_{ij} the distance between the centres of bacteria i and j (Figure 4.1a).

Similarly, a bacterium escaping its predators experiences a repulsive force (Figure 4.1b) given by

$$\mathbf{F}_i = \beta \sum_{j=1}^n \begin{cases} \frac{-\mathbf{r}_{ij}}{d_{ij}^2}, & \text{if } i \text{ is a prey of } j, \\ \mathbf{0} & , \text{ if } i \text{ is not a prey of } j. \end{cases} \quad (4.3)$$

This motility comes on top of the adapted movement mechanism described by Eq. 4.1. Note that this motile behaviour is an absolute advantage and does not come with any trade-off, unlike in the real world, where motility imposes a certain metabolic load.

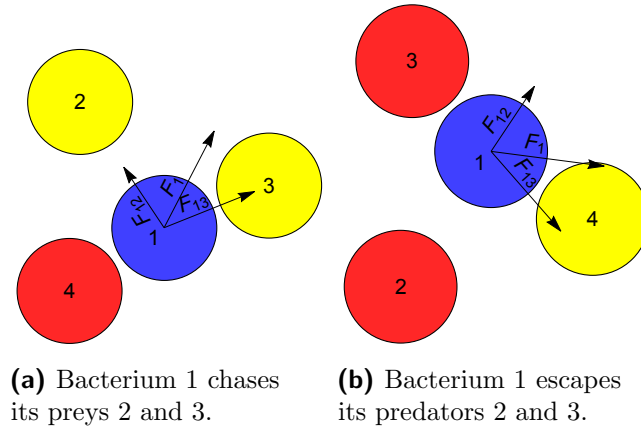


Figure 4.1: Visualisation of the force \mathbf{F}_1 and its components exerted on bacterium 1 due to attraction by chasing its preys (a) or escaping its predators (b).

Species always chase their prey species and escape their predator species according to the intransitive competition structure in Figure 2.2b, where the blue species dominates the yellow species, the yellow species dominates the red species, and the red species dominates the blue species. We now introduce a shorthand three-letter notation, with the first letter representing the ability of the blue species to chase (C) the yellow species, to escape (E) the red species or no motile ability (N); and the second and third letter accordingly for respectively the yellow and red species. For example, a system denoted by CEN contains a blue species that chases the yellow species, a yellow species that escapes the blue species, and a red species that has no special ability.

4.4 Experimental setup

4.4.1 Adapted movement mechanism

The experimental setup described in Section 3.4 was used, with the exception of the adapted movement mechanism (Section 4.2). To test whether mobility is proportional to $M \propto \epsilon d_{max}^2 N^{-1}$, the model was run for different combinations of ϵ and d_{max} representing the same M . This was done by choosing ϵ between 10 and 60 and subsequently calculating the corresponding d_{max} to obtain a predefined value of M , chosen between 5×10^{-4} and 3×10^{-3} . We calculated 10 000 generations, with 50 simulations for each parameter combination.

To investigate the influence of mobility M on the system, M was varied between 2×10^{-5} and 4.5×10^{-3} , by choosing $\epsilon = 20$ and varying d_{max} accordingly between 0.1 and 1.5. We calculated 10 000 generations, with 50 simulations for each parameter combination.

4.4.2 Chasing predators and escaping preys

The model was adapted to encompass chasing or escaping behaviour as described in Section 4.3. These abilities were assigned asymmetrically to the species, in different combinations. Scenarios with species having multiple abilities were not investigated in order to avoid confounding effects. This gave a total of $3^3 = 27$ different scenarios. The CCC and EEE scenarios were not investigated since the focus of this experiment was on asymmetric competition. Moreover, by acknowledging symmetry (e.g. CNE and ECN are symmetric), the total number of unique scenarios was reduced to eight: CNN, CNE, CCN, CCE, CEN, CEE, ENN, and EEN. The NNN scenario was included as a benchmark, and corresponds with the one studied in Section 4.4.1. The weight β was always set to 1, while the mobility M was set to 1.5×10^{-3} , with $\epsilon = 20$ and $d_{max} = 0.86$, since for this mobility $P_{ext} \approx 0.5$ (see further). We calculated 10 000 generations, with 50 simulations for each parameter combination. Apart from the data gathered described in Section 3.4, the probability of a monoculture dominated by either the blue (P_{blue}), the yellow (P_{yellow}), or the red (P_{red}) species were obtained by calculating the fraction of simulations ending in each of these situations.

4.5 Results and discussion

4.5.1 Adapted movement mechanism

Figure 4.2 shows the probability of extinction P_{ext} for different values of ϵ , with d_{max} chosen so that M equals a predefined value, and this for several values of M . The extinction probability P_{ext} is almost constant for all values of mobility M , regardless of the underlying ϵ and d_{max} . As long as ϵd_{max}^2 remains constant, the maintenance of coexistence is the same. Similarly, the final average evenness is roughly constant for all values of mobility M (Figure 4.3). Moreover, the spiral structures are of comparable size for the same mobility M , again independent of ϵ and d_{max} (Figure 4.4). This supports our hypothesis that, macroscopically speaking, moving small distances at a high rate results in the same mobility as moving larger distances at a low rate. However, when looking at higher values of ϵ , one can see a slightly lower extinction probability. Closer inspection of the underlying simulations reveals that these have not been given enough time to collapse to extinction. A higher ϵ at the same mobility M means that individuals are more often engaged in movement events than reproduction and competition. It therefore takes longer for the dynamics to emerge, and extinctions to occur. We can conclude that $M \propto \epsilon d_{max} N^{-1}$, as long as the time-scale is sufficiently large for the dynamics to emerge.

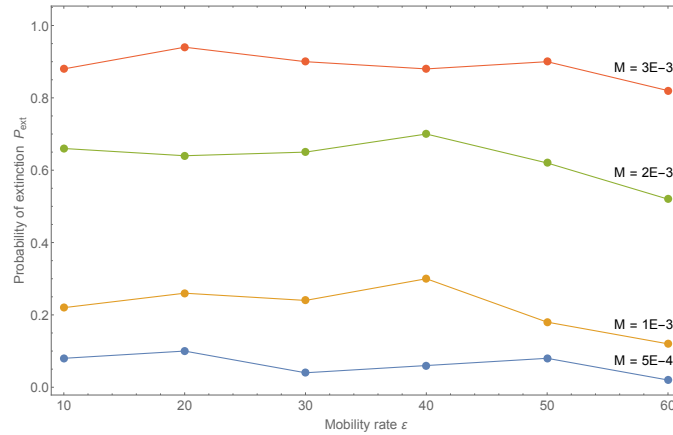


Figure 4.2: Probability of extinction P_{ext} (50 simulations, 10 000 generations) versus mobility rate ϵ for different mobilities M , obtained by varying d_{max} accordingly.

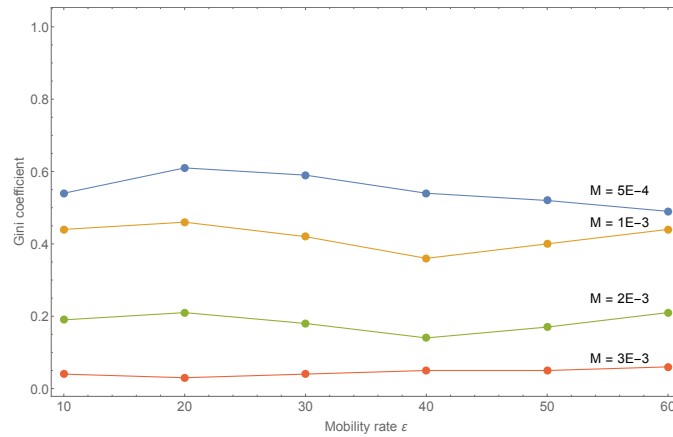
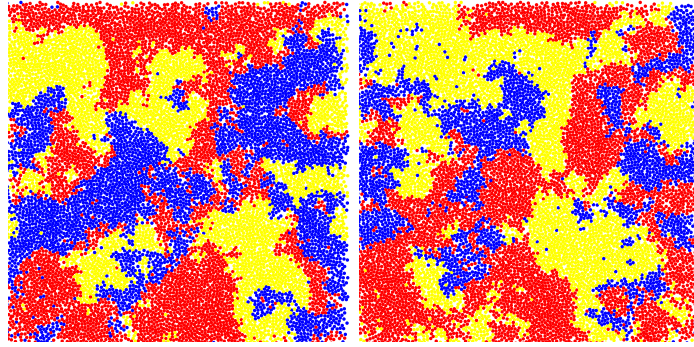


Figure 4.3: Final average community evenness (50 simulations, 10 000 generations), measured by the Gini coefficient, versus mobility rate ϵ for different mobilities M , obtained by varying d_{max} accordingly.

Figure 4.5 shows the probability of extinction P_{ext} as a function of the mobility M . A relationship similar to Figure 3.14 can be seen, where increased mobility leads to a higher extinction probability. The critical mobility is $3.5 (\pm 0.5) \times 10^{-3}$. This shows that the same qualitative behaviour emerges in a model with the adapted movement mechanism. This movement mechanism is however more realistic than the previously used one with bacteria switching their positions (Section 3.3). Although it introduces an additional parameter d_{max} , the complexity of the model does not really increase as ϵ and d_{max} are linked by M .



(a) $\epsilon = 20$ and $d_{max} = 0.71$. (b) $\epsilon = 40$ and $d_{max} = 0.5$.

Figure 4.4: Example of the spatial dynamics arising when $M = 1 \times 10^{-3}$ for two different combinations of ϵ and d_{max} .

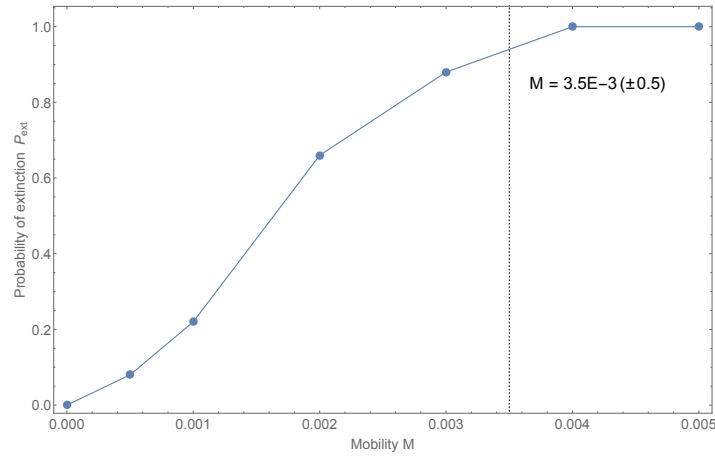


Figure 4.5: Probability of extinction P_{ext} (50 simulations, 10 000 generations) versus mobility M .

4.5.2 Chasing predators and escaping preys

Scenarios analysis

Table 4.1 lists the probability of extinction P_{ext} and the probability of a monoculture dominated by either the blue (P_{blue}), the yellow (P_{yellow}), or the red (P_{red}) species, for the nine scenarios described in Section 4.4.2. For the reference scenario NNN, P_{ext} is 0.52. One can see that some scenarios result in a higher P_{ext} than the benchmark, such as CNE, CCE, CEE, and ENN. Some scenarios result in a lower P_{ext} than the benchmark, such as CNN, CCN, and EEN. In one scenario, we do not see an effect P_{ext} as compared to the benchmark, namely CEN.

Table 4.1: Probability of extinction P_{ext} and probability of a monoculture dominated by either the blue (P_{blue}), yellow (P_{yellow}), or red (P_{red}) species (50 simulations, 10 000 generations).

Scenario	P_{ext}	P_{blue}	P_{yellow}	P_{red}
NNN	0.52	0.14	0.18	0.20
CNN	0.82	0.00	0.04	0.78
CNE	0.04	0.00	0.00	0.04
CCN	1.00	0.00	0.00	1.00
CCE	0.14	0.08	0.00	0.06
CEN	0.56	0.22	0.20	0.14
CEE	0.16	0.02	0.02	0.12
ENN	0.38	0.08	0.24	0.06
EEN	0.82	0.14	0.50	0.18

To gain a better insight into the dynamics influencing the maintenance of coexistence, we visualised representative temporal evolutions for each scenario, together with a simplex plot in Figures 4.6-4.11. Additionally, Appendix C gives the evenness and patchiness as a function of time for these evolutions. An example is considered representative if at least 80% of the simulations follows the same dynamics. When the simulation produces a wide range of different outcomes, no evolution is visualised.

Figure 4.6 shows a representative evolution of the CNN scenario, where the blue species chases the yellow species. Space is randomly and evenly initialised, meaning the species are initially dispersed and spiral patterns have not yet emerged, visible by the low initial patchiness (Figure C.1a). During this initial phase, the chasing behaviour increases the chance that the blue species encounters its predator and is subsequently defeated. Chasing behaviour is thus an initial disadvantage, visible by a decreasing density of the blue species. The lower density of the blue species gives an advantage to the yellow species, allowing it to expand its territory at the expense of the red species. Later on, spiral form, indicated by a higher patchiness. The chasing behaviour of the blue species now becomes an advantage. By chasing, the blue species can quickly capture the territory of the yellow species without the danger of encountering the red species on its way. The substantial advantage of the chasing behaviour allows the blue species to drive the yellow species extinct, causing its own demise by removing the predator of its predator. As $P_{ext} = 0.82$, the system maintains coexistence less frequently than the benchmark ($P_{ext} = 0.52$).

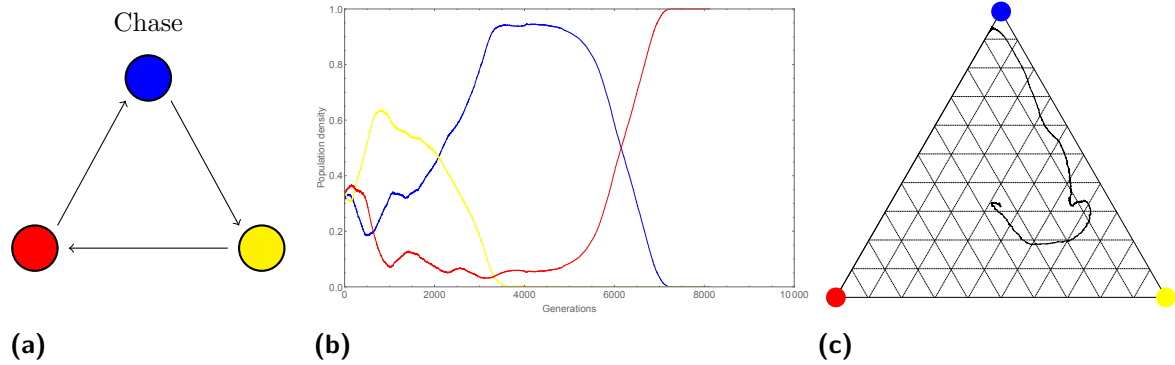


Figure 4.6: Tournment graph (a), population density plotted through time (b) and as a trajectory on a simplex (c) for a representative evolution of the CNN scenario.

Figure 4.7 shows a representative evolution of the CNE scenario, where the blue species chases the yellow species and the red species escapes the yellow species. The motile behaviour of the blue species and the red species gives them an initial disadvantage by increasing their mobility, allowing the yellow species to quickly expand its territory. Later on, when spirals emerge, the blue species penetrates into the territory of the yellow species. However, when the red species escapes from the yellow species, it leaves its former territory open for the yellow species to colonise. The escaping behaviour of the red species thus gives the yellow species an advantage, allowing it to compensate for the threat of the blue species. The yellow species can maintain its dominant position, with the blue species and the red species being present in low numbers. At $P_{ext} = 0.04$, the system maintains coexistence more frequently than the benchmark ($P_{ext} = 0.52$), albeit with low evenness (Figure C.1b).

Figure 4.8 shows a representative evolution of the CCN scenario, where the blue species chases the yellow species and the yellow species chases the red species. The chasing behaviour initially decreases the density of both the blue species and the yellow species, allowing the red species to expand quickly. After the emergence of spirals, the yellow species chases the red species, who is temporarily dominant, and becomes dominant itself. The blue species then chases the yellow species, thereby driving it extinct and thus allowing the red species to become the sole survivor. At $P_{ext} = 1$, the system maintains coexistence less frequently compared to the benchmark ($P_{ext} = 0.52$).

Figure 4.9 shows a representative evolution of the CCE scenario, where the blue species chases the yellow species, the yellow species chases the red species, and the red species escapes from the yellow species. Since all species exhibit motile behaviour, their mobility is equal. However, the escaping behaviour of the red species appears to give it an initial advantage. Whereas the chasing behaviour of the yellow species and the blue species increases the chance

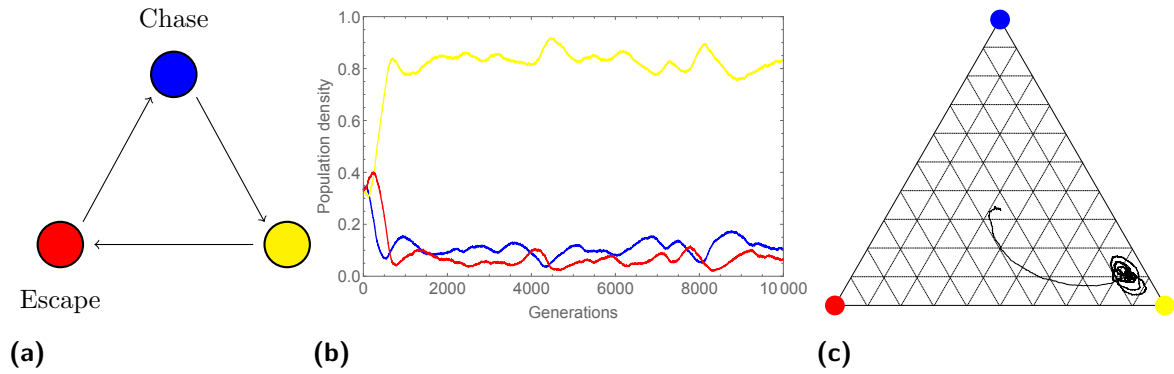


Figure 4.7: Tournament graph (a), population density plotted through time (b) and as a trajectory on a simplex (c) for a representative evolution of the CNE scenario.

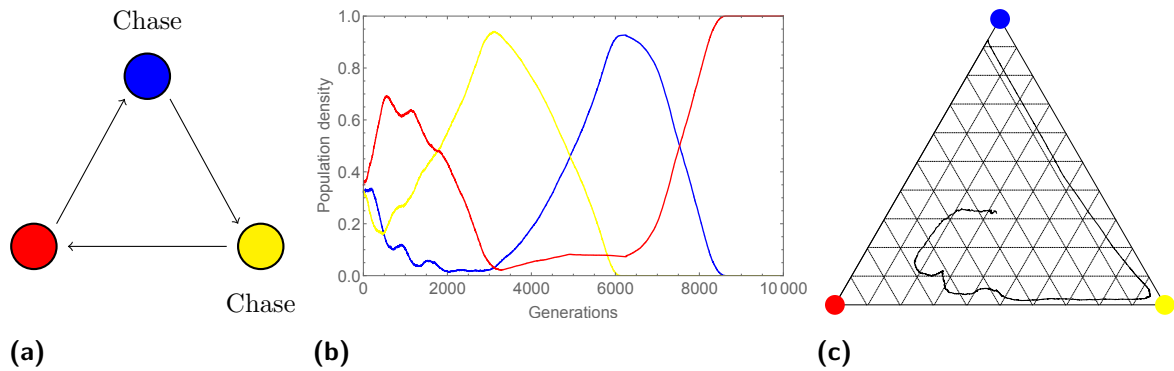


Figure 4.8: Tournament graph (a), population density plotted through time (b) and as a trajectory on a simplex (c) for a representative evolution of the CCN scenario.

of encountering a predator, the escaping behaviour of the red species makes it move away from its predator. The chance of the red species encountering a predator is therefore lower, allowing it to increase its density. When the spirals are formed, the yellow species expands into the territory of the red species, aided by the red species opening up space by fleeing away from the yellow species. This allows the yellow species to dominate the system, a position it can maintain by offsetting its disadvantage of being chased by the blue species with the advantage of the red species escaping. At $P_{ext} = 0.14$, the system maintains coexistence less frequently than the benchmark ($P_{ext} = 0.52$), although with low evenness (Figure C.1d).

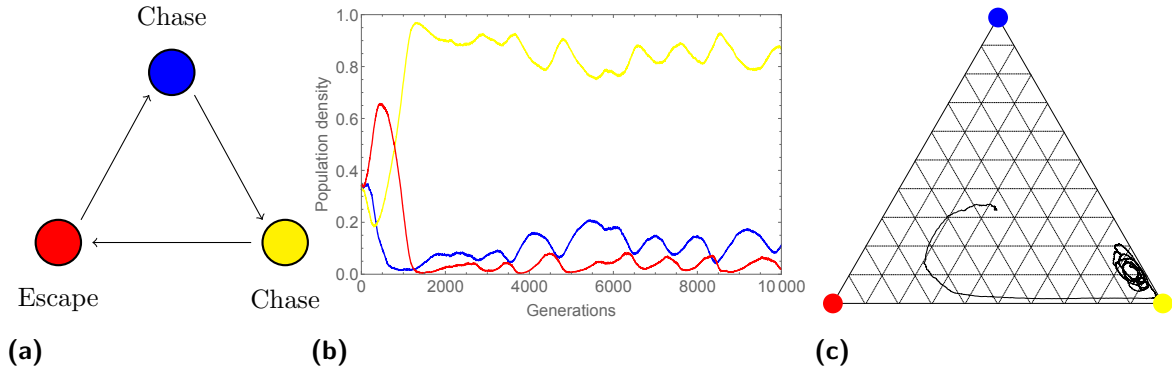


Figure 4.9: Tournament graph (a), population density plotted through time (b) and as a trajectory on a simplex (c) for a representative evolution of the CCE scenario.

No example of an evolution for the CEN scenario is visualised, since this scenario produces diverse dynamics. When the blue species chases the yellow species and the yellow species escapes the blue species, these two abilities tend to neutralise each other. At $P_{ext} = 0.56$, this scenario does not seem to have a significant effect on the maintenance of coexistence compared to the benchmark ($P_{ext} = 0.52$).

Figure 4.10 shows a representative evolution of the CEE scenario, where the blue species chases the yellow species, the yellow species escapes the blue species, and the red species escapes from the yellow species. The escaping behaviour of the yellow species appears to give it an advantage in the beginning, which explains its ability to increase its density. This allows the blue species to expand into the territory of the yellow species, aided by the escaping yellow species, and becomes temporarily dominant. The red species can now expand, but the yellow species quickly bypasses the red species. The red species never becomes the dominant species, as can be seen in the simplex plot. With $P_{ext} = 0.16$, the system maintains coexistence more frequently than the benchmark ($P_{ext} = 0.52$).

Figure 4.11 shows a representative evolution of the ENN scenario, where the blue species escapes from the red species. Initially, the escaping behaviour of the blue species gives it a disadvantage, decreasing its density. Later on, when spirals have emerged, the escaping behaviour of the blue species gives an advantage to the red species, by freeing up empty space for the red species to reproduce in. This advantage gives the red species the ability to continuously dominate the system, with only short interruptions of its dominant position by the yellow species and the blue species. With $P_{ext} = 0.38$, the system maintains coexistence slightly more often than the benchmark ($P_{ext} = 0.52$). When the system loses coexistence, the yellow species prevails due to the red species driving the blue species extinct.

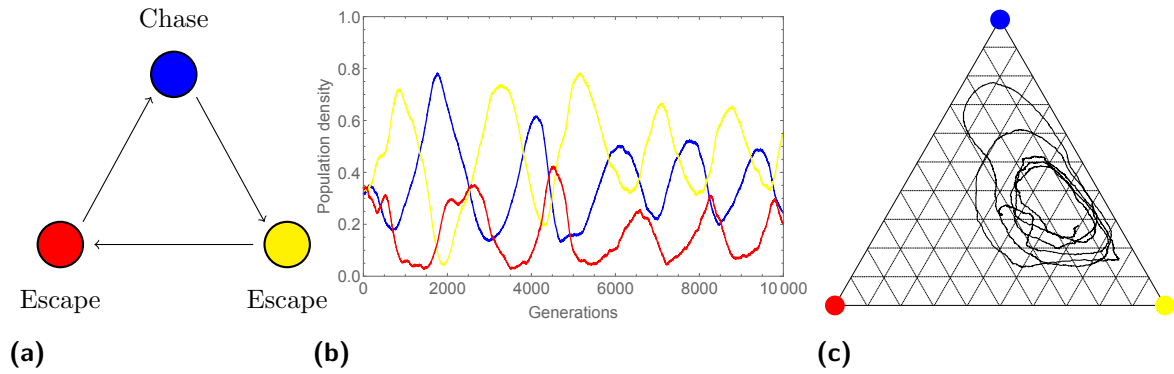


Figure 4.10: Tournament graph (a), population density plotted through time (b) and as a trajectory on a simplex (c) for a representative evolution of the CEE scenario.

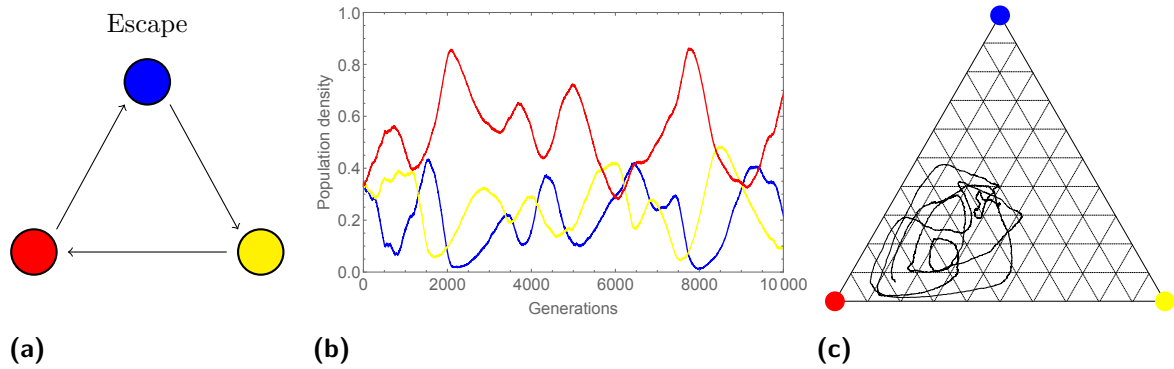


Figure 4.11: Tournament graph (a), population density plotted through time (b) and as a trajectory on a simplex (c) for a representative evolution of the ENN scenario.

An example of an evolution of the EEN scenario is not visualised, since this scenario produces a wide range of outcomes. With the blue species escaping from the red species and the yellow species escaping from the blue species, the red species has an initial advantage as the only non-motile species, increasing its density. Later on, the blue species and the yellow species give their respective predators an advantage due to their escaping behaviour by creating empty space for their predators to reproduce in. Diverse dynamics occur, often ending in the red species driving the blue species extinct, allowing the yellow species to survive. With $P_{ext} = 0.82$, the system maintains coexistence less frequently than the benchmark ($P_{ext} = 0.52$).

Motile dynamics

Some general dynamics can be derived from these simulations. Initially, the chasing or escaping behaviour seems to be a disadvantage when non-motile species are present. Because of the random and even initialization of the system, the species are dispersed and disaggregated from their conspecifics, indicated by a low initial patchiness (Figure C.1). Therefore, one's prey is often located close to one's predator. Chasing behaviour thus increases the chance of an encounter with a predator, possibly leading to a competition interaction and subsequent death. Similarly, escaping behaviour gives an initial disadvantage to the species by increasing its mobility. This is visible in the scenarios CNN, CNE, CCN, ENN, and EEN, where the density of motile species tends to decrease in the initial evolution of the system, to the advantage of a non-motile species.

However, when all species are motile, the mobility of all species is increased. Escaping behaviour now becomes an initial advantage, as can be seen in scenarios CCE and CEE. Whereas both chasing and escaping behaviour increase mobility, only chasing behaviour increases the chance of encountering a predator, since escaping behaviour makes species move away from their predator. We can conclude that motile behaviour is thus an initial disadvantage when non-motile species are present, but escaping behaviour becomes an initial advantage when only motile species are present.

However, after the emergence of spatial structures, visible by an increased patchiness (Figure C.1), motile behaviour can turn into an advantage. Chasing behaviour allows a species to expand into the territory of its prey, without the danger of encountering its predator. This is visible in scenarios CNN, CCN, and CCE, where a chasing species rapidly increases its density at the expense of its prey.

However, escaping behaviour is not always an advantage when spirals are present. It seems to be an advantage when a species is chased by its predator, as in scenarios CCE, CEN, and CEE (yellow). However, when escaping from a predator without chasing behaviour, it seems to be a disadvantage for the escaping species and an advantage for its predator, as is visible in scenarios CNE, CEE (red), and ENN. When a species escapes from a predator without chasing behaviour, it will leave space empty for the predator to colonise by reproduction, thereby allowing their predator to increase its density. Contrarily, when a species escapes from a chasing predator, it flees territory that a predator would move into, thereby avoiding a competition event resulting in its death, and thus preserving its density. Whereas escaping a non-chasing species is a disadvantage, escaping a chasing species is an effective survival strategy.

Influence on the maintenance of coexistence

The extinction probability P_{ext} for the reference scenario NNN is 0.52. The scenarios can be divided into those promoting the maintenance of coexistence ($P_{ext} \ll 0.52$), those jeopardising the maintenance of coexistence ($P_{ext} \gg 0.52$), and those with no influence on the maintenance of coexistence ($P_{ext} \approx 0.52$).

The scenarios promoting the maintenance of coexistence ($P_{ext} \ll 0.52$) can be divided into two categories. The first maintains coexistence in a highly uneven way, with one species dominating while the others are present in low numbers. Both the CNE ($P_{ext} = 0.04$) and CCE ($P_{ext} = 0.14$) scenario allow the yellow species to dominate early on. Thereafter, the yellow species is able to maintain this dominant position by balancing its disadvantage of being chased by the blue species against its advantage of an escaping red species, thereby never allowing the blue species or the red species to become the dominant species.

The second category promoting maintenance of coexistence leads to oscillating species densities, albeit with one or more dominant species. The communities arising from the CEE ($P_{ext} = 0.16$) scenario are dominated by the blue species and the yellow species. The blue species has an advantage as a consequence of its chasing behaviour, the yellow species offsets the disadvantage of a chasing predator by escaping, and has an advantage due to the escaping behaviour of the red species. The red species, being the inferior species, remains present at lower densities. Similarly, in the ENN ($P_{ext} = 0.38$) scenario, the red species has an advantage due to the escaping behaviour of the blue species. The scenario maintains coexistence, with the red species oscillating at a higher density than the blue species and the yellow species. When coexistence is lost, this is because of the red species driving the blue species out of existence, allowing the yellow species to survive.

The scenarios jeopardising the maintenance of coexistence ($P_{ext} \gg 0.52$) lose coexistence because one species has a substantial advantage, thereby driving its prey extinct. In the CNN scenario ($P_{ext} = 0.82$), the blue species drives the yellow species extinct by chasing it, giving the red species the possibility to survive. The same dynamics happen in the CCN scenario ($P_{ext} = 1.00$), with the blue species driving the yellow species extinct; and the EEN scenario ($P_{ext} = 0.82$), with the red species driving the blue species extinct.

Lastly, the CEN scenario ($P_{ext} = 0.56$) does not appear to affect the maintenance of coexistence. The advantage of the blue species chasing the yellow species is offset by the yellow species escaping the blue species, resulting in balanced dynamics and no significant difference from the benchmark scenario.

4.6 Conclusion

The movement mechanism of the lattice-free model described in Chapter 3 has been adapted to mimic movement more realistically. Similar qualitative dynamics have been found as compared to the lattice-free model, with spiral structures emerging, facilitating coexistence. Likewise, when the mobility increases, the extinction probability P_{ext} increases as well.

Subsequently, the model was extended by allowing species to either chase their prey or escape their predator. We investigated different scenarios, with certain scenarios promoting the maintenance of coexistence, with others jeopardising it or having no influence compared to the benchmark scenario of all non-motile species. We found that, when species are disaggregated and no spatial structures are present, motile behaviour is a disadvantage by increasing the mobility of species and thus the probability of encountering a predator. However, when spatial structures are present, chasing behaviour is an advantage. Escaping behaviour can be an advantage when a species is being chased, mitigating the advantage of its chasing predator. However, escaping behaviour is not beneficial when not being chased, opening up space for its predator to expand into. Thus, the system dynamics are dependent on the spatial characteristics, namely the presence or absence of spirals.

CHAPTER 5

Substrate-dependent dynamics

5.1 Introduction

The models used in Chapters 2-4 assume that a bacterium can only reproduce when the carrying capacity (i.e., the maximum population size that can be sustained indefinitely) in its neighbourhood has not been reached. In the lattice-based model, this is implemented by requiring an empty cell to reproduce into. In the lattice-free model, this is done by assuming that reproduction can only happen if an individual's neighbourhood is not overpopulated (Section 3.3.2). However, this is not in accordance with reality. *In vivo* bacteria neither search for empty spots, nor count their neighbours before reproducing. Reproduction happens when a bacterium attains a certain size through growth, splitting itself into two smaller bacteria. Growth, on the other hand, is limited by the availability of substrate, which in turn is influenced by the presence of other bacteria (Power and Marshall, 1988; Tilman et al., 1997). To model reproduction more realistically, we will extend the model from Chapter 4 with substrate-dependent growth.

5.2 Substrate-dependent reproduction

For simplicity, bacterial growth is assumed to be limited by only one substrate type. A substrate lattice is superimposed on the space inhabited by the bacteria, and is filled with an initial concentration. The centre of a bacterium determines which cell it uses for substrate uptake. Bacteria grow following Monod kinetics (Monod, 1949)

$$\frac{d(\frac{4}{3}\pi r^3)}{dt} = Y_{max} \frac{\mu_{max} S^t(i, j)}{K_s + S^t(i, j)} \frac{4}{3}\pi r^3, \quad (5.1)$$

with $\frac{4}{3}\pi r^3$ the volume of a bacteria modelled as a sphere, Y_{max} the apparent yield (i.e., the amount of substrate converted into microbial biomass), μ_{max} the maximum growth rate, $S^t(i, j)$ the substrate concentration of cell (i, j) that contains the centre of the bacterium at time t , and K_s the half-saturation constant. During growth, the radius of the bacteria

increases and the substrate content of the resource cell is decreased accordingly. The substrate concentration in a given cell cannot become negative. No maximal radius is specified, since reproduction will reduce the size of large bacteria.

Reproduction is only possible if the radius of a bacterium is larger than the minimum reproduction radius r_{rep} , regardless of the number of bacteria present in its neighbourhood. A bacterium splits into two bacteria centred at the coordinates given by Eq. 3.2. The volume of the mother bacterium is equally divided over its daughters, minus a certain amount since reproduction is not considered fully efficient. Hence, the radius of the daughters is calculated by

$$\begin{aligned} \eta \frac{4}{3}\pi r^3 &= 2 \frac{4}{3}\pi r_d^3, \\ \text{thus } r_d &= r \sqrt[3]{\frac{\eta}{2}}, \end{aligned} \tag{5.2}$$

with η the reproduction efficiency, r the radius of the mother bacterium, and r_d the radius of its daughters. The overlap avoidance scheme described in Section 3.3.3 makes sure there is space available for both bacteria.

Diffusion of the substrate across the substrate lattice takes place according to

$$S^{t+1}(i, j) = S^t(i, j) + D_s [S^t(i-1, j) + S^t(i+1, j) + S^t(i, j-1) + S^t(i, j+1) - 4S^t(i, j)], \tag{5.3}$$

with $S^t(i, j)$ the substrate concentration at substrate lattice cell (i, j) at time t and D_s the diffusion coefficient. Periodic boundary conditions apply. Ten diffusion steps are carried out per diffusion event. Diffusion thus occurs at a time scale faster than the individual interaction processes of the bacteria, since otherwise substrate would be depleted very quickly and no dynamics can be observed.

Each generation, substrate flows into the grid at a fixed inflow rate F_{in} . This is comparable to a colony growing on an agar plate, where the substrate available for the bacteria is replenished by diffusion from deeper layers or a reservoir (Matsushita and Fujikawa, 1990). An excess of environmental substrate (an atypical situation in natural systems) is avoided through the choice of F_{in} . When a bacterium dies, its substrate is instantaneously released into the environment.

The model then proceeds as follows. At the start of each generation, diffusion takes place. Next, each bacterium is allowed to grow according to the Monod kinetics. Thereafter, the cell and Verlet lists are constructed and the interactions are executed as in the substrate-free model (Section 4.2). Figure 5.1 gives a flowchart outlining the processes taking place in one generation.

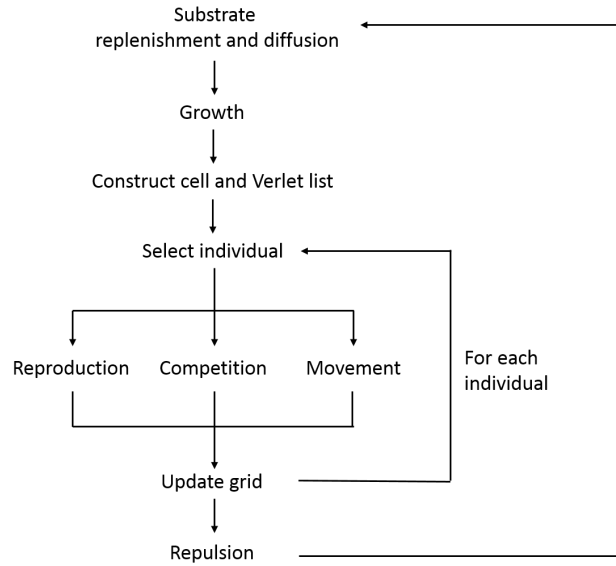


Figure 5.1: Flowchart outlining the processes making up one generation according to the algorithm by Gillespie (1976).

5.3 Experimental set-up

The experimental set-up described in Section 4.4.1 was used, with addition of the substrate dynamics described in Section 5.2. The parameters of the Monod equation were taken from literature relating to *E. coli* strains (Kreft et al., 1998; Daly et al., 2016). The apparent yield Y_{max} was set at 0.44, the maximum growth rate μ_{max} was set at 0.05, and the half-saturation constant K_s was set at 0.05. The minimal cell radius at replication r_{rep} was set at 0.5 and the reproduction efficiency η at 0.85. The substrate diffusion coefficient D_s was set at 0.1, the initial substrate concentration was 0.01, with the substrate inflow rate F_{in} varied between 0.002 and 0.01. As before, we choose to omit units, although dimensions are consistent. The mobility M was set at 1.5×10^{-3} , with $\epsilon = 20$ and $d_{max} = 0.86$. We calculated 10 000 generations, with 50 simulations for each value of the substrate inflow rate F_{in} . Apart from the data gathered described in Section 3.4, the average substrate concentration and total number of individuals are recorded.

5.4 Results and discussion

Figure 5.2 shows the final average substrate concentration in the environment as a function of the substrate inflow rate F_{in} . Logically, a higher substrate inflow leads to a higher substrate concentration in the environment. Figure 5.3 shows the final average number of individuals present in the system. As can be seen, the final population size is dependent on the substrate inflow. A lower substrate inflow limits the growth and thus reproduction of the bacteria,

thereby limiting the number of individuals present. A higher substrate inflow allows the bacteria to grow and reproduce faster, and thus allows the ecosystem to support more individuals. However, the overlap avoidance mechanism only works when fewer bacteria are present than can pack into space. If the substrate inflow is too high, more species will be present than can pack into space, resulting in overlapping bacteria. Spatial dynamics are then not accounted for, and the results should be considered invalid.

We will investigate simulation conditions more closely: a system with a low substrate inflow rate $F_{in} = 0.003$, and a system with a high substrate inflow rate $F_{in} = 0.008$. Figure 5.4 shows the Monod growth curve as described by Eq. 5.1. Taking the average final substrate concentrations for these systems, as shown in Figure 5.2, the following respective growth rates can be computed by

$$\begin{aligned}\mu_{0.003} &= Y_{max} \frac{\mu_{max} S}{K_s + s} \\ &= 0.44 \frac{0.05 \times 0.0058}{0.05 + 0.0058} \\ &\approx 0.0023 , \\ \mu_{0.008} &= 0.44 \frac{0.05 \times 0.019}{0.05 + 0.019} \\ &\approx 0.0061 .\end{aligned}$$

The number of growth steps x needed between two subsequent reproduction events can be calculated as

$$\begin{aligned}r \sqrt[3]{\frac{\eta}{2}} (1 + \mu)^x &= r , \\ \text{thus } x &= \frac{\log \left(\sqrt[3]{\frac{2}{\eta}} \right)}{\log(1 + \mu)} .\end{aligned}$$

Using this formula, bacteria in the high-inflow system can reproduce on average each 46 steps, whereas in the low-inflow system this is each 122 steps, a factor 2.66 slower. This ratio is similar to the ratio between the substrate inflow $0.008/0.003 \approx 2.66$. This similarity can be explained by the substrate concentration levels. When $S \ll K_s$, the Monod equation (Eq. 5.1) can be approximated by a linear curve

$$\frac{d\left(\frac{4}{3}\pi r^3\right)}{dt} = Y_{max} \frac{\mu_{max} S}{K_s} \frac{4}{3}\pi r^3 .$$

Since both substrate concentrations are far smaller than K_s , this approximation holds. Therefore, the volume increase of a bacterium is linearly dependent on the substrate concentration, and the number of growth steps x is inversely related to the substrate concentration. This explains the similarity between the ratios.

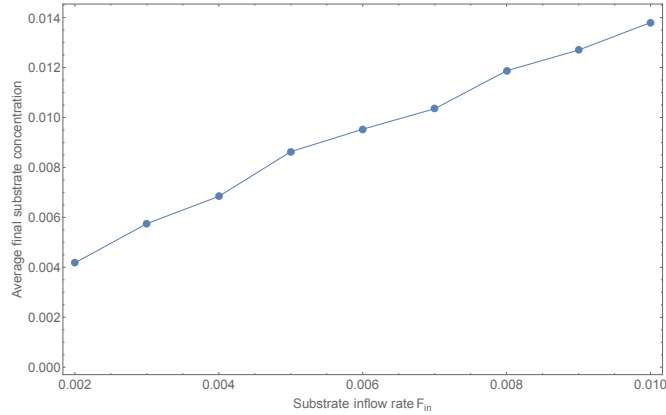


Figure 5.2: Average substrate concentration (50 simulations, 10 000 generations) as a function of substrate inflow rate F_{in} .

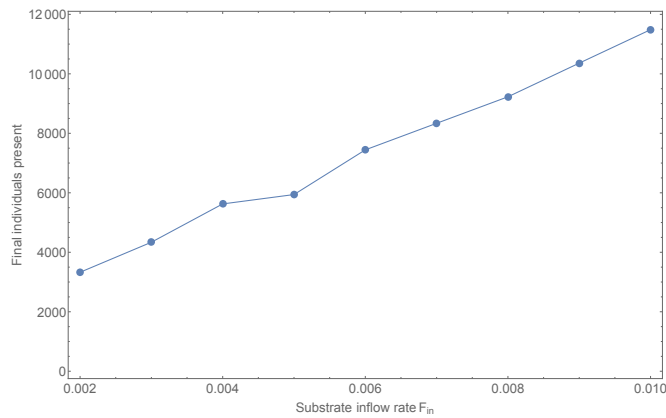


Figure 5.3: Final average number of individuals (50 simulations, 10 000 generations) as a function of substrate inflow rate F_{in} .

Figures 5.5a and 5.5d show the population size for the three species and the total population size plotted through time of a representative evolution of both systems. For both simulations, an initial drop in population size is noticeable. This is due to the dispersed initialisation of the system, enabling many successful competition events, and thereby killing a large number of bacteria. Later on, when spirals have emerged, the bacteria can grow and the oscillating behaviour starts. However, the low-inflow system leads to a greater decline (around 2500 individuals) compared to the high-inflow system (around 5000 individuals). Moreover, the high-inflow system recovers faster and supports a higher number of individuals. This is logical, since reproduction is slower in the low-inflow system, whereas the competition rate σ is equal for both systems. Furthermore, the amplitude of the oscillations is higher in the high-inflow system. Because of the faster growth and thus reproduction, species in the high-inflow system can expand more rapidly into the territory of their prey, thereby producing larger variations in the system composition. However, plotted as density on a simplex, the trajectories look similar for the low-inflow (Figure 5.5b) and high-inflow system (5.5e). Lastly, Figures 5.5c and

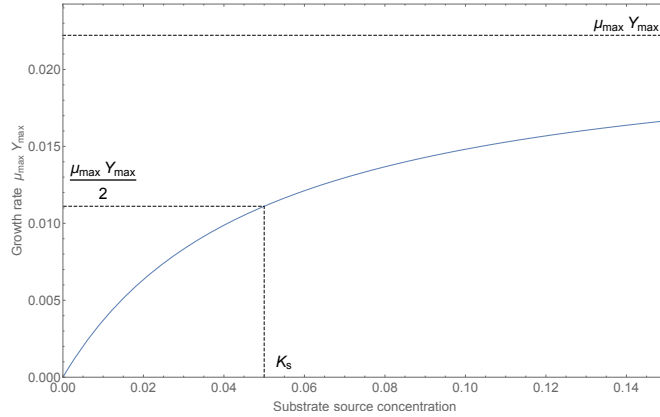


Figure 5.4: Monod growth-curve for $Y_{max} = 0.44$, $\mu_{max} = 0.05$, and $K_s = 0.05$.

5.5f show the final spatial configuration of both systems. Both systems show spiral structures of approximately the same size, preserving coexistence. However, while the high-inflow system is densely packed by the bacteria, the individuals in the low-inflow system are more dispersed.

These results show that the macroscopic concept of carrying capacity can be retrieved using the bottom-up approach of an IBM. By making the reproduction process of the bacteria dependent on substrate dynamics, the model reproduces macroscopic behaviour without explicitly incorporating it, thereby making the model more realistic and justifying the use of the IBM approach.

Figure 5.6 gives the probability of extinction P_{ext} as a function of the substrate inflow rate F_{in} . An inverse relationship is visible, with a higher substrate inflow promoting the maintenance of coexistence. As noted before, a high-inflow system produces oscillations with a larger amplitude (Figure 5.5d) than one with a low-inflow system (Figure 5.5a). The latter has a lower growth rate, suggesting that a low-inflow system maintains coexistence better. However, the number of species in the low-inflow system is lower than the high-inflow system (Figure 5.3). This lower population size leads to smaller communities, who are more prone to extinction. This explains the lower probability of extinction. This is comparable to the findings of Reichenbach et al. (2007), who found a higher P_{ext} when fewer species are present.

The probability of extinction P_{ext} of the model without substrate dynamics at mobility $M = 1.5 \times 10^{-3}$ is 0.52 (Figure 4.5). For the model including substrate dynamics at the same mobility with comparable population size (i.e., $F_{in} = 0.008$ supports $\pm 10\,000$ individuals (Figure 5.3), the P_{ext} is 0.26 (Figure 5.6). Inclusion of substrate-dependent growth thus promotes the maintenance of coexistence. In the model without substrate dynamics, a bacterium can immediately reproduce when empty space is available due to the killing of its prey. Furthermore, its daughter bacteria can already reproduce themselves in the next generation. This allows bacteria to quickly expand into the territory of its prey. On the other

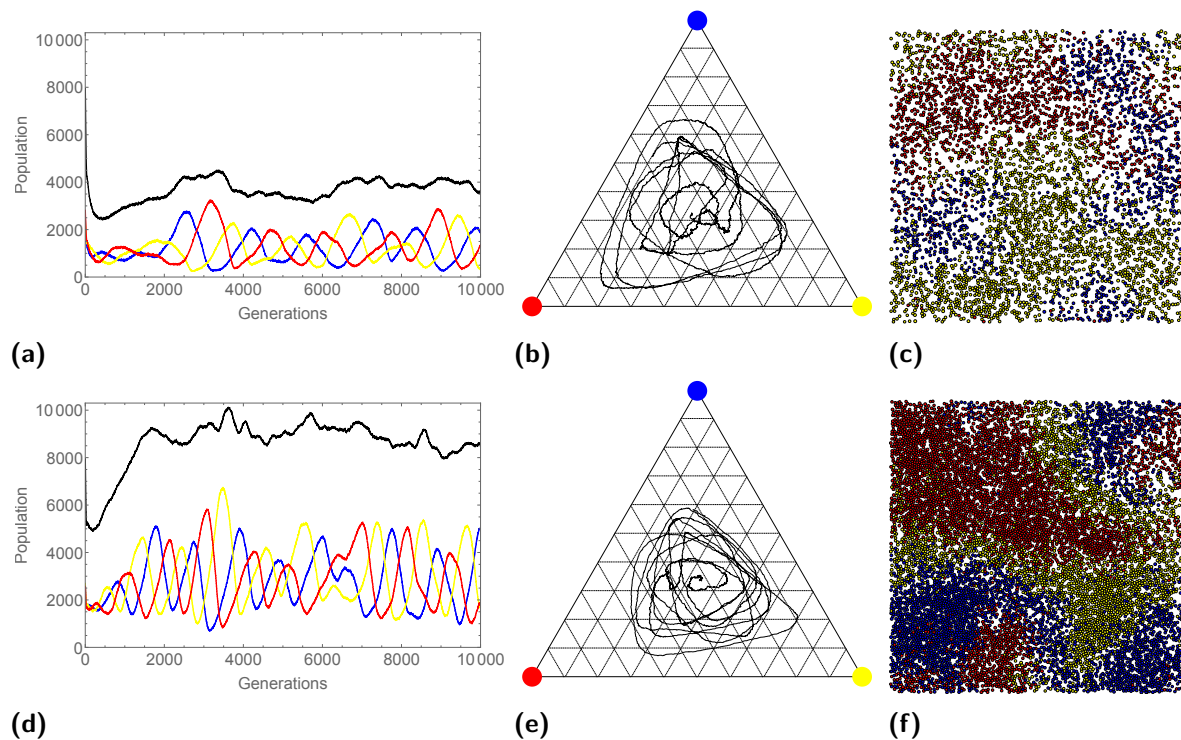


Figure 5.5: The population size plotted through time for the three species (blue, yellow, red) and total population size (black) (a and d), population density as a trajectory on a simplex (b and e), and spatial configuration for 10 000 generations (c and f) for a representative evolution with substrate inflow rate $F_{in} = 0.003$ (a-c) and $F_{in} = 0.008$ (d-f).

hand, a bacterium in the model including substrate dynamics can only reproduce when it attains a certain size. Furthermore, its daughter bacteria are only able to reproduce themselves after multiple growth steps. This slows down the ability of bacteria to expand into the territory of its prey. Hence, due to the dampening effect on reproduction of the substrate dynamics, the maintenance of coexistence is promoted.

5.5 Conclusion

By incorporating substrate-dependent growth and substrate diffusion into our model, reproduction is modelled more realistically. It is shown that higher levels of available substrate allow the system to support more individuals, thereby proving that the macroscopic concept of carrying capacity is retrieved through the bottom-up approach of an IBM. Furthermore, it is found that a higher substrate availability promotes the maintenance of coexistence, mainly as a consequence of the higher number of individuals. Lastly, inclusion of substrate-dependent growth promotes the maintenance of coexistence by lowering the rate of reproduction.

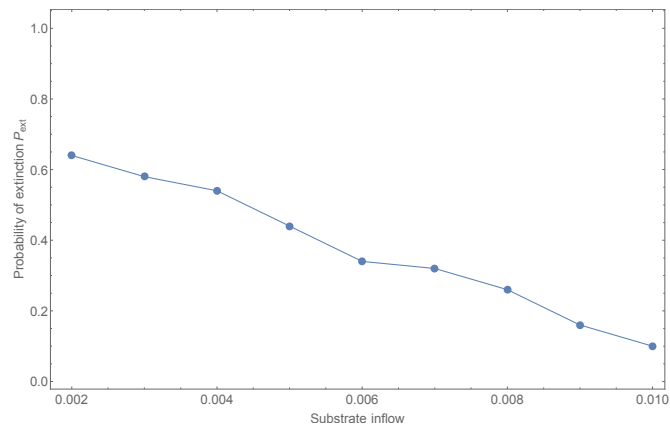


Figure 5.6: Probability of extinction P_{ext} (50 simulations, 10 000 generations) as a function of substrate inflow rate F_{in} .

CHAPTER 6

Conclusion

6.1 Conclusion

In this thesis, we have addressed several research questions. First, we investigated the effect on the maintenance of coexistence of a lattice-free approach to modelling microbial and spatial dynamics. Thereafter, we implemented a more realistic movement mechanism, and explored the effect of motility on biodiversity. Lastly, we studied the effect of substrate-dependent reproduction on the maintenance of coexistence.

We addressed these research questions with the help of IBMs. These models are increasingly appreciated, especially in microbial sciences, due to their ability to account for local interactions, variability among individuals, and adaptive behaviour. We used a three-species intransitive competition structure as basis for the competitive dynamics among the individuals. Since no single species has an absolute advantage, this competition structure offers an interesting simplification to study the basic interaction in communities. We used the probability of extinction as the main metric for measuring the maintenance of coexistence.

In Chapter 3, we investigated the effect how space is represented. Therefore, we constructed and compared a lattice-free model to the original lattice-based model. We found that the former maintains coexistence better, as shown by a higher critical mobility rate, and can thus be considered more robust. Both models show the same qualitative behaviour, with spiral patterns allowing for the maintenance of coexistence. However, by having more spatial degrees of freedom, the spirals in the lattice-free model tend to be more robust in terms of the maintenance of coexistence. Small refuges can form and persist, thereby maintaining coexistence, whereas these refuges would go extinct in the lattice-based model. This finding agrees with the spatial dynamics seen in experimental studies. However, the increased realism comes at a computational cost. Although we implemented several computational improvements, namely cell

and Verlet lists, one needs to consider if the advantages are worth the cost. Furthermore, the effect of the interaction range has been investigated. A larger interaction range diminishes the localisation of interactions, thereby increasing the probability of extinction, in agreement with previous studies linked to the localisation of interactions. We can conclude that the lattice-free approach is more realistic and allows us to retrieve behaviour not seen with lattice-based models.

In Chapter 4, we adapted the movement mechanism of the model to mimic movement more realistically. We found similar qualitative dynamics compared to the previous model, namely emerging spiral patterns, facilitating coexistence. Likewise, an increase in mobility induces an increase in the probability of extinction P_{ext} . Although this mechanism introduces an extra parameter d_{max} , the complexity of the model is not increased when it is acknowledged that ϵ and d_{max} can be linked by M .

Subsequently, we extended the model from Chapter 4 by allowing species to either chase their prey or escape their predator, a form of motile behaviour. Different scenarios were investigated, with some scenarios promoting maintenance of coexistence, with others threatening it or having no influence compared to the benchmark scenario of all non-motile species. We found that, when species are disaggregated and no spatial structures are present, motile behaviour is a disadvantage by increasing the mobility of species and thus the probability of encountering a predator. However, when spirals are present, chasing behaviour is an advantage. Escaping behaviour can be an advantage when a species is being chased, mitigating the advantage of its chasing predator. However, escaping behaviour is not beneficial when not being chased, as it leads to open space for its predator to expand into. Thus, the system dynamics are dependent on the spatial characteristics, namely the presence or absence of spirals.

In Chapter 5, we incorporated substrate-dependent growth and substrate diffusion into the model, allowing us to model reproduction more realistically. We found that higher levels of substrate availability allow the system to support more individuals, thereby proving that the macroscopic concept of carrying capacity can be retrieved through the bottom-up approach of an IBM. Furthermore, we found that a higher substrate availability promotes the maintenance of coexistence, mainly as a consequence of the higher number of individuals present. Lastly, inclusion of substrate-dependent growth promotes the maintenance of coexistence compared to the model without substrate dynamics by lowering the rate of reproduction.

6.2 Perspectives

To make the model even more realistic, further adaptations can be made. First, although the model developed in this thesis allows for bacteria of different sizes, they are modelled as spheres. *In vivo* bacteria have a wide range of different shapes, such as spherical (e.g. *Coccus*), rod-shaped (e.g. *Bacillus*), spiral (e.g. *Spirillum*), or even pleomorphic (without a defined shape). These different shapes can be included in an extended version of the model, since in a lattice-free approach, there is no need to fix a certain pre-defined shape (Cabeen and Jacobs-Wagner, 2005).

Furthermore, certain bacteria tend to aggregate. Some cluster together with two (e.g. *Diplococci*), four (e.g. *Tetragenococcus*), or eight (e.g. *Sarcinae*) of their conspecifics, whereas others form long chains (e.g. *Streptococcus*). To investigate the dynamics arising from these specific arrangements, these can be included in an adapted version of the model (Dusenbery, 2009).

Moreover, as noted in Section 2.1.2, a competitive advantage does not only arise from killing one's prey, accounted for in the model, but also due to a metabolic advantage. The intransitive competition dynamics found in *E. coli* is only partially based on toxin production, with two species having a relative metabolic advantage. However, this competition structure is implemented as if all three species produce toxins. Competition through a metabolic advantage can be implemented by imposing a certain metabolic cost on some of the species, possibly leading to a decrease in size. Bacteria that fall below a certain size are removed from the system. This allows a species with a metabolic advantage to outcompete the other species.

We briefly explored this approach, where one species kills its prey and the other two have a relative metabolic advantage. We found spiral structures emerging, comparable to the other models (Figure 6.1). However, the boundaries of these structures tended to be less defined, and the blue species tended to mix with the red species. Exploring the parameter range maintaining coexistence is, among other possible ways to analyse this system, a promising idea for further research.

Finally, real microbial ecosystems often contain more than three species, with plenty of species having relative advantages to one another. The model can be extended to incorporate higher-order competition structures to investigate the dynamics of such systems.

To make the model more representative of a particular microbial system, it could be calibrated with *in vivo* data. During this thesis, an attempt was made to obtain data in a lab experiment based on the intransitive *E. coli* community described by Kerr et al. (2002). Yet, due to practical problems and time restrictions, we decided not to proceed with these experiments.

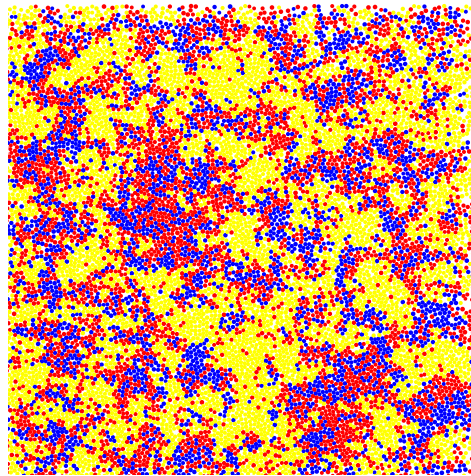


Figure 6.1: Visualisation of spatial structures emerging with modified competition structure.

Still, the potential of a calibrated model is tremendous. A calibrated model can be used to make predictions under conditions not yet investigated empirically, or simulate experiments that might be troublesome to execute in the field or lab, and can therefore contribute to the understanding of coexistence. For the purpose of calibrating stochastic IBMs, Bayesian approximate computation is often used to calibrate a stochastic IBM (Beaumont, 2010; Csilléry et al., 2010; van der Vaart et al., 2015).

Furthermore, our model can be used to investigate the dynamics of certain behaviour. Similar to the escaping and chasing behaviour described in Section 4.3, other forms of motility can be included, such as chemotaxis, where bacteria move along a substrate gradient. We briefly explored the effect of chemotaxis on the system, and found that chemotaxis increases the probability of extinction P_{ext} (Figure 6.2). Chemotaxis allows bacteria to migrate to substrate-rich positions, thereby increasing their reproduction rate, and decreasing the maintenance of coexistence. However, this effect is less pronounced at high substrate inflow rates. This is probably because more substrate is available to the bacteria, making chemotaxis less of an advantage. An in-depth study of the effects of chemotaxis by some or all species could yield interesting insights.

Other competitive advantages (e.g. quorum sensing) could be included and investigated as well. A trade-off for an advantage in the form of a metabolic cost could be included, making a cost-benefit analysis of certain strategies possible. Furthermore, complex communities, where bacteria have a combination of these different advantages could be studied, and the relative strength of these advantages could be varied.

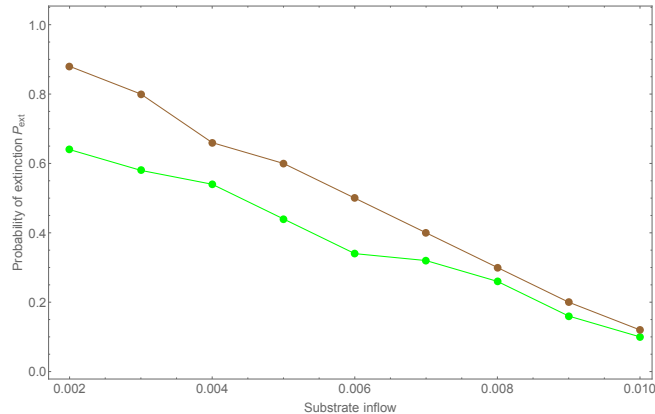


Figure 6.2: Probability of extinction (50 simulations, 10 000 generations) as a function of the substrate inflow rate F_{in} for a system with (brown) and without chemotaxis behaviour (green).

The ultimate goal of such an approach would be to construct a general microbial IBM framework. This framework would characterise the species and their mutual interactions as input and then evolve this hypothetical microbial community. This framework would allow for *in silico* study of hypotheses of ecological theories. Furthermore, this framework would aid the design of a synthetic microbial community, helping with the selection of the individual bacteria (De Roy et al., 2014). Because of their reduced complexity and increased controllability, synthetic microbial communities have great promise as a tool for a deeper understanding of microbial communities and optimisation of engineered systems.

However, such a model would be computationally demanding. Rewriting and compiling the model in a faster low-level programming language (e.g. C) might lower the demand, and parallelisation of the execution can bring some improvements as well. When available, one can consider running the model on graphics processing units (GPU) through e.g. the CUDA environment produced by nVidia.

In conclusion, we demonstrated the effects of a lattice-free approach, a more realistic movement mechanism, the effect of motility and the effect of substrate-dependent reproduction on the dynamics of *in silico* microbial communities described by means of an IBM, thereby making existing models more realistic. The flexible nature of the developed IBMs will allow further progress in this scientific field.

Bibliography

- Abrudan, M., You, L., St, K., and Thuijsman, F. (2016). A Game Theoretical Approach to Microbial Coexistence. In Thuijsman, F. and Wagener, F., editors, *Advances in Dynamic and Evolutionary Games*, chapter 13, pages 267–282. Springer International Publishing, Switzerland.
- Achtman, M., Mercer, A., Kusecek, B., Pohl, A., Aaronson, W., Sutton, A., and Silver, P. (1983). Six widespread bacterial clones among *Escherichia coli* K1 isolates. *Infection and Immunity*, 39(1):315–335.
- Adamson, M. W. and Morozov, A. Y. (2012). Revising the Role of Species Mobility in Maintaining Biodiversity in Communities with Cyclic Competition. *Bulletin of Mathematical Biology*, 74(9):2004–2031.
- Allesina, S. and Levine, J. M. (2011). A competitive network theory of species diversity. *Proceedings of the National Academy of Sciences of the United States of America*, 108(14):5638–5642.
- An, D., Danhorn, T., Fuqua, C., and Parsek, M. R. (2006). Quorum sensing and motility mediate interactions between *Pseudomonas aeruginosa* and *Agrobacterium tumefaciens* in biofilm cocultures. *Proceedings of the National Academy of Sciences, USA*, 103(10):3828–3833.
- Arnoldi, M., Kacher, C. M., Bäuerlein, E., Radmacher, M., and Fritz, M. (1998). Elastic properties of the cell wall of *Magnetospirillum gryphiswaldense* investigated by atomic forcemicroscopy. *Applied Physics A: Materials Science and Processing*, 66(SUPPL. 1):613–617.
- Ashby, M. N., Rine, J., Mongodin, E. F., Nelson, K. E., and Dimster-Denk, D. (2007). Serial analysis of rRNA genes and the unexpected dominance of rare members of microbial communities. *Applied and Environmental Microbiology*, 73(14):4532–4542.
- Avelino, P. P., Bazeia, D., Losano, L., Menezes, J., and Oliveira, B. F. (2012). Junctions and spiral patterns in generalized rock-paper-scissors models. *Physical Review E - Statistical, Nonlinear, and Soft Matter Physics*, 86(3):2–6.

- Beaumont, M. A. (2010). Approximate Bayesian Computation in Evolution and Ecology. *Annual Review of Ecology, Evolution, and Systematics*, 41(1):379–406.
- Bell, T., Newman, J. A., Silverman, B. W., Turner, S. L., and Lilley, A. K. (2005). The contribution of species richness and composition to bacterial services. *Nature*, 436(7054):1157–1160.
- Ben-Jacob, E., Schochet, O., Tenenbaum, A., Cohen, I., Czirók, A., and Vicsek, T. (1994). Generic modelling of cooperative growth patterns in bacterial colonies. *Nature*, 368(6466):46–49.
- Berr, M., Reichenbach, T., Schottenloher, M., and Frey, E. (2009). Zero-one survival behavior of cyclically competing species. *Physical Review Letters*, 102(4):1–4.
- Buss, L. W. (1979). Competitive Networks : Nontransitive Competitive Relationships in Cryptic Coral Reef Environments. *The American Naturalist*, 113(2):223–234.
- Buss, L. W. (1990). Competition within and between encrusting clonal invertebrates. *Trends in Ecology and Evolution*, 5(11):352–356.
- Cabeen, M. T. and Jacobs-Wagner, C. (2005). Bacterial cell shape. *Nature Reviews Microbiology*, 3(8):601–610.
- Cardinale, B. J., Palmer, M. A., and Collins, S. L. (2002). Species diversity enhances ecosystem functioning through interspecific facilitation. *Nature*, 415(6870):426–429.
- Chao, L. and Levin, B. R. (1981). Structured habitats and the evolution of anticompertitor toxins in bacteria. *Proceedings of the National Academy of Sciences of the United States of America*, 78(10):6324–6328.
- Cheng, H., Yao, N., Huang, Z.-G., Park, J., Do, Y., and Lai, Y.-C. (2014). Mesoscopic Interactions and Species Coexistence in Evolutionary Game Dynamics of Cyclic Competitions. *Scientific Reports*, 4:7486.
- Chesson, P. (2000). Mechanisms of maintenance of species diversity. *Annual Review of Ecology and Systematics*, 31(1):343–366.
- Csilléry, K., Blum, M. G. B., Gaggiotti, O. E., and François, O. (2010). Approximate Bayesian Computation (ABC) in practice. *Trends in Ecology and Evolution*, 25(7):410–418.
- Czárán, T. L., Hoekstra, R. F., and Pagie, L. (2002). Chemical warfare between microbes promotes biodiversity. *Proceedings of the National Academy of Sciences of the United States of America*, 99(2):786–790.

- Daly, A. J., Baetens, J. M., and De Baets, B. (2015). The impact of initial evenness on biodiversity maintenance for a four-species in silico bacterial community. *Journal of Theoretical Biology*, 387:189–205.
- Daly, A. J., Baetens, J. M., and De Baets, B. (2016). In silico substrate dependence increases community productivity but threatens biodiversity. *Physical Review E*, 93(4):042414.
- De Roy, K., Marzorati, M., Negroni, A., Thas, O., Balloi, A., Fava, F., Verstraete, W., Daffonchio, D., and Boon, N. (2013). Environmental conditions and community evenness determine the outcome of biological invasion. *Nature Communications*, 4:1383.
- De Roy, K., Marzorati, M., Van den Abbeele, P., Van de Wiele, T., and Boon, N. (2014). Synthetic microbial ecosystems: an exciting tool to understand and apply microbial communities. *Environmental Microbiology*, 16(6):1472–1481.
- Descamps-Julien, B. and Gonzalez, A. (2005). Stable coexistence in a fluctuating environment: An experimental demonstration. *Ecology*, 86(10):2815–2824.
- Diggle, S. P., Griffin, A. S., Campbell, G. S., and West, S. A. (2007). Cooperation and conflict in quorum-sensing bacterial populations. *Nature*, 450(7168):411–414.
- Domach, M. M., Leung, S. K., Cahn, R. E., Cocks, G. G., and Shuler, M. L. (1984). Computer model for Glucose-limited growth of a single cell of *Escherichia Coli*. *Biotechnology and Bioengineering*, 26(3):203–216.
- Durrett, R. and Levin, S. A. (1997). Allelopathy in Spatially Distributed Populations. *Journal of Theoretical Biology*, 185(2):165–171.
- Durrett, R. and Levin, S. A. (1998). Spatial aspects of interspecific competition. *Theoretical population biology*, 53(1):30–43.
- Dusenbery, D. B. (2009). *Living at Micro Scale: The Unexpected Physics of Being Small*. Harvard University Press.
- Ermentrout, G. and Edelstein-Keshet, L. (1993). Cellular Automata Approaches to Biological Modeling. *Journal of Theoretical Biology*, 160:97–133.
- Evans, M. R., Grimm, V., Johst, K., Knuuttila, T., de Langhe, R., Lessells, C. M., Merz, M., O’Malley, M. A., Orzack, S. H., Weisberg, M., Wilkinson, D. J., Wolkenhauer, O., and Benton, T. G. (2013). Do simple models lead to generality in ecology? *Trends in Ecology and Evolution*, 28(10):578–583.
- Ferrer, J., Prats, C., and López, D. (2008). Individual-based modelling: An essential tool for microbiology. *Journal of Biological Physics*, 34:19–37.

- Fink, K. A. and Wilson, S. D. (2011). Invasion of a Native Grassland: Diversity and Resource Reduction. *Botany*, 89(3):157–164.
- Flannagan, R. S., Valvano, M. A., and Koval, S. F. (2004). Downregulation of the motA gene delays the escape of the obligate predator Bdellovibrio bacteriovirus 109J from bdelloplasts of bacterial prey cells. *Microbiology*, 150(3):649–656.
- Frean, M. and Abraham, E. R. (2001). Rock-scissors-paper and the survival of the weakest. *Proceedings. Biological sciences / The Royal Society*, 268(1474):1323–7.
- Frey, E. and Reichenbach, T. (2011). *Bacterial games*. Springer, Berlin Heidelberg.
- Gause, F. (1934). *The Struggle for Existence*. Hafner Publishing Company, New York.
- Gillespie, D. T. (1976). A general method for numerically simulating the stochastic time evolution of coupled chemical reactions. *Journal of Computational Physics*, 22(4):403–434.
- Ginovart, M. (2002). INDISIM, An Individual-based Discrete Simulation Model to Study Bacterial Cultures. *Journal Of Theoretical Biology*, 214(2):305–319.
- Grimm, V. (1999). Ten years of individual-based modelling in ecology: What have we learned and what could we learn in the future? *Ecological Modelling*, 115(2-3):129–148.
- Grimm, V., Berger, U., Bastiansen, F., Eliassen, S., Ginot, V., Giske, J., Goss-Custard, J., Grand, T., Heinz, S. K., Huse, G., Huth, A., Jepsen, J. U., Jørgensen, C., Mooij, W. M., Müller, B., Pe'er, G., Piou, C., Railsback, S. F., Robbins, A. M., Robbins, M. M., Rossmanith, E., Rüger, N., Strand, E., Souissi, S., Stillman, R. A., Vabø, R., Visser, U., and DeAngelis, D. L. (2006). A standard protocol for describing individual-based and agent-based models. *Ecological Modelling*, 198(1-2):115–126.
- Grimm, V., Berger, U., DeAngelis, D. L., Polhill, J. G., Giske, J., and Railsback, S. F. (2010). The ODD protocol: A review and first update. *Ecological Modelling*, 221(23):2760–2768.
- Grman, E., Lau, J. A., Schoolmaster, D. R., and Gross, K. L. (2010). Mechanisms contributing to stability in ecosystem function depend on the environmental context. *Ecology Letters*, 13(11):1400–1410.
- Hales, D., Rouchier, J., and Edmonds, B. (2003). Model-To-Model Analysis. *Journal of Artificial Societies and Social Simulation*, 6(4):5.
- Hardin, G. (1960). The competitive exclusion principle. *Science*, 131:1292–1297.
- Harpole, W. S. and Suding, K. N. (2007). Frequency-dependence stabilizes competitive interactions among four annual plants. *Ecology Letters*, 10(12):1164–1169.

- Hassell, M. P., Comins, H. N., and May, R. M. (1994). Species coexistence and self-organizing spatial dynamics. *Nature*, 370(6487):290–292.
- Hawick, K. A. (2011). Cycles, diversity and competition in rock-paper-scissors-lizard-spock spatial game agent simulations. *Proceedings of the 2011 International Conference on Artificial Intelligence*, 1:115–121.
- Heinz, T. N. and Hunenberger, P. H. (2004). A fast pairlist-construction algorithm for molecular simulations under periodic boundary conditions. *Journal of Computational Chemistry*, 25(12):1474–1486.
- Hellweger, F. L. and Bucci, V. (2009). A bunch of tiny individuals-Individual-based modeling for microbes. *Ecological Modelling*, 220(1):8–22.
- Hellweger, F. L., Clegg, R. J., Clark, J. R., Plugge, C. M., and Kreft, J.-U. (2016). Advancing microbial sciences by individual-based modelling. *Nature Reviews Microbiology*, 14(7):461–471.
- Henke, J. M. and Bassler, B. L. (2004). Bacterial social engagements. *Trends in Cell Biology*, 14(11):648–656.
- Hibbing, M. E., Fuqua, C., Parsek, M. R., and Peterson, S. B. (2010). Bacterial competition: surviving and thriving in the microbial jungle. *Nature Reviews. Microbiology*, 8(1):15–25.
- Hillebrand, H., Bennett, D. M., and Cadotte, M. W. (2008). Consequences of dominance: a review of evenness effect on local and regional ecosystem processes. *Ecology*, 89(6):1510–1520.
- Holcombe, M., Adra, S., Bicak, M., Chin, S., Coakley, S., Graham, A. I., Green, J., Greenough, C., Jackson, D., Kiran, M., MacNeil, S., Maleki-Dizaji, A., McMinn, P., Pogson, M., Poole, R., Qwarnstrom, E., Ratnieks, F., Rolfe, M. D., Smallwood, R., Sun, T., and Worth, D. (2012). Modelling complex biological systems using an agent-based approach. *Integrative Biology*, 4(November):53–64.
- Hooper, D. U., Chapin, F. S., Ewel, J. J., Hextor, A., Inchausti, P., Lavorel, S., Lawton, J. H., Lodge, D. M., Loreau, M., Naeem, S., Schmid, B., Setälä, H., Symstad, J., Vandermeer, J., and Wardle, D. A. (2005). Effects of biodiversity on ecosystem functioning: a consensus of current knowledge. *America*, 75(July 2004):3–35.
- Huisman, J., Johansson, A. M., Folmer, E. O., and Weissing, F. J. (2001). Towards a solution of the plankton paradox: The importance of physiology and life history. *Ecology Letters*, 4(5):408–411.
- Huisman, J. and Weissing, F. J. (1999). Biodiversity of plankton by species oscillations and chaos. *Nature*, 402(6760):407–410.

- Hutchinson, G. . E. . (1961). The Paradox of the Plankton. *The American Naturalist*, 95(882):137–145.
- Isbell, F. I., Polley, H. W., and Wilsey, B. J. (2009). Species interaction mechanisms maintain grassland plant species diversity. *Ecology*, 90(7):1821–1830.
- Jackson, J. B. C. (1983). Biological determinants of present and past sessile animal distributions. In Tevesz, M. J. S. and McCall, P. L., editors, *Biotic interactions in recent and fossil benthic communities.*, chapter 2, pages 39–120. Springer US.
- James, R., Lazdunski, C., and Pattus, F. (2013). *Bacteriocins, microcins and lantibiotics*, volume 65. Springer Science & Business Media.
- Jeong, J. W., Snay, J., and Ataai, M. M. (1990). A mathematical model for examining growth and sporulation processes of *Bacillus subtilis*. *Biotechnology and Bioengineering*, 35(2):160–184.
- Kang, Y., Pan, Q., Wang, X., and He, M. (2013). A golden point rule in rock-paper-scissors-lizard-spock game. *Physica A: Statistical Mechanics and its Applications*, 392(11):2652–2659.
- Karolyi, G., Neufeld, Z., and Scheuring, I. (2005). Rock-scissors-paper game in a chaotic flow: The effect of dispersion on the cyclic competition of microorganisms. *Journal of Theoretical Biology*, 236(1):12–20.
- Keddy, P. (2001). *Competition (2nd edition)*. Kluwer, Dordrecht.
- Kéfi, S., Rietkerk, M., Alados, C. L., Pueyo, Y., Papanastasis, V. P., ElAich, A., and de Ruiter, P. C. (2007). Spatial vegetation patterns and imminent desertification in Mediterranean arid ecosystems. *Nature*, 449(7159):213–7.
- Kennedy, T. A., Naeem, S., Howe, K. M., Knops, J. M. H., Tilman, D., and Reich, P. (2002). Biodiversity as a barrier to ecological invasion. *Nature*, 417(6889):636–638.
- Kerr, B., Riley, M. A., Feldman, M. W., and Bohannan, B. J. M. (2002). Local dispersal promotes biodiversity in a real-life game of rock-paper-scissors. *Nature*, 418(6894):171–174.
- Kinkel, L. L., Schlatter, D. C., Xiao, K., and Baines, A. D. (2014). Sympatric inhibition and niche differentiation suggest alternative coevolutionary trajectories among Streptomycetes. *The ISME Journal*, 8(2):249–56.
- Kirkup, B. C. and Riley, M. A. (2004). Antibiotic-mediated antagonism leads to a bacterial game of rock-paper-scissors in vivo. *Nature*, 428(6981):412–4.
- Klapper, I. and Dockery, J. (2010). Mathematical Description of Microbial Biofilm. *SIAM Review*, 52(2):221–265.

- Kreft, J. U., Booth, G., and Wimpenny, J. W. T. (1998). BacSim, a simulator for individual-based modelling of bacterial colony growth. *Microbiology*, 144(12):3275–3287.
- Kreft, J. U., Plugge, C. M., Grimm, V., Prats, C., Leveau, J. H. J., Banitz, T., Baines, S., Clark, J., Ros, A., Klapper, I., Topping, C. J., Field, A. J., Schuler, A., Litchman, E., and Hellweger, F. L. (2013). Mighty small: Observing and modeling individual microbes becomes big science. *Proceedings of the National Academy of Sciences of the United States of America*, 110(45):18027–18028.
- Laird, R. A. (2014). Population interaction structure and the coexistence of bacterial strains playing 'rock-paper-scissors'. *Oikos*, 123(4):472–480.
- Laird, R. A. and Schamp, B. S. (2006). Competitive intransitivity promotes species coexistence. *The American Naturalist*, 168(2):182–193.
- Laird, R. A. and Schamp, B. S. (2008). Does local competition increase the coexistence of species in intransitive networks? *Ecology*, 89(1):237–247.
- Laird, R. A. and Schamp, B. S. (2009). Species coexistence, intransitivity, and topological variation in competitive tournaments. *Journal of Theoretical Biology*, 256(1):90–95.
- Laird, R. A. and Schamp, B. S. (2015). Competitive intransitivity, population interaction structure, and strategy coexistence. *Journal of Theoretical Biology*, 365:149–158.
- Landau, L. and Lifshitz, E. (1986). *EM Lifshitz Theory of elasticity*. Pergamon Press, 3 edition.
- Lankau, R. A. and Strauss, S. Y. (2007). Genetic and Species Diversity in a Plant Community. *Science*, 317(5844):1561–1563.
- Lemieux, J. and Cusson, M. (2014). Effects of habitat-forming species richness, evenness, identity, and abundance on benthic intertidal community establishment and productivity. *PLoS ONE*, 9(10).
- Levin, B. R., Antonovics, J., and Sharma, H. (1988). Frequency-dependent selection in bacterial populations [and discussion]. *Philosophical Transactions of the Royal Society B: Biological Sciences*, 319(1196):459–472.
- Levin, S. A. (1974). Dispersion and Population Interactions. *The American Naturalist*, 108(960):207–228.
- Levine, J. M. and D'Antonio, C. M. (1999). Elton Revisited : A Review of Evidence Linking Diversity and Invasibility. *Nordic Society Oikos*, 87(1):15–26.
- Matsushita, M. and Fujikawa, H. (1990). Diffusion-limited growth in bacterial colony formation. *Physica A: Statistical Mechanics and its Applications*, 168(1):498–506.

- Mattson, W. and Rice, B. M. (1999). Near-neighbor calculations using a modified cell-linked list method. *Computer Physics Communications*, 119(2):135–148.
- May, R. M. and Leonard, W. J. (1975). Nonlinear Aspects of Competition Between Three Species Author. *ociety for Industrial and Applied Mathematics*, 29(2):243–253.
- Michaelis, L., Menten, M. L., Goody, R. S., and Johnson, K. A. (1913). Die Kinetik der Invertinwirkung The Kinetics of Invertase Action translated by. *Biochem.*, 49:333–369.
- Miller, M. B. and Bassler, B. L. (2001). Quorum sensing in bacteria. *Annual Review of Microbiology*, 55(1):165–199.
- Mimura, M. and Tohma, M. (2015). Dynamic coexistence in a three-species competition-diffusion system. *Ecological Complexity*, 21:215–232.
- Mirams, G. R., Arthurs, C. J., Bernabeu, M. O., Bordas, R., Cooper, J., Corrias, A., Davit, Y., Dunn, S. J., Fletcher, A. G., Harvey, D. G., Marsh, M. E., Osborne, J. M., Pathmanathan, P., Pitt-Francis, J., Southern, J., Zemezmi, N., and Gavaghan, D. J. (2013). Chaste: An Open Source C++ Library for Computational Physiology and Biology. *PLoS Computational Biology*, 9(3).
- Miyazaki, T., Tainaka, K. I., Togashi, T., Suzuki, T., and Yoshimura, J. (2006). Spatial coexistence of phytoplankton species in ecological timescale. *Population Ecology*, 48(2):107–112.
- Monod, J. (1949). The Growth of Bacterial Cultures. *Annual Review of Microbiology*, 3(1):371–394.
- Naeem, S. (2009). Ecology: Gini in the bottle. *Nature*, 458(7238):579–580.
- Naeem, S. and Li, S. (1997). Biodiversity enhances ecosystem reliability. *Nature*, 390(6659):507–509.
- Narisawa, N., Haruta, S., Arai, H., Ishii, M., and Igarashi, Y. (2008). Coexistence of antibiotic-producing and antibiotic-sensitive bacteria in biofilms is mediated by resistant bacteria. *Applied and Environmental Microbiology*, 74(12):3887–3894.
- Nisbet, R. M., Martin, B. T., and de Roos, A. M. (2016). Integrating ecological insight derived from individual-based simulations and physiologically structured population models. *Ecological Modelling*, 326:101–112.
- Perc, M., Szolnoki, A., and Szabó, G. (2007). Cyclical interactions with alliance-specific heterogeneous invasion rates. *Physical Review E - Statistical, Nonlinear, and Soft Matter Physics*, 75(5):3–6.

- Petraitis, P. S. (1979). Competitive networks and measures of intransitivity. *The American Naturalist*, 114(6):921–925.
- Picioreanu, C., Loosdrecht, M., and Heijnen, J. J. (1998a). Mathematical Modeling of Biofilm Structure with a Hybrid Differential-Discrete Cellular Automata Approach. *Biotechnology and Bioengineering*, 58(November):101–116.
- Picioreanu, C., van Loosdrecht, M. C. M., and Heijnen, J. J. (1998b). A new combined differential discrete cellular automaton approach for biofilm modelling Application for growth in gel beads. *Biotechnology and Bioengineering*, 58(March):101–116.
- Polley, H. W., Wilsey, B. J., and Derner, J. D. (2003). Do species evenness and plant density influence the magnitude of selection and complementarity effects in annual plant species mixtures? *Ecology Letters*, 6(3):248–256.
- Popławski, N. J., Shirinifard, A., Swat, M., and Glazier, J. A. (2008). Simulation of single-species bacterial-biofilm growth using the Glazier-Graner-Hogeweg model and the CompuCell3D modeling environment. *Mathematical Biosciences and Engineering*, 5(2):355–88.
- Power, K. and Marshall, K. C. (1988). Cellular growth and reproduction of marine bacteria on surfacebound substrate. *Biofouling*, 1(2):163–174.
- Proulx, R., Wirth, C., Voigt, W., Weigelt, A., Roscher, C., Attinger, S., Baade, J., Barnard, R. L., Buchmann, N., Buscot, F., Eisenhauer, N., Fischer, M., Gleixner, G., Halle, S., Hildebrandt, A., Kowalski, E., Kuu, A., Lange, M., Milcu, A., Niklaus, P. A., Oelmann, Y., Rosenkranz, S., Sabais, A., Scherber, C., Scherer-Lorenzen, M., Scheu, S., Schulze, E. D., Schumacher, J., Schwichtenberg, G., Soussana, J. F., Temperton, V. M., Weisser, W. W., Wilcke, W., and Schmid, B. (2010). Diversity promotes temporal stability across levels of ecosystem organization in experimental grasslands. *PLoS ONE*, 5(10):1–8.
- Reichenbach, T., Mobilia, M., and Frey, E. (2007). Mobility promotes and jeopardizes biodiversity in rock-paper-scissors games. *Nature*, 448(7157):1046–1049.
- Reichenbach, T., Mobilia, M., and Frey, E. (2008). Self-organization of mobile populations in cyclic competition. *Journal of Theoretical Biology*, 254(2):368–383.
- Reusch, T. B. H., Ehlers, A., Hämmerli, A., and Worm, B. (2005). Ecosystem recovery after climatic extremes enhanced by genotypic diversity. *Proceedings of the National Academy of Sciences*, 102(8):2826–2831.
- Richerson, P., Armstrong, R., and Goldman, C. R. (1970). Contemporaneous disequilibrium, a new hypothesis to explain the "paradox of the plankton". *Proceedings of the National Academy of Sciences of the United States of America*, 67(4):1710–1714.

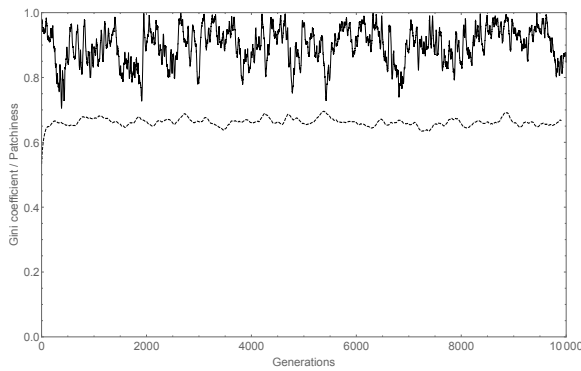
- Riley, M. A. and Gordon, D. M. (1992). A survey of Col plasmids in natural isolates of *Escherichia coli* and an investigation into the stability of Col-plasmid lineages. *Journal of General Microbiology*, 138(7):1345–1352.
- Riley, M. A. and Gordon, D. M. (1999). The ecological role of bacteriocins in bacterial competition. *Trends in Microbiology*, 7(3):129–133.
- Rohani, P., Lewis, T. J., Grünbaum, D., and Ruxton, G. D. (1997). Spatial self-organization in ecology: Pretty patterns or robust reality? *Trends in Ecology and Evolution*, 12(2):70–74.
- Rojas-Echenique, J. and Allesina, S. (2011). Interaction rules affect species coexistence in intransitive networks. *Ecology*, 92(5):1174–1180.
- Roman, A., Dasgupta, D., and Pleimling, M. (2016). A theoretical approach to understand spatial organization in complex ecologies. *ArXiv*, 403:10–16.
- Rosenzweig, M. L. and MacArthur, R. H. (1963). Graphical Representation and Stability Conditions of Predator-Prey. *The American Naturalist*, 97(895):209–223.
- Rousseau, R. and Van Hecke, P. (1999). Measuring Biodiversity. *Acta Biotheoretica*, 47:1–5.
- Roy, S. and Chattopadhyay, J. (2007). Towards a resolution of 'the paradox of the plankton': A brief overview of the proposed mechanisms. *Ecological Complexity*, 4(1-2):26–33.
- Rudge, T. J., Steiner, P. J., Phillips, A., and Haseloff, J. (2012). Computational modeling of synthetic microbial biofilms. *ACS Synthetic Biology*, 1(8):345–352.
- Sale, A. U. (2007). Getting the measure of well-being. *Community Care*, 405(1691):16–17.
- Sankaran, M. and McNaughton, S. J. (1999). Determinants of biodiversity regulate compositional stability of communities. *Nature*, 401(6754):691–693.
- Scanlon, T. M., Caylor, K. K., Levin, S. A., and Rodriguez-Iturbe, I. (2007). Positive feedbacks promote power-law clustering of Kalahari vegetation. *Nature*, 449(7159):209–212.
- Scheffer, M., Baveco, J. M., Deangelis, D. L., Rose, K. A., and Vannes, E. H. (1995). Super-Individuals A Simple Solution For Modeling Large Populations On An Individual Basis. *Ecological Modelling*, 80(1995):161–170.
- Scheffer, M., Rinaldi, S., Huisman, J., and Weissing, F. J. (2003). Why plankton communities have no equilibrium: Solutions to the paradox. *Hydrobiologia*, 491:9–18.
- Shapiro, J. A. (1998). Thinking about bacterial populations as multicellular organisms. *Annual Review of Microbiology*, 52:81–104.

- Sinervo, B. R., Heulin, B., Surget-Groba, Y., Clobert, J., Miles, D. B., Corl, A., Chaine, A. S., and Davis, A. R. (2007). Models of Density-Dependent Genic Selection and a New Rock-Paper-Scissors Social System. *The American Naturalist*, 170(5):663–680.
- Smith, V. H. (2002). Effects of resource supplies on the structure and function of microbial communities. *Antonie van Leeuwenhoek*, 81:99–106.
- Standaert, A. R., Poschet, F., Geeraerd, A. H., Uylbak, F. V., Kreft, J. U., and Van Impe, J. F. (2004). A novel class of predictive microbial growth models: implementation in an individual-based framework. *Computer Applications in Biotechnology*, pages 183–188.
- Szabó, G. and Fáth, G. (2007). Evolutionary games on graphs. *Physics Reports*, 446(4-6):97–216.
- Szolnoki, A., Mobilia, M., Jiang, L. L., Szczesny, B., Rucklidge, A. M., and Perc, M. (2014). Cyclic dominance in evolutionary games: a review. *Journal of the Royal Society, Interface / the Royal Society*, 11(100):20140735.
- Taylor, D. R. and Aarssen, L. W. (1990). Complex Competitive Relationships Among Genotypes of Three Perennial Grasses : Implications for Species Coexistence. *The American Society of Naturalist*, 136(3):305–327.
- Tilman, D. (1996). Biodiversity: population versus ecosystem stability. *Ecological Society of America*, 77(2):350–363.
- Tilman, D., Knops, J. M. H., Wedin, D., Reich, P., Ritchie, M., and Siemann, E. (1997). The Influence of Functional Diversity and Composition on Ecosystem Processes. *Science*, 277(5330):1300–1302.
- Touhami, A., Nysten, B., and Dufrêne, Y. (2003). Nanoscale Mapping of the Elasticity of Microbial Cells by Atomic Force Microscopy. *Langmuir*, (19):4539–4543.
- Tracy, B. F. and Sanderson, M. A. (2004). Forage productivity, species evenness and weed invasion in pasture communities. *Agriculture, Ecosystems and Environment*, 102(2):175–183.
- van der Vaart, E., Beaumont, M. A., Johnston, A. S., and Sibly, R. M. (2015). Calibration and evaluation of individual-based models using Approximate Bayesian Computation. *Ecological Modelling*, 312:182–190.
- Verlet, L. (1967). Computer "Experiments" on Classical Fluids. *Physical Review*, 159(1):98–103.
- Vetsigian, K., Jajoo, R., and Kishony, R. (2011). Structure and evolution of streptomyces interaction networks in soil and in silico. *PLoS Biology*, 9(10).

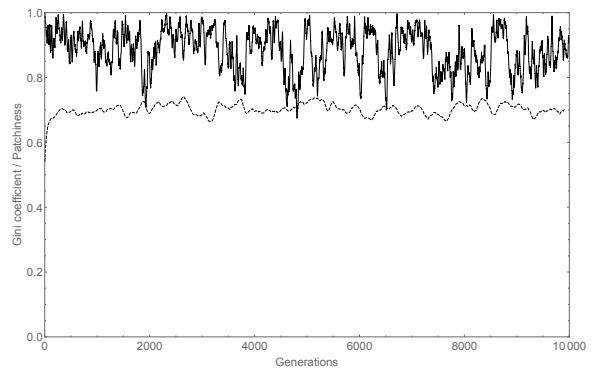
- Vukov, J., Szolnoki, A., and Szabó, G. (2013). Diverging fluctuations in a spatial five-species cyclic dominance game. *Physical Review E - Statistical, Nonlinear, and Soft Matter Physics*, 88(2):1–8.
- Waters, C. M. and Bassler, B. L. (2005). Quorum Sensing : Communication in Bacteria. *Annual Reviews in Cell Development Biology*, 21(1):319–346.
- Wessel, A. K., Hmelo, L., Parsek, M. R., and Whiteley, M. (2013). Going local: technologies for exploring bacterial microenvironments. *Nature reviews. Microbiology*, 11(5):337–48.
- Wiggert, J. D., Haskell, A. G. E., Paffenhöfer, G. A., Hofmann, E. E., and Klinck, J. M. (2005). The role of feeding behavior in sustaining copepod populations in the tropical ocean. *Journal of Plankton Research*, 27(10):1013–1031.
- Wilensky, U. (1999). Netlogo.
- Wills, C., Harms, K. E., Condit, R., King, D., Thompson, J., He, F., Muller-Landau, H. C., Ashton, P., Losos, E., Comita, L., Hubbell, S., LaFrankie, J., Bunyavejchewin, S., Dattaraja, H. S., Davies, S., Esufali, S., Foster, R., Gunatilleke, N., Gunatilleke, S., Hall, P., Itoh, A., John, R., Kiratiprayoon, S., de Lao, S. L., Massa, M., Nath, C., Noor, M. N. S., and Kassim, A. R. (2006). Diversity in tropical forests. *Science*, 311(5766):527.
- Wilsey, B. J. (2004). Realistically Low Species Evenness Does Not Alter Grassland Species-Richness Productivity Relationships. *Ecology*, 85(10):2693–2700.
- Wilsey, B. J. and Polley, H. W. (2002). Reductions in grassland species evenness increase dicot seedling invasion and spittle bug infestation. *Ecology Letters*, 5(5):676–684.
- Wilsey, B. J. and Potvin, C. (2000). Biodiversity and ecosystem functioning: Importance of species evenness in an old field. *Ecology*, 81(4):887–892.
- Wilsey, B. J., Teaschner, T. B., Daneshgar, P. P., Isbell, F. I., and Polley, H. W. (2009). Biodiversity maintenance mechanisms differ between native and novel exotic-dominated communities. *Ecology Letters*, 12(5):432–442.
- Wimpenny, J. W. T. (1992). *Microbial Systems*, pages 469–522. Springer US, Boston, MA.
- Wimpenny, J. W. T. and Colasanti, R. (1997). A unifying hypothesis for the structure of microbial biofilms based on cellular automaton models. *FEMS Microbiology Ecology*, 22:1–16.
- Wittebolle, L., Marzorati, M., Clement, L., Balloi, A., Daffonchio, D., De Vos, P., Heylen, K., Verstraete, W., and Boon, N. (2009). Initial community evenness favours functionality under selective stress. *Nature*, 458(7238):623–626.

APPENDIX A

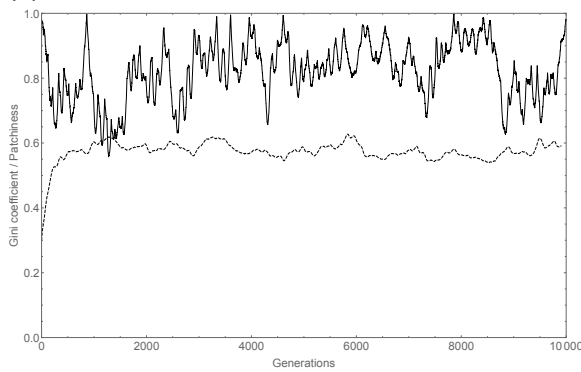
Evenness and patchiness for the systems under study in Chapter 3



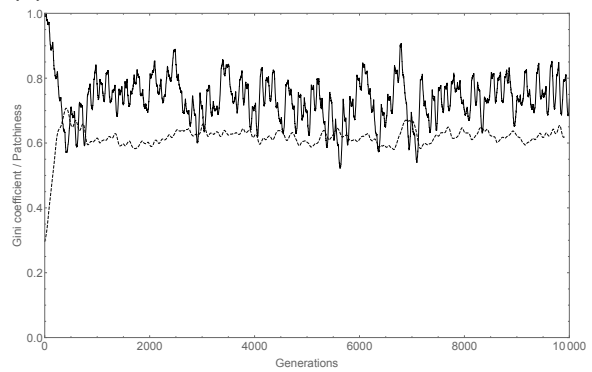
(a) Lattice-free approach with $\epsilon = 1$.



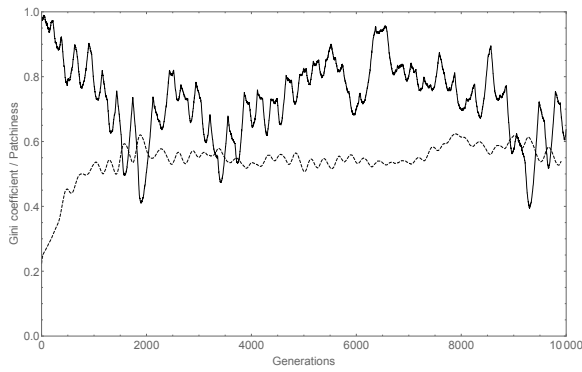
(b) Lattice-based approach with $\epsilon = 1$.



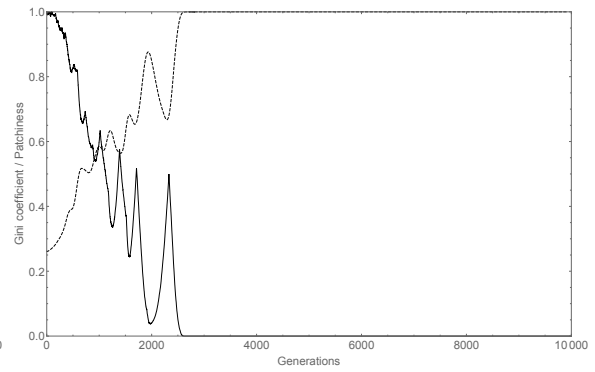
(c) Lattice-free approach with $\epsilon = 10$.



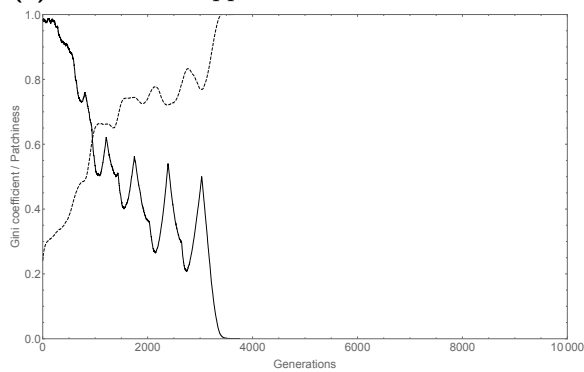
(d) Lattice-based approach with $\epsilon = 10$.



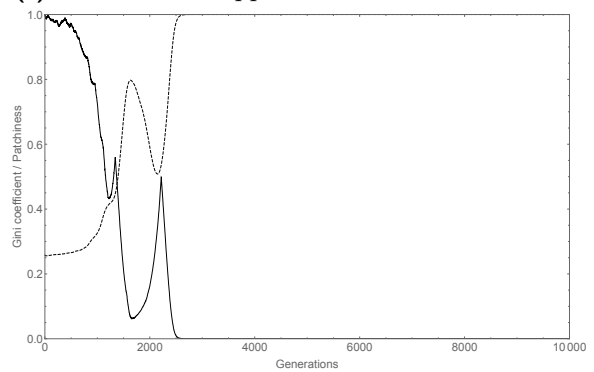
(e) Lattice-free approach with $\epsilon = 30$.



(f) Lattice-based approach with $\epsilon = 30$.



(g) Lattice-free approach with $\epsilon = 60$.



(h) Lattice-based approach with $\epsilon = 60$.

Figure A.1: Evenness (solid), measured as the Gini coefficient, and patchiness (dashed) plotted through time for a representative evolution of for different values of mobility rate ϵ for the lattice-free (a and c) and lattice-based model (b and d).

APPENDIX B

Step-by-step derivation of the expected value of total distance

The expected value of the Euclidean distance travelled during one movement event is given by

$$\begin{aligned} E(\sqrt{x^2 + y^2}) &= \int_{-d}^d \int_{-d}^d \sqrt{x^2 + y^2} f_X(x) f_Y(y) dx dy \\ &= \int_{-d}^d \int_{-d}^d \sqrt{x^2 + y^2} \frac{1}{d - (-d)} \frac{1}{d - (-d)} dx dy \\ &= \frac{1}{4d^2} \int_{-d}^d \int_{-d}^d \sqrt{x^2 + y^2} dx dy , \end{aligned}$$

with f_X and f_Y the probability distribution function of a uniform distribution.

Transformation in polar coordinates and using symmetry to simplify the equation gives (Figure B.1)

$$\begin{aligned} E(\sqrt{x^2 + y^2}) &= \frac{2}{d^2} \int_0^{\frac{\pi}{4}} \int_0^{d \sec \theta} r r dr d\theta \\ &= \frac{2}{d^2} \int_0^{\frac{\pi}{4}} \frac{d^3}{3} \sec^3 \theta d\theta \\ &= \frac{2d}{3} \int_0^{\frac{\pi}{4}} \sec^3 \theta d\theta . \end{aligned} \tag{B.1}$$

To evaluate this integral, integration by parts is used

$$\begin{aligned}
\int_0^{\frac{\pi}{4}} \sec^3 \theta \, d\theta &= [\sec \theta \tan \theta]_0^{\frac{\pi}{4}} - \int_0^{\frac{\pi}{4}} \tan^2 \theta \sec \theta \, d\theta \\
&= [\sec \theta \tan \theta]_0^{\frac{\pi}{4}} - \int_0^{\frac{\pi}{4}} (\sec^2 \theta - 1) \sec \theta \, d\theta \\
&= [\sec \theta \tan \theta]_0^{\frac{\pi}{4}} - \int_0^{\frac{\pi}{4}} \sec^3 \theta \, d\theta + \int_0^{\frac{\pi}{4}} \sec \theta \, d\theta \\
&= \left[\frac{\sec \theta \tan \theta}{2} \right]_0^{\frac{\pi}{4}} + \frac{\int_0^{\frac{\pi}{4}} \sec \theta \, d\theta}{2} \\
&= \left[\frac{\sec \theta \tan \theta + \ln(\sec \theta + \tan \theta)}{2} \right]_0^{\frac{\pi}{4}} .
\end{aligned} \tag{B.2}$$

Substitution of Equation B.2 in Equation B.1 gives

$$\begin{aligned}
E(\sqrt{x^2 + y^2}) &= \frac{2d}{3} \left[\frac{\sec \theta \tan \theta + \ln(\sec \theta + \tan \theta)}{2} \right]_0^{\frac{\pi}{4}} \\
&= \frac{d}{3} (1 \cdot \sqrt{2} + \ln(\sqrt{2} + 1)) \\
&= \frac{d}{3} (\sqrt{2} + \sinh^{-1}(1)) \\
&\approx 0.76 \, d .
\end{aligned}$$

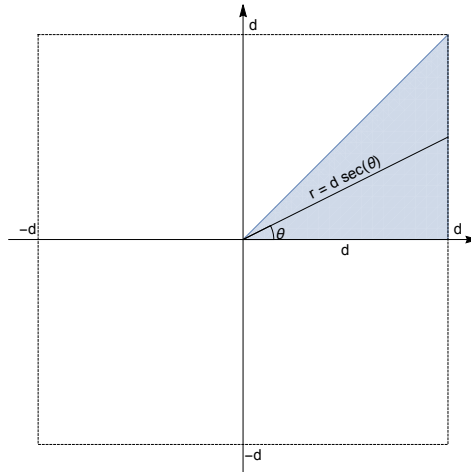
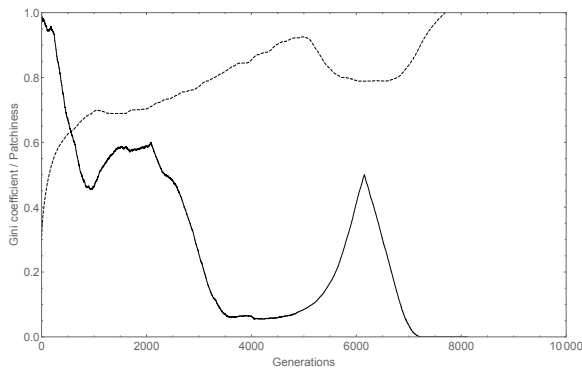


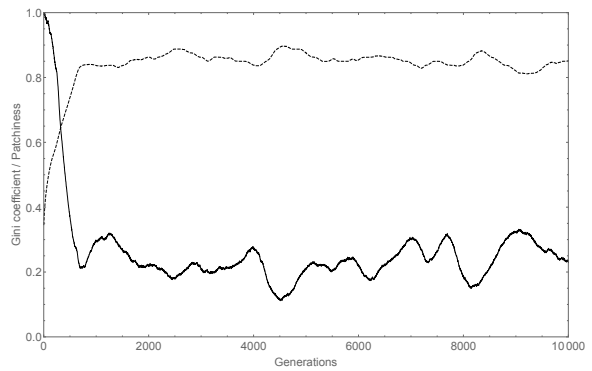
Figure B.1: Visualisation of the limits of the integration.

APPENDIX C

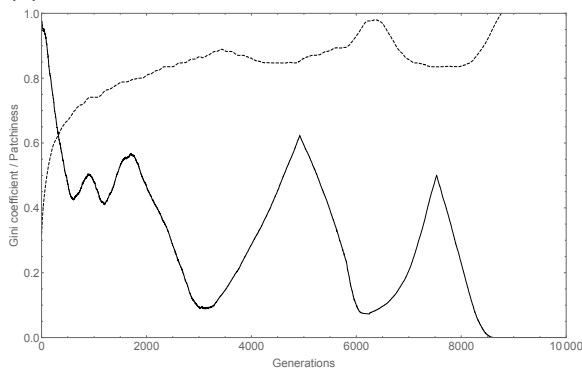
Evenness and patchiness for the systems under study in Chapter 4



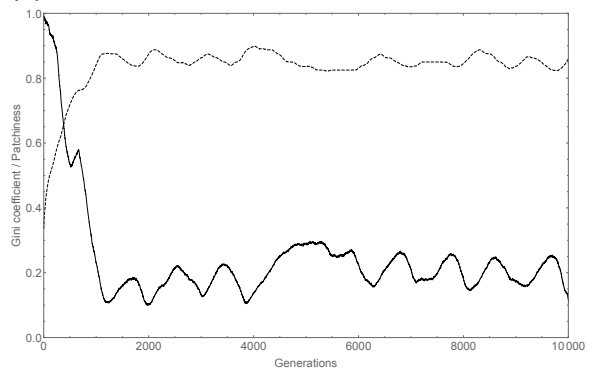
(a) CNN



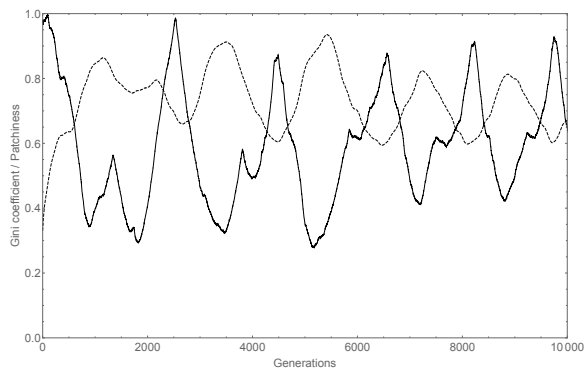
(b) CNE



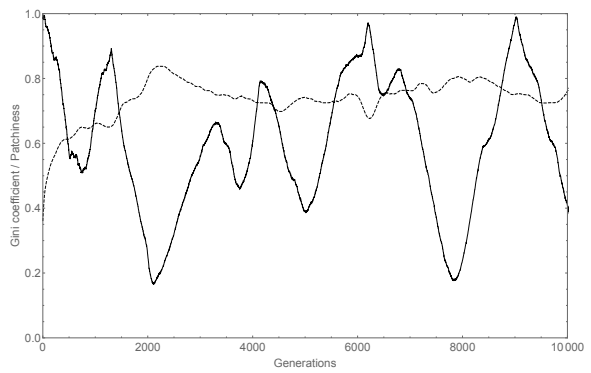
(c) CCN



(d) CCE



(e) CEE



(f) ENN

Figure C.1: Evenness (solid), measured as the Gini coefficient, and patchiness (dashed) plotted through time for a representative evolution of different scenarios.